DR. SUJAY PATTANAYAK M.SC. PH.D

CONTACT NO.

- **Mob. 9830048975**

E-MAIL

- **sujayp69@gmail.com**

POSITION HELD

- **ASSOCIATE PROFESSOR**
  DEPARTMENT OF CHEMISTRY, BANGABASI COLLEGE

RESEARCH INTEREST

- **ORGANOMETALLIC CHEMISTRY**

THESIS

- **CHEMISTRY OF NEW COORDINATION AND ORGANOMETALLIC COMPOUNDS OF d-BLOCK ELEMENTS**

TEACHING INTEREST

- **ORGANOMETALLIC CHEMISTRY**
- **COORDINATION CHEMISTRY**
- **ORGANIC CHEMISTRY**
- **INORGANIC CHEMISTRY**
- **ANALYTICAL CLINICAL BIOCHEMISTRY**
- **PHARMACEUTICALS CHEMISTRY**

MRP

- "**STUDIES OF DECARBONYLATION REACTIONS BY IRIDIUM PHOSPHINE CATALYSTS**"
  UGC Reference No. : F. PSW- 040/03-04(ERO) Dated 12-March –04; Grants: Rs. 83,000

- "**STUDIES OF NEW ORGANOMETALLIC COMPOUNDS WITH ANTICANCER ACTIVITY**"
  Grants: Rs. 25,000 (COLLEGE SEED MONEY)

RECENT SEMINARS/WORKSHOP ATTENDED

- **One day workshop on "Hand on Training of NAAC methodology and Preparation" Sponsored by the department of Higher Education, Government of West Bengal. Organized by Women's College, Calcutta on 09.01.2024**

- **One day workshop on the newly introduced UG Chemistry Syllabus for the 4 year Honours Degree Course & the 3 year MDC of the University of Calcutta organized by the Department of Chemistry, SCC in collaboration with the UG Board of Studies in Chemistry, University of Calcutta and Supported by IQAC SCC on 4th August 2023.**

- **One day International Seminar on "Non-Conventional Renewable Energy: Impact on Environment" organized by Bangabasi College, Ramakrishna Mission Residential College Narendrapur, Acharya Jagadish Chandra Bose College, Ananda Mohan College, City College of Commerce and Business Administration on 08.04.2023**

- **One day Online International Seminar on "Solar Cell & Solar Energy" delivered by Prof. Dr. Mool C. Gupta, Prof. & Director for NSFI/UCRC Laser center, University of Virginia, U.S.A. Organized by Bangabasi College on 07.03.2022**

PUBLICATIONS.

- Ruthenium Antitumor Compounds.
  ***Bangabasi College Academic Journal* 2014,** *20,* 1419-1423.
  Sujay Pattanayak.

- Rhodium(III) Organometallic Anticancer Agent, an Intercalative DNA Coordinator.
  ***Bangabasi College Academic Journal* 2013,** *20,* 1419-1423. **Sujay Pattanayak.**

- Alkyne Insertion into the Ru-C Bond of a Four-Membered Metallacycle. Insertion Rate and Reaction Pathway.
  ***Organometallics* 2001,** *20,* 1419-1423.
  Kaushik Ghosh, Swarup Chattopadhyay, **Sujay Pattanayak**, and Animesh Chakravorty.

- A family of organoruthenium nitrites: alkyne insertion, linkage isomerization and ring nitration.
  J. Chem. Soc., Dalton Trans., **2001**, 1259-1265
  Swarup Chattopadhyay, Kaushik Ghosh, **Sujay Pattanayak** and Animesh Chakravorty.

- Nitrite Linkage Isomersation Promoted by Alkyne Insertion in Ruthenium Organometallics.
  Indian Journal of Chemistry, 2001, pp1-3
  Swarup Chattopadhyay, Kaushik Ghosh, **Sujay Pattanayak,** and Animesh Chakravorty.

- A New Family of Acylrhodium Organometallics.
  ***Organometallics,* 1999**, 18, 1486.
  Sujay Pattanayak, Swarup Chattopadhyay, Kaushik Ghosh, Sanjib Ganguly, Prasanta Ghosh and Animesh Chakravorty.

- Metallacycle Expansion by Alkyne Insertion. Chemistry of a New Family of Ruthenium Organometallics.
  ***Organometallics,* 1998,** *17,* 1956-1960
  Kaushik Ghosh, **Sujay Pattanayak**, and Animesh Chakravorty.

- Valence specific chelation of ruthenium to Schiff mono-bases of 2,6-diformyl-4-methylphenol : synthesis and structure of trivalent salicylaldiminato species of coordination type RuN,OzPCl
  Polyhedron, Vol. 16, No. 17, pp. 2951-2956, **1997**
  Sujay Pattanayak, Kausikisankar Pramanik, Nilkamal Bag, Prasanta Ghosh and Animesh Chakravorty.

- Synthesis, Structure and Metal Redox of a Family of Copper Complexes Derived from Hexadentate Ligands Incorporating Thioether and Triazene 1-Oxide Functions.
  Polyhedron, Vol. 15. No 7. pp I I21 1127. **1996**
  Sujay Pattanayak, Partha Chakraborty, Swapan Kumar Chandra and Animesh Chakravorty.

- Binding of Thioether Sulfur to Trivalent Chromium. A Family of CrSzNzOz Complexes Derived from Acyclic Ligands.
  ***Inorg. Chem.* 1995**, 34**,** 6556-6558
  Sujay Pattanayak, Diganta Kumar Das, Partha Chakraborty, and Animesh Chakravorty.

Alkyne Insertion into the Ru−C Bond of a Four-Membered Metallacycle. Insertion Rate and Reaction Pathway

Kaushik Ghosh, Swarup Chattopadhyay, Sujay Pattanayak, and Animesh Chakravorty*

Department of Inorganic Chemistry, Indian Association for the Cultivation of Science, Calcutta 700032, India

Received July 28, 2000

The insertion of $HOCH_2C{\equiv}CH$ (ha) into the Ru−C bond of $Ru^{II}(RL^1)(PPh_3)_2(CO)Cl$, **1**, has afforded $Ru^{II}(RL^3)(PPh_3)_2(CO)Cl$, **3**, which has been structurally characterized. Insertion rates in CH_2Cl_2−MeOH for ha as well as for $PhC{\equiv}CH$ (pa), which inserts similarly into **1** affording $Ru^{II}(RL^2)(PPh_3)_2(CO)Cl$, **2**, are proportional to the product of the concentrations of alkyne and methanol. The insertion rate of ha is nearly 5 times faster than that of pa, and for a given alkyne the rate increases as R becomes more electron-withdrawing (OMe < Me < Cl). A reaction model implicating the adduct **1**·MeOH, which binds and activates the alkyne via displacement of MeOH, is proposed.

Introduction

A few instances of insertion of alkynes into the Ru−C σ-bond have been documented in the literature,[1−6] but rarely have mechanistic proposals been authenticated by rate studies.[6] The concern of the present work is the two-carbon metallacycle expansion via insertion of alkynes generally abbreviated as xa, eq 1. The reaction

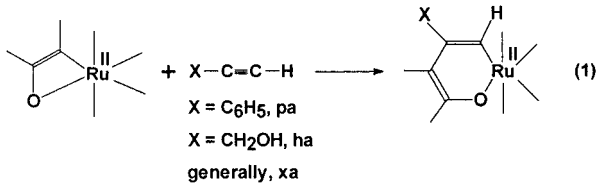

was recently authenticated by us via isolation and structure determination of the expanded cycle in the case of phenylacetylene, pa (as well as unsubstituted acetylene).[1]

Further scrutiny has revealed that the reaction is suitable for facile rate determination by spectrophotometric methods in the cases of pa and hydroxymethylacetylene, ha. This has provided an opportunity for probing the reaction pathway. Rates have been measured in CH_2Cl_2−MeOH mixtures, revealing that the four-membered metallacycle itself is *not* reactive but its methanol adduct present in equilibrium *is*. The observed rate law has been rationalized on this basis, and a mechanistic model is proposed. The substituents in the alkyne and the reactive metallacycle have notable effects on reaction rates. The insertion of hydroxymethylacetylene, ha according to eq 1, is being reported here for the first time, necessitating product characterization, which forms a part of the present work.

Results and Discussion

Substrates and Products. The concerned metallacycles, their abbreviations, and numberings are set out in Figure 1. Three substrates[7] of type **1** have been used. The pa-inserted products of type **2** are already known.[1] The reaction of ha with **1** proceeds smoothly in CH_2Cl_2−MeOH mixtures under mild conditions, affording the type **3** species in virtually quantitative yield. To our knowledge, this reaction represents the first authentic example of insertion of ha into the Ru−C bond.

Characterization of $Ru(RL^3)(PPh_3)_2(CO)Cl$, 3. Spectral and other physical features of **3** are listed in the Experimental Section. The N^+−H and C═N stretches occur at ∼3440 and ∼1620 cm^{-1}, respectively, consistent with the zwitterionic iminium−phenolato function. In ^1H NMR, the N^+−H and O−H signals occur near δ 12.0 and δ 2.3, respectively (both signals disappear upon shaking with D_2O). The σ-vinyl 10-H proton occurs near δ 6.3 as a singlet.

The structure of **3a** has been determined (Figure 2, Table 1). In the distorted octahedral coordination sphere, the nearly linear P−Ru−P axis lies approximately perpendicular to the plane (mean deviation of 0.02 Å) of the RuC_2ClO meridian. The hydroxymethyl group is tilted away from the meridian and lies closer to P2 than P1, their distances from the O3 atom being 5.176(16)

(1) Ghosh, K.; Pattanayak, S.; Chakravorty, A. *Organometallics* **1998**, *17*, 1956 and references therein.
(2) Bruce, M. I.; Catlaw, A.; Cifuentes, M. P.; Snow, M. R.; Tiekink, E. R. T. *J. Organomet. Chem.* **1990**, *397*, 187.
(3) Lutsenko, Z. L.; Aleksandrov, G. G.; Petrovskii, P. V.; Shubina, E. S.; Andrianov, V. G.; Struchkov, Yu. T.; Rubezhov, A. Z. *J. Organomet. Chem.* **1985**, *281*, 349.
(4) Garn, D.; Knoch, F.; Kish, H. *J. Organomet. Chem.* **1993**, *444*, 155.
(5) Barns, R. M.; Hubbard, J. L. *J. Am. Chem. Soc.* **1994**, *116*, 9514.
(6) Ferstl, W.; Sakodinskaya, I. K.; Beydoun-Sutter, N.; Borgne, G. L.; Pfeffer, M.; Ryabov, A. D. *Organometallics* **1997**, *16*, 411.
(7) Ghosh, P.; Bag, N.; Chakravorty, A. *Organometallics* **1996**, *15*, 3042. (b) Bag, N.; Choudhury, S. B.; Pramanik, A.; Lahiri, G. K.; Chakravorty, A. *Inorg. Chem.* **1990**, *29*, 5013. (c) Bag, N.; Choudhury, S. B.; Lahiri, G. K.; Chakravorty, A. *J. Chem. Soc., Chem. Commun.* **1990**, 1626.

10.1021/om000649c CCC: $20.00
Publication on Web 03/09/2001

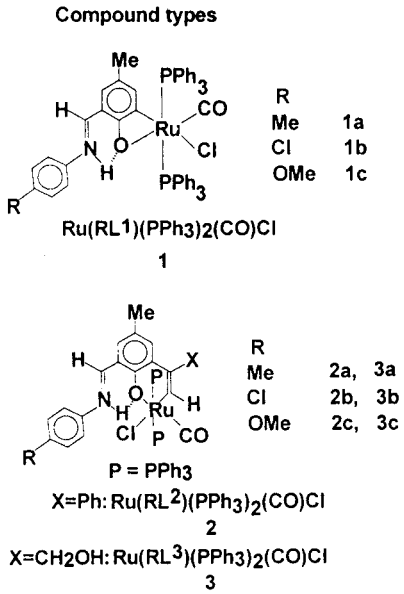

Figure 1. Substrates and alkyne-inserted organometallics of this work.

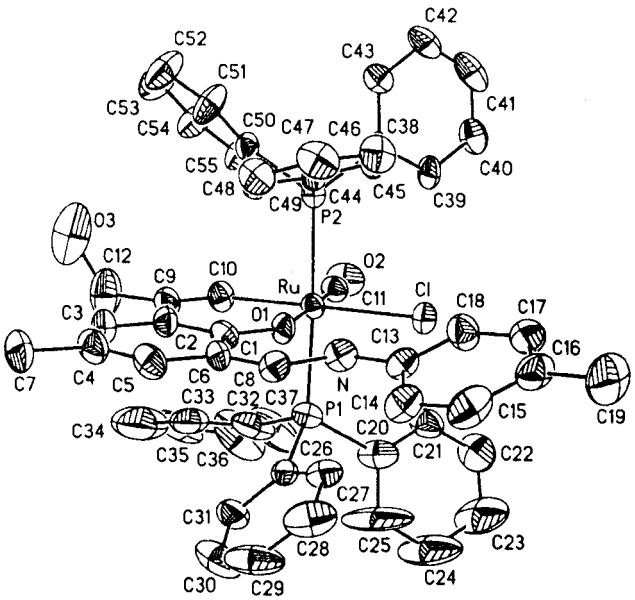

Figure 2. ORTEP plot (30% probability ellipsoids) and atom-labeling scheme for **3a**.

and 6.275(18) Å, respectively. The chelate ring is nearly planar (mean deviation of 0.02 Å), and indeed, the $RuRL^3$ fragment excluding MeC_6H_5, Me, and CH_2OH groups is approximately planar (mean deviation of 0.04 Å). The Ru−C10 (sp^2) bond is ∼0.2 Å longer than Ru−C11 (sp) bond. The Ru−Cl bond is longer than usual because of the trans influence of the *σ*-vinyl site as observed previously.[1]

Insertion Rates. These have been determined spectrophotometrically in CH_2Cl_2−MeOH mixtures over a range of temperature. The two reactions studied in detail are stated in eq 2. The spectra of the reacting

$$\mathbf{1a} + \text{xa} \rightarrow \mathbf{2a, 3a} \qquad (2)$$

solutions (Figure 3, case of ha) are characterized by multiple isosbestic points, strongly implicating[9] that **1a** and the expanded metallacycle are the only stable absorbing species. Studies in 2:1 CH_2Cl_2−MeOH mixtures in the presence of a large excess (>10-fold) of xa over **1a** have revealed the rate law of eq 3, the pseudo-

$$\text{rate} = k_{obs}[\mathbf{1a}] \qquad (3)$$

first-order rate constant k_{obs} being proportional to the concentration of xa. It was further observed *that the insertion process failed to proceed in pure* CH_2Cl_2. This prompted us to examine the rate as a function of methanol concentration at constant xa concentration. The rate was found to be proportional to the concentration of methanol. The consolidated concentration dependence of k_{obs} is stated in eq 4 where k'_{xa} is a constant, vide infra.

$$k_{obs} = k'_{xa}[\text{xa}][\text{MeOH}] \qquad (4)$$

Table 1. Selected Bond Lengths [Å] and Angles [deg] for $Ru(RL^3)(PPh_3)_2(CO)Cl$, 3A

Distances			
Ru−C(11)	1.820(13)	Ru−Cl	2.530(3)
Ru−C(10)	2.020(11)	O(1)−C(1)	1.284(13)
Ru−O(1)	2.100(7)	O(2)−C(11)	1.153(13)
Ru−P(1)	2.365(4)	N−C(8)	1.325(14)
Ru−P(2)	2.376(3)	C(9)−C(10)	1.363(16)
N···O(1)	2.608(12)		

Angles			
C(11)−Ru−C(10)	91.4(5)	P(1)−Ru−P(2)	177.26(12)
C(11)−Ru−O(1)	178.1(4)	C(11)−Ru−Cl	99.6(4)
C(10)−Ru−O(1)	86.9(4)	C(10)−Ru−Cl	168.8(4)
C(11)−Ru−P(1)	89.2(4)	O(1)−Ru−Cl	82.2(2)
C(10)−Ru−P(1)	89.4(3)	P(1)−Ru−Cl	93.08(12)
O(1)−Ru−P(1)	90.0(2)	P(2)−Ru−Cl	89.12(11)
C(11)−Ru−P(2)	92.0(4)	C(1)−O(1)−Ru	131.0(7)
C(10)−Ru−P(2)	88.1(3)	C(9)−C(10)−Ru	129.8(10)
O(1)−Ru−P(2)	88.7(2)	O(2)−C(11)−Ru	177.6(11)

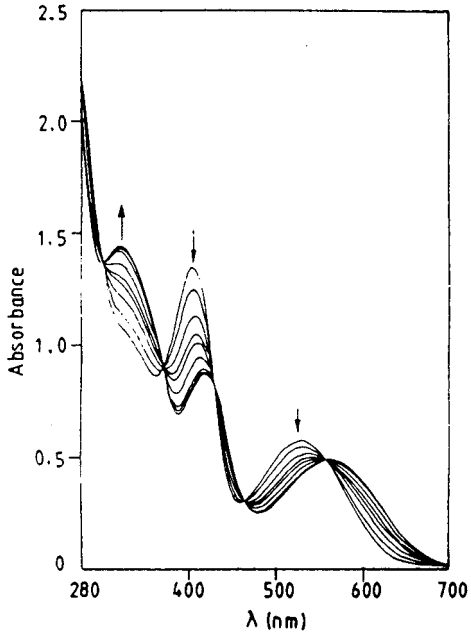

Figure 3. Spectral time evolution in the reaction of **1a** (1.27×10^{-4} M) with ha (9.97×10^{-3} M) in CH_2Cl_2−MeOH (8.14 M in MeOH) solution at 308 K.

(8) Chevalier, P.; Sandorfy, C. *Can. J. Chem.* **1960**, *38*, 2524. (b) Bohme, H.; Haake, M. In *Advances in Organic Chemistry*; Bohme, H., Vieche, H. G., Eds.; Interscience: New York, 1976; Part 1, Vol. 9, p 1. (c) Farvot, J.; Vocelle, D.; Sandorpy, C. *Photochem. Photobiol.* **1979**, *30*, 417. (d) Sandorfy, C.; Vocelle, D. *Mol. Phys. Chem. Biol.* **1989**, *4*, 195.

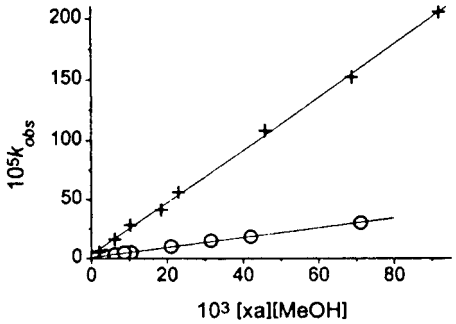

Figure 4. Plots of k_{obs} vs [xa][MeOH] at 313 K: (+) ha; (○) pa.

Table 2. Rate Data for Reaction of 1a and pa in CH_2Cl_2−MeOH Mixture

T, K	10^4[**1a**], M	10^3[pa], M	10^3[pa][MeOH], M^2	10^5k_{obs},[a] s^{-1}	$10^3k_{pa}K$, s^{-1} M^{-2}
308	1.11	1.32	10.74	3.3(1)	
		2.64	21.49	5.6(4)	2.6(4)
		3.96	32.23	7.4(2)	
		5.28	42.98	11.9(1)	
313	1.19	1.29	10.50	4.9(2)	
		2.58	21.00	9.9(1)	
		3.87	31.50	14.8(3)	
		5.16	42.00	18.2(3)	
	0.19	0.50	1.23	0.9(1)	4.2(1)
			3.70	1.9(3)	
			6.17	3.3(2)	
			8.64	4.8(4)	
	1.38	9.61	71.11	30.1(1)	
318	1.10	1.32	10.74	6.9(4)	
		2.64	21.49	14.7(1)	6.0(5)
		3.96	32.23	18.8(2)	
		5.28	42.98	27.0(1)	
323	1.27	1.29	10.50	9.6(1)	
		2.58	21.00	17.0(3)	7.1(1)
		3.87	31.50	24.0(1)	
		5.16	42.00	32.0(2)	

[a] Least-squares deviations are given in parentheses.

The plots of observed rate constants vs [xa][MeOH] encompassing large variations in the concentrations of xa and MeOH are excellently (correlation factor of 0.99) linear (Figure 4). Rate data are listed in Tables 2 (for pa) and 3 (for ha).

Methanol Adduct. The relation of eq 4 is consistent with the presence of a methanol adduct occurring in equilibrium, the equilibrium constant being *K*, eqs 5 and 6. The methanol adduct is taken as the reactive inter-

$$\mathbf{1a} + \mathrm{MeOH} \overset{K}{\rightleftharpoons} \mathbf{1a}\cdot\mathrm{MeOH} \tag{5}$$

$$K = \frac{[\mathbf{1a}\cdot\mathrm{MeOH}]}{[\mathbf{1a}][\mathrm{MeOH}]} \tag{6}$$

mediate as in eq 7, which is the rate-determining step

$$\mathbf{1a}\cdot\mathrm{MeOH} + \mathrm{xa} \xrightarrow[\text{rds}]{k_{xa}} \mathbf{2a},\mathbf{3a} + \mathrm{MeOH} \tag{7}$$

(rds). The corresponding rate law given in eq 8 is characterized by the rate constant k_{xa}. The relation of

$$\text{rate} = k_{xa}[\mathbf{1a}\cdot\mathrm{MeOH}][\mathrm{xa}] \tag{8}$$

(9) Wilkins, R. G. *Kinetics and Mechenism of Reactions of Transition Metal Complexes*, 2nd ed.; VCH: New York, 1991; p 156.

Table 3. Rate Data for Reaction of 1a and ha in CH_2Cl_2−MeOH Mixture

T, K	10^4[**1a**], M	10^3[ha], M	10^3[ha][MeOH], M^2	10^5k_{obs},[a] s^{-1}	$10^3k_{ha}K$, s^{-1} M^{-2}
298	1.79	2.82	22.95	23.0(4)	
		5.64	45.90	43.0(3)	7.2(4)
		8.46	68.86	56.0(2)	
		11.28	91.82	74.0(3)	
303	1.83	2.92	23.77	24.0(3)	
		5.84	47.54	52.0(2)	11.1(4)
		8.76	71.31	77.0(3)	
308	1.83	2.92	23.77	35.0(1)	
		5.84	47.54	67.0(3)	13.2(1)
		8.76	71.31	98.0(4)	
313	1.79	2.82	22.95	56.0(3)	
		5.64	45.90	108.0(4)	
		8.46	68.86	152.0(2)	
		11.28	91.82	205.0(4)	22.0(3)
	0.49	0.83	2.04	5.2(2)	
			6.14	16.0(3)	
			10.24	28.0(1)	
			18.43	41.0(3)	

[a] Least-squares deviations are given in parentheses.

eq 4 is readily derived by combining eqs 3, 6, and 8, the constant k'_{xa} of eq 4 being related to *K* and k_{xa} as in eq 9.

$$k'_{xa} = Kk_{xa} \tag{9}$$

The value of k'_{xa} increases with increasing temperature (Tables 2 and 3), and the Eyring equation is obeyed. The corresponding activation enthalpies ($\Delta H^{\#}$) are 12.9(1.0) and 12.5(1.0) kcal mol^{-1} and the activation entropies ($\Delta S^{\#}$) are −28.9(2.9) and −26.7(2.7) eu, respectively, for the pa and ha insertions. The rate-determining step is thus associative in nature. We have not succeeded, however, in determining k_{xa} and *K* separately, and both quantities are expected to be temperature-dependent. This has vitiated estimation of true activation parameters, which must relate only to k_{xa}. It is possible, however, to estimate genuine relative rate constants for the pa and ha reactions with a given type **1** substrate by virtue of eq 10, which follows from eq 9. Scrutiny of

$$\frac{k'_{ha}}{k'_{pa}} = \frac{k_{ha}}{k_{pa}} \tag{10}$$

Table 2 reveals that at a given temperature $k_{ha} \approx 5k_{pa}$. This is qualitatively reflected in the much higher slope of the ha line in Figure 4.

Reaction Model. Solutions of **1a** in CH_2Cl_2−MeOH are nonconducting, and the insertion rate is not affected by the presence of even large excess of (>10-fold) chloride (Et_4NCl/LiCl) and PPh_3 in the reaction medium. These observations militate against possible displacement of chloride and phosphine ligands by methanol. On the other hand, the Ru−O(phenolato) bond in type **1** species is relatively weak and is known to be readily displaced by Lewis bases.[10] It is proposed that methanol acts as a Lewis base, generating the reactive adduct stylized as **4**. Alkyne π-anchoring and activation is believed to occur via displacement of methanol as in **5**. Rapid 2 + 2 addition between C≡C and Ru−C (aryl) and reestablishment of the Ru−

(10) Ghosh, P.; Pramanik, A.; Chakravorty, A. *Organometallics* **1996**, *15*, 4147. (b) Ghosh, P.; Chakravorty, A. *Inorg. Chem.* **1997**, *36*, 64.

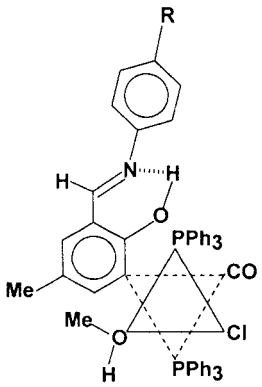

4

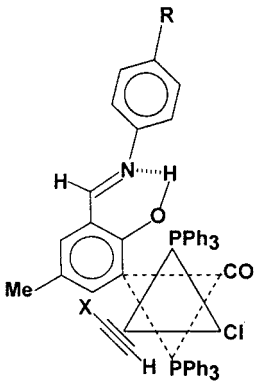

5

O(phenolato) bond complete the metallacycle expansion, affording **2** or **3**.

Space-filling models reveal that the 2 + 2 addition reaction is subject to steric crowding[1] from Cl and PPh_3 ligands, and this can explain the regiospecificity of the insertion reaction characterized by the addition of ≡CX and ≡CH fragments, respectively, to the carbon and metal ends of Ru−C bond.

To our knowledge, the only other reported kinetic study of alkyne insertion into Ru−C bond concerns certain orthoruthenated *N*,*N*-dimethylbenzylamine species[6] wherein, unlike in our system, the reaction involves displacement of chloride by methanol.

Effect of Substituents. The 2 + 2 addition process involves nucleophilic attack on the metal. Electron withdrawal from metal via the Schiff base ligand should therefore make insertion more facile. The k_{obs} (Table 4) values for all three type **1** species were determined for both pa and ha under invariant conditions of temperature (40 °C) and concentrations (alkyne and MeOH). The R substituents are found to affect k_{obs} significantly, and it increased with increasing electron withdrawal: OMe < Me < Cl. Indeed, the plots of log k_{obs} vs Hammett constants[11] of R are found to be linear for both pa and ha insertions.

Electron-rich alkynes would be expected to insert more quickly, as ha does compared to pa. The smaller steric bulk of CH_2OH compared to Ph is also an advantage of ha over pa. The net observed effect is that ha reacts 5 times faster than pa.

Concluding Remarks

The main finding of this work will now be summarized. The insertion of ha into **1** has afforded the expanded metallacycle **3** in nearly quantitative yields. Rate studies in the cases of pa and ha in CH_2Cl_2−MeOH mixtures have revealed that the reactive intermediate is the methanol adduct **1**·MeOH presumably belonging to structural type **4**. The latter anchors and activates the alkyne via displacement of MeOH as in **5**. Sterically controlled regiospecific 2 + 2 addition between C≡C and Ru−C (aryl) bonds follows, finally affording **2** and **3**.

Electronic and steric features make ha 5 times more reactive than pa. The R substituents affect the reactivity of **1**, the rate increasing with increasing electron withdrawal (OMe < Me < Cl).

Table 4. Observed Rate Constants for the Insertion of pa and ha into $Ru(RL^1)(PPh_3)_2(CO)Cl$ for Different R at 313 K in CH_2Cl_2−MeOH Mixture[a]

	pa insertion			ha insertion		
R	10^4[**1a**], M	10^4[pa], M	10^3k_{obs}, min^{-1}	10^4[**1a**], M	10^4[ha], M	10^3k_{obs}, min^{-1}
Me	0.15		4.1(1)	0.45		14.3(1)
Cl	0.15	4.68	8.6(1)	0.43	9.20	24.7(3)
OMe	0.17		3.8(1)	0.44		12.2(1)

[a] [MeOH] = 22.21 M.

Experimental Section

Materials. The compounds $Ru(PPh_3)_3Cl_2$[12] and $Ru(RL^1)(PPh_3)_2(CO)Cl$[7] were prepared as reported. Phenylacetylene and hydroxymethylacetylene (propargyl alcohol) were obtained from Aldrich. The purification of dichloromethane and methanol was done as described before.[13] All other chemicals and solvents were of analytical grade and were used as received.

Physical Measurements. Electronic and IR spectra were recorded with a Shimadzu UV-1601PC spectrophotometer (thermostated cell compartment) and Perkin-Elmer 783 IR spectrophotometer. ^{1}H NMR spectra were obtained using a Bruker 300 MHz FT NMR spectrophotometer (tetramethylsilane internal standard). Microanalyses (C, H, N) were done by using a Perkin-Elmer 240 C elemental analyzer. Solution electrical conductivity was measured by a Philips PR 9500 bridge using a platinized conductivity cell with a cell constant of 1.0.

Preparation of Complexes. $Ru(RL^3)(PPh_3)_2(CO)Cl$ complexes were synthesized in nearly quantitative (∼98%) yield by reacting $Ru(RL^1)(PPh_3)_2(CO)Cl$ in a CH_2Cl_2−MeOH mixture with excess ha. Details of a representative case are given below. The other compounds were prepared analogously.

$[Ru(MeL^3)(PPh_3)_2(CO)Cl]$ (3a). In a round-bottom flask $Ru(MeL^1)(PPh_3)_2(CO)Cl$ (50 mg, 0.054 mmol) was dissolved in a 2:1 (by volume) CH_2Cl_2−MeOH mixture and ha (30 mg, 0.536 mmol) was added to it. The mixture was stirred at 40 °C for 15 min on a magnetic stirrer. The color of the solution changed from violet to green. When the solution was concentrated and cooled, a green crystalline solid separated, which was collected, washed thoroughly with methanol, and dried in vacuo. Yield, 52 mg (98%); mp, 152 °C. Anal. Calcd for $RuC_{55}H_{48}NO_3P_2Cl$: C, 68.14; H, 4.99; N, 1.44. Found: C, 68.19; H, 4.91; N, 1.46. ^{1}H NMR ($CDCl_3$, δ): 6.44 (s, 1H arom), 6.34 (s, 1H, C=CH-(Ru)), 3.71−3.79 (m, 2H, $-CH_2-$), 2.29 (s, 1H, OH), 12.72 (m, 1H, $=N^+H$), 7.04−7.92 (m, 35 H, arom and $-HC=N^+$), 2.12 (s, 3H, $-CH_3$), 2.29 (s, 3H, $-CH_3$). IR (KBr, cm^{-1}): ν(C=N) 1620; ν(C≡O) 1900; ν(N−H, hexachlorobutadiene) 3440. UV−vis (CH_2Cl_2, λ_{max}, nm (ϵ, M^{-1} cm^{-1})): 575 (2600), 420 (5070), 320 (8050).

$[Ru(ClL^3)(PPh_3)_2(CO)Cl]$ (3b). Yield, 51 mg (96%); mp, 155 °C. Anal. Calcd for $RuC_{54}H_{45}NO_3P_2Cl_2$: C, 65.52; H, 4.58; N, 1.42. Found: C, 65.57; H, 4.53; N, 1.45. ^{1}H NMR ($CDCl_3$, δ): 6.43 (s, 1H arom), 6.33 (s, 1H, C=CH(Ru)), 3.71−3.79 (m, 2H, $-CH_2-$), 2.31 (s, 1H, OH), 12.66 (m, 1H, $=N^+H$), 7.11−7.96 (m, 35 H, arom and $-HC=N^+$), 2.11 (s, 3H, $-CH_3$). IR (KBr, cm^{-1}): ν(C=N) 1610; ν(C≡O) 1890; ν(N−H, hexachlorobutadiene) 3440. UV−vis (CH_2Cl_2, λ_{max}, nm (ϵ, M^{-1} cm^{-1})): 570 (4650), 420 (8850), 320 (14400).

$[Ru(MeOL^3)(PPh_3)_2(CO)Cl]$ (3c). Yield, 52 mg (98%); mp, 153 °C. Anal. Calcd for $RuC_{55}H_{48}NO_4P_2Cl$: C, 67.04; H, 4.91; N, 1.42. Found: C, 67.01; H, 4.88; N, 1.43. ^{1}H NMR ($CDCl_3$,

(11) Finar, I. L. *Organic Chemistry, Vol. 1: Fundamental Principles*, 6th ed.; ELBS, Longman Group: Essex, England, 1990; p 605.

(12) Stephenson, T. A.; Wilkinson, G. J. *Inorg. Nucl. Chem.* **1966**, *28*, 945.

(13) Vogel, A. I. *Practical Organic Chemistry*, 3rd ed.; ELBS and Longman Group: Harlow, England, 1965; pp 176, 169.

δ): 6.44 (s, 1H arom), 6.34 (s, 1H, C═CH(Ru)), 3.71−3.76 (m, 5H, $-CH_2-$ and −OMe), 2.31 (s, 1H, OH), 12.71 (m, 1H, $=N^+H$), 7.13−7.90 (m, 35H, arom and $-HC=N^+$), 2.12 (s, 3H, $-CH_3$). IR (KBr, cm^{-1}): ν(C═N) 1610; ν(C≡0) 1890; ν(N−H, hexachlorobutadiene) 3440. UV−vis (CH_2Cl_2, λ_{max}, nm(ϵ, M^{-1} cm^{-1})): 570 (2460), 420 (4510), 320 (9120).

Rate Measurements. Measurements were carried out in CH_2Cl_2−MeOH mixtures by observing the change in absorbances at 403 nm for pa and at 408 nm for ha. The k_{obs} values were calculated from a linear plot of $-\ln(A_t - A_\infty)$ vs t, where A_t and A_∞ are the absorbances at time t and at the end of reaction (48 h), respectively. The activation enthalpy ($\Delta H^\#$) and entropy ($\Delta S^\#$) were calculated from the variable-temperature rate constant, using the Eyring equation, eq 11 (k_B and h are the Boltzmann constant and Planck's constant, respectively).

$$k = \frac{k_B T}{h}\left[\exp\left(\frac{-\Delta H^\#}{RT}\right)\exp\left(\frac{\Delta S^\#}{R}\right)\right] \qquad (11)$$

The plots of $-\ln[k'_{xa}h/(k_B T)]$ vs $^1/_T$ were satisfactorily linear (correlation factor of 0.98). The curve fit and all other calculations were done with the Microcal Origin, version 4.0, software package.

X-ray Structure Determination. Single crystals of Ru(MeL^3)$(PPh_3)_2$(CO)Cl, **3a** ($0.25 \times 0.25 \times 0.40$ mm^3) were grown (at 298 K) by slow diffusion of hexane into dichloromethane solution followed by evaporation. The crystals were inherently poor in quality, giving rise to broadened diffraction peaks, and only moderately good refinement could be achieved. The thermal parameters are relatively high, especially for one phenyl ring on the P1 atom. Cell parameters were determined by a least-squares fit of 30 machine-centered reflections ($2\theta = 15-30°$). Data were collected with the ω-scan technique in the range $3° \le 2\theta \le 45°$ on a Siemens R3m/V four-circle diffractometer with graphite-monochromated Mo Kα radiation ($\lambda = 0.710\ 73$ Å). Two check reflections measured after every 198 reflections showed no significant intensity reduction in any case. All data were corrected for Lorentz polarization effects, and an empirical absorption correction[14] was done on the basis of an azimuthal scan of six reflections for the crystal.

The metal atom was located from Patterson maps, and the rest of the non-hydrogen atoms emerged from successive Fourier syntheses. The structures were refined by a full-matrix least-squares procedure on F^2. All non-hydrogen atoms were refined anisotropically. Hydrogen atoms were included at calculated positions. Calculations were performed using the SHELXTL, version 5.03,[15] program package. Significant crystal data are listed in Table 5.

Table 5. Crytal, Data Collection, and Refinement Parameters for Ru(RL^3)$(PPh_3)_2$(CO)Cl, 3a

mol formula	$C_{55}H_{48}ClNO_3P_2Ru$
mol wt	969.40
cryst syst	monoclinic
space group	$P2_1/c$
a, Å	14.655(8)
b, Å	15.091(6)
c, Å	21.949(14)
β, deg	92.93(5)
V, $Å^3$	4848(5)
Z	4
λ, Å	0.710 73
μ, cm^{-1}	4.88
D_{calcd}, g cm^{-3}	1.328
R^a, wR2^b [$I > 2\ \sigma(I)$]	7.95, 18.19

^{a} $R = \sum||F_o| - |F_c||/\sum|F_o|$. ^{b} wR2 $= [\sum w(F_o^2 - F_c^2)^2/\sum(F_o^2)^2]^{1/2}$.

Acknowledgment. We thank the Department of Science and Technology, Indian National Science Academy and the Council of Scientific and Industrial Research, New Delhi, for financial support. Affiliation with Jawaharlal Nehru Centre for Advanced Scientific Research, Bangalore, India, is acknowledged. We are thankful to Prof. P. Banerjee for helpful discussions.

Supporting Information Available: X-ray crystallography files, in CIF format, for the structure determination of **3a**. This material is available free of charge via the Internet at http://pubs.acs.org.

OM000649C

(14) North, A. C. T.; Phillips, D. C.; Mathews, F. A. *Acta Crystallogr., Sect. A* **1968**, *24*, 351.

(15) Sheldrick, G. M. *SHELXTL*, version 5.03; Bruker Analytical X-ray Systems: Madison, WI, 1994.

Journal of the Chemical Society, Dalton Transactions
Issue 8, 2001

A family of organoruthenium nitrites: alkyne insertion, linkage isomerization and ring nitration

Swarup Chattopadhyay,[a] Kaushik Ghosh,[a] Sujay Pattanayak[a] and Animesh Chakravorty*[a]

J. Chem. Soc., Dalton Trans., 2001, 1259-1265

Abstract

The reaction of [Ru(C_6H_2OH-2-CHNR-3-Me-5)(PPh_3)$_2$(CO)(NO_2)] **1** (R = Et, *p*-MeC_6H_4 or *p*-ClC_6H_4) with an excess of alkyne HC≡CX (X = H, Ph or CH_2OH) in CH_2Cl_2–MeOH medium was accompanied by linkage isomerization of nitrite (*O*,*O′*-bonded → *N*-bonded) and formation of a six-membered vinyl–phenolato chelate ring to give [Ru(η^2-C_6H_2CXCH-1-*O*-2-CHNHR-3-Me-5)(PPh_3)$_2$(CO)(NO_2)] **4**. The active substrate is the solvate **1**·MeOH, and the 2 + 2 addition of the bulky ≡CX (X = Ph or CH_2OH) group proceeds regiospecifically to the carbon end of the Ru–C bond. Compound **4** has also been obtained metathetically by treating **3** (the chloro analogue of**4**) with $NaNO_2$ in neutral media. However in acid media ring nitration of **3** (R = Et, X = Ph) occurs furnishing [Ru(η^2-C_6HCPhCH-1-*O*-2-CHNHEt-3-NO_2-4-Me-5)(PPh_3)$_2$(CO)Cl] **7** which can metathetically be converted into the corresponding *N*-bonded NO_2 analogue, **8**. The iminium proton is hydrogen bonded to the phenolato oxygen in **4**, **7** and **8** and also weakly to a nitro oxygen in **4** and **8** (IR and ^{1}H NMR data). All the species display a quasireversible cyclic voltammetric Ru^{III}–Ru^{II} couple, the $E_{1/2}$ of which shifts to higher potential by ≈200 mV upon replacing chloride by nitrite (**3** → **4**; **7** → **8**) as well as upon aromatic nitration (**3** → **7**). The crystal structures of the solvate **4b**·C_6H_6 in which R = *p*-MeC_6H_4 and X = H, **4h** in which R = *p*-ClC_6H_4 and X = CH_2OH and **7** have been determined. The *σ*-vinyl–phenolato chelate ring is approximately planar. The Ru–N bond in the planar $RuNO_2$ fragment of **4b**·C_6H_6 and **4h** is lengthened by ≈0.1 Å due to the *trans* influence of the vinyl group. The Ru–C(vinyl) bond in **7** is significantly shortened due to electron withdrawal by the nitro group, thus promoting Ru–ligand back bonding. The distances of the iminium nitrogen from phenolic oxygen and a nitrito oxygen (in **4b**·C_6H_6 and **4h**) lie in the ranges 2.55–2.67 and 2.90–2.98 Å respectively.

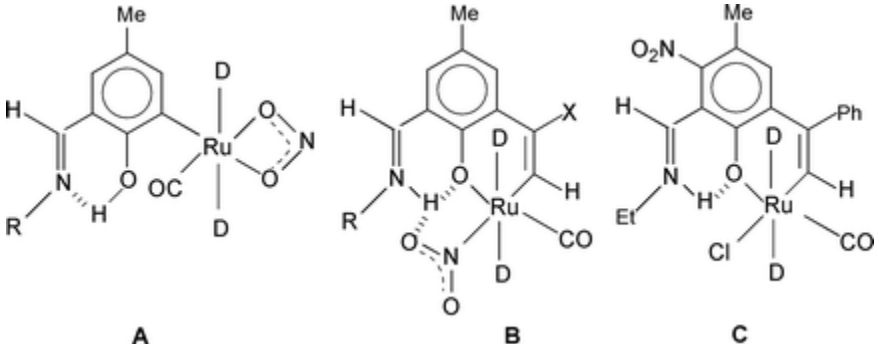

Indian Journal of Chemistry
Vol.40A, January 2001, pp.1-3

Rapid Communication

Nitrite linkage isomerization promoted by alkyne insertion in ruthenium organometallics

Swarup Chattopadhyay, Kaushik Ghosh,
Sujay Pattanayak & Animesh Chakravorty*

Department of Inorganic Chemistry, Indian Association for the Cultivation of Science, Calcutta 700 032, India

Received 5 December 2000

The title transformation is of type η^2-nitrite → η^1-nitrite and it occurs upon reacting carbonyl(η^2-nitrito)[4-methyl-6-(N-*p*-tolyl-imino)phenol] bis (triphenylphosphine) ruthenium(II) with acetylene in warm CH_2Cl_2-MeOH medium affording carbonyl (η^1-nitrito) [2 – vinyl –4 - methyl -6-(N-*p*-tolyl-imino) phenolato] bis(triphenylphosphine) ruthenium(II) in which the iminium function is involved in weak bifurcated hydrogen bonding with phenolato oxygen and a nitrite oxygen atom.

Linkage isomerization[1] of ambidentate ligands is of inherent interest in inorganic chemistry, the first reported example[2] being the nitrite ligand which is also the concern of the present work. Herein we

1 2 (1)

report the $\eta^2 \rightarrow \eta^1$ transformation of Eq (1) promoted by alkyne insertion at the metal site. The parent compound incorporating the η^2 motif **1** is **3** which was prepared[3] by reacting **4**(ref. 4) with NO_2^-.

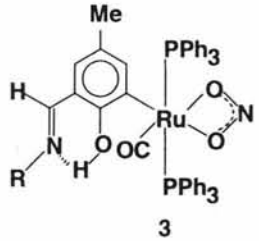

3

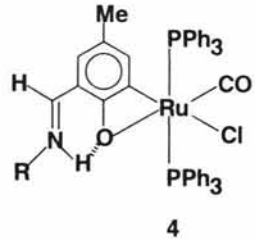

4

Instances of alkyne insertion into the Ru-C bond are relatively sparse[5-7]. Such insertion into the four-membered chelate ring of **4** is, however, facile[5]. This has prompted us to scrutinize the behaviour of alkynes towards **3** in which the Ru-C(aryl) bond is unsupported by chelation. Insertion is indeed found to occur, the process being attended with the reaction of Eq (1). The representative case of R = *p*-MeC_6H_4 is reported here, the alkyne being acetylene.

Experimental

IR (KBr disc) and ^{1}H NMR ($CDCl_3$ solvent, standard $SiMe_4$) spectra were recorded on Perkin-Elmer 783 spectrophotometer and Bruker 300 MHz FT NMR spectrometer respectively. The X-ray structure was determined using a Siemens R3m/V diffractometer (Mo-Kα radiation) and SHELXTL-Ver. 5.03 software[8]. Further details can be found elsewhere[9].

A warm solution of **3**(R=*p*-MeC_6H_4) (50 mg, 0.054 mmol) in 2:1 dichloromethane-methanol mixture (50 mL) was purged with acetylene gas and

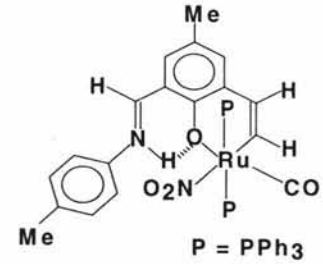

P = PPh3

5

then the solution was heated to reflux for 14 hr in an acetylene atmosphere with the help of a balloon filled with acetylene. The solution colour turned from yellow to violet. The solvent was then removed under reduced pressure and the desired compound, **5**, was isolated as a violet solid in 80% yield. Analytical data: Found (Calcd, %): C, 68.21 (68.27); H, 4.82 (4.88); N, 2.91 (2.95).

Table 1 — Selected bond distances (Å) and angles (°) for complex $5{\cdot}C_6H_6$

Distances		Angles	
Ru-P1	2.410(2)	N2-Ru-P1	92.01(11)
Ru-P2	2.383(2)	N2-Ru-C10	170.43(14)
Ru-C10	2.050(3)	P1-Ru-C11	89.5(2)
Ru-O1	2.106(3)	N2-Ru-O1	83.21(14)
Ru-C11	1.808(5)	P1-Ru-C10	88.81(11)
Ru-N2	2.217(4)	P1-Ru-P2	175.11(4)
O1-C1	1.302(5)	N2-Ru-C11	97.3(2)
O2-C11	1.157(5)	C10-Ru-C11	92.2(2)
N1-C8	1.304(6)	P1-Ru-O1	90.67(10)
C9-C10	1.334(1)	O1-Ru-C10	87.25(13)
O1···N1	2.668(10)	O1-Ru-C11	179.4(2)
N1···O3	2.981(6)	Ru-C11-O2	177.1(4)

Results and discussion

A warm solution of **3** (R = *p*-MeC_6H_4) in dichloromethane-methanol mixture was heated to reflux in an acetylene atmosphere. The colour of the solution changed from yellow to violet and upon removal of the solvent under reduced pressure **5** was isolated as a violet solid in excellent yield. The reaction is stated in Eq (2).

$$\mathbf{3}(R = p\text{-}MeC_6H_4) + H{-}C{\equiv}C{-}H \longrightarrow \mathbf{5} \qquad (2)$$

The X-ray structure (excluding solvent) of $5{\cdot}C_6H_6$ is shown in Fig. 1 and selected bond lengths and angles are listed in Table 1. In the structure the six-membered vinyl-phenolato chelate ring is only approximately planar (mean deviation 0.06 Å), there being a 9.2° fold along the C10···O1 line. The $RuNO_2$ fragment is nearly perfectly planar and the Ru-N length is ~0.1Å longer than usual (2.06-2.09 Å)[10] due to the *trans* influence of the σ-vinyl group. It is noteworthy that the reaction of Eq (2) is attended with a rotation of the Schiff base ligand such that the coordinated phenolato function and the CO ligand are placed *trans* to each other (in **3** the uncoordinated phenolic group and the CO ligand lie *cis* to each other[3]).

The N1···O1 length (2.668(10) Å) is consistent with the zwitterionic iminium-phenolato hydrogen bonding (in **3** the bonding is of imine-phenol type[3]). Significantly, the coordinated NO_2 group makes a dihedral angle of only 19.8° with the plane of the O1, C1, C6, C8 and N1 atoms and the N1···O3 length is 2.981(6) Å implicating that the iminium function is involved in weak bifurcated hydrogen bonding as depicted in **6**.

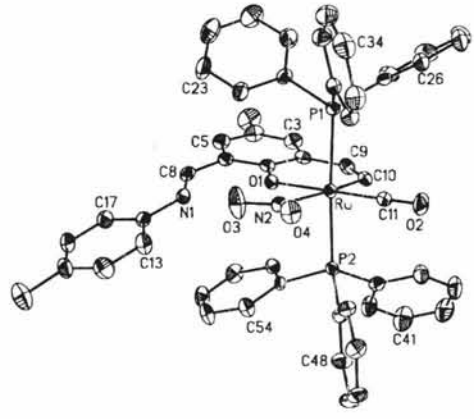

Fig. 1 — ORTEP plot (30% probability ellipsoids) and atom-labeling scheme for $5{\cdot}C_6H_6$ (excluding C_6H_6).

The iminium proton is observed in ^1H NMR as a doublet (δ 13.99, J_{HH} 15.0 Hz) due to coupling with the azomethine proton (δ 7.43, J_{HH} 15.0 Hz). Significantly, the iminium chemical shift in the chloride analogue[5] (NO_2^- replaced by Cl^-) of **5** is δ 12.87 (J_{HH} 21.0 Hz). The weak hydrogen bond

between coordinated NO_2^- and N^+-H, noted above, is believed to contribute to the 1 ppm downfield shift in **5**. In IR the N^+-H stretch occurs as a broad feature of medium intensity at 3440 cm^{-1} and $\nu_{C=N}$ is relatively high (1620 cm^{-1}) consistent with protonation of nitrogen[11].

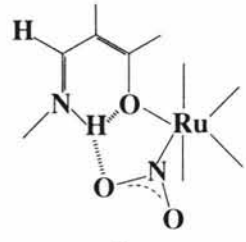

6

The four-membered aryl-phenolato Ru (C,O) chelate ring in **4** is highly strained (Ru-O, 2.235(4) Å) and once nitrite replaces chloride the four-membered nitrite Ru (O,O) chelate ring (as in **3**) is preferred. Alkyne insertion, however, makes six-membered vinyl-phenolato Ru (C,O) chelation feasible (as in **5**; Ru-O, 2.106(3) Å) and this provides the thermodynamic driving force for the observed nitrite isomerization from the bidentate chelation mode to the monodentate mode. It is likely that the initial π-anchoring of the alkyne to the metal occurs *via*

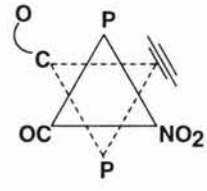

P = PPh_3

7

cleavage of a Ru-O bond generating monodentate nitrite presumably N-bonded as stylized in **7**. The **7**→**5** transformation can then proceed *via* 2+2 addition. Further work is in progress.

Acknowledgement

We are grateful to the Department of Science and Technology, New Delhi, India, the Indian National Science Academy, New Delhi, India and the Council of Scientific and Industrial Research, New Delhi, India for financial support. Affiliation with the Jawaharlal Nehru Centre for Advanced Scientific Research, Bangalore, India is acknowledged.

References

1 Huheey J E, Keiter E A & Keiter R L, *Inorganic chemistry : Principles of structure and reactivity*, 4th edn (Harper Collins College Publishers, New York), 1993, p. 513-521; Shriver D F & Atkins P W, *Inorganic chemistry*, 3rd edn (Oxford University Press, Oxford),1999, p. 221.

2 Jorgensen S M, *Z anorg Chem*, 5 (1894) 169.

3 Ghosh P & Chakravorty A, *Inorg Chem*, 36 (1997) 64.

4 Ghosh P, Bag N & Chakravorty A, *Organometallics*, 15 (1996) 3042.

5 Ghosh K, Pattanayak S & Chakravorty A, *Organometallics*, 17 (1998) 1956 and refs therein.

6 Ferstl W, Sakodinskaya I K, Beydoun-Sutter N, Borgne G L, Pfeffer M & Ryabov A D, *Organometallics*, 16 (1997) 411.

7 Burns R M & Hubbard J L, *J Am chem Soc*, 116 (1994) 9514.

8 Sheldrick G M, SHELXTL Version 5.03, *Structure determination software programs* (Siemens Analytical X-ray Instruments Inc., Madison, WI), 1994.

9 Ghosh K, *Ph.D. Thesis*, Jadavpur University, Calcutta, India, April 2000.

10 Szczepura L F, Kubow S A, Leising R A, Perez W J, Huynh M H V, Lake C H, Churchill D G, Churchill M R & Takeuchi K J, *J chem Soc, Dalton Trans*, (1996) 1463.

11 Sandorfy C & Vocelle D, *Mol Phys, Chem Biol*, 4 (1989) 195.

A New Family of Acylrhodium Organometallics

Sujay Pattanayak, Swarup Chattopadhyay, Kaushik Ghosh, Sanjib Ganguly, Prasanta Ghosh, and Animesh Chakravorty*

Department of Inorganic Chemistry, Indian Association for the Cultivation of Science, Calcutta 700 032, India

Received September 3, 1998

The Schiff mono bases of 2,6-diformyl-4-methylphenol, **1**, react with $RhCl_3 \cdot 3H_2O$ and PPh_3 in ethanol, affording dichloro[4-methyl-6-((arylimino)methyl)phenolato-C^1,O]bis(triphenylphosphine)rhodium(III), $Rh(XL_{sb})(PPh_3)_2Cl_2$ (**5**; X = H, Me, OMe, Cl). Organometallics of the type (carboxylato)[4-methyl-6-formylphenolato-C^1,O]bis(triphenylphosphine)rhodium(III), $Rh(L_{al})(PPh_3)_2(RCO_2)$ (**6**; R = H, Me, Et, Ph), have been synthesized by oxidative addition of **1** to $RhCl(PPh_3)_3$ in the presence of dilute RCO_2H in ethanol. Replacement of RCO_2H by dilute HNO_3 has afforded the nitrate analogue $Rh(L_{al})(PPh_3)_2(NO_3)$ (**7**). Species of type **5** are susceptible to aldiminium → aldehyde hydrolysis in a dichloromethane−acetone−water mixture with concomitant chloride dissociation, furnishing $Rh(L_{al})(PPh_3)_2Cl$ (**8a**), from which the N-bonded nitrite $Rh(L_{al})(PPh_3)_2(NO_2)$ (**8b**) has been generated metathetically. The four types of species **5**−**8** are interconvertible, and a possible reaction pathway involving pentacoordinate intermediates is proposed. The X-ray structures of $Rh(MeL_{sb})(PPh_3)_2Cl_2$ (**5b**; bis(dichloromethane) adduct), $Rh(L_{al})(PPh_3)_2(MeCO_2)$ (**6b**), $Rh(L_{al})(PPh_3)_2(NO_3)$ (**7**), and $Rh(L_{al})(PPh_3)_2(NO_2)$ (**8b**) have been determined. Among these, **5b**, **6b**, and **7** are pseudooctahedral—the bonds *trans* to the acyl function being longer by 0.2−0.4 Å compared to those *trans* to phenolato oxygen. Complex **8b** is square pyramidal, there being no ligand *trans* to the acyl function. In **5b** iminium−phenolato (N···O, 2.66(1) Å) and in the remaining species aldehyde−phenolato (C···O, 2.86(1) Å) hydrogen bonding is present. Internal charge balance is crucial for the stability of the present organometallics.

Introduction

The reaction of $Ru(PPh_3)_3Cl_2$ with the Schiff mono base of 2,6-diformyl-4-methylphenol, **1**, has been shown to afford organometallics of type **2**.[1,2] The unusual four-membered metallacycle has been proposed to arise from reductive (Ru(IV) → Ru(II)) decarbonylation of an elusive acyl intermediate incorporating the ring **3** formed *via* oxidative (Ru(II) → Ru(IV)) aldehyde addition. The richness of the chemistry[1−5] of **2** has prompted us to search for organorhodium species based on **1**, with special reference to the status of the acylrhodium moiety **4**.

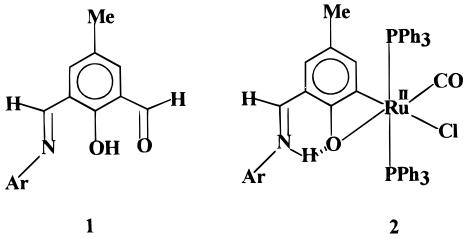

1 **2**

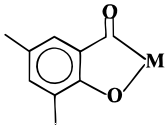

3 M = Ru^{IV}

4 M = Rh^{III}

In the present work we have scrutinized the reaction of **1** with $RhCl(PPh_3)_3$. Aldehydes are usually decarbonylated[6−9] by $RhCl(PPh_3)_3$ (eq 1), a reaction that finds use

(1) (a) Bag, N.; Choudhury, S. B.; Pramanik, A.; Lahiri, G. K.; Chakravorty, A. *Inorg. Chem.* **1990**, *29*, 5013. (b) Bag, N.; Choudhury, S. B.; Lahiri, G. K.; Chakravorty, A. *J. Chem. Soc., Chem. Commun.* **1990**, 1626.

(2) Ghosh, P.; Bag, N.; Chakravorty, A. *Organometallics* **1996**, *15*, 3042.

(3) Ghosh, P.; Pramanik, A.; Chakravorty, A. *Organometallics* **1996**, *15*, 4147.

(4) Ghosh, P.; Chakravorty, A. *Inorg. Chem.* **1997**, *36*, 64.

(5) Ghosh, K.; Pattanayak, S.; Chakravorty, A. *Organometallics* **1998**, *17*, 1956.

(6) Hughes, R. P. In *Comprehensive Organometallic Chemistry*; Wilkinson, G., Stone, F. G. A., Abel, F. W., Eds.; Pergamon Press: Oxford, U.K., 1982; Vol. 5, pp 277−540.

(7) Doughty, D. H.; Pignolet, L. H. In *Homogeneous Catalysis with Metal Phosphine Complexes*; Pignolet, L. H., Ed.; Plenum: New York, 1983.

(8) O'Connor, J. M.; Ma, J. *Inorg. Chem.* **1993**, *32*, 1866.

(9) (a) Baird, M. C.; Mague, J. T.; Osborn, J. A.; Wilkinson, G. *J. Chem. Soc. A* **1967**, 1347. (b) O'Connor, J. M.; Ma, J. *J. Org. Chem.* **1992**, *57*, 5075. (c) Baird, M. C.; Nyman, C. J.; Wilkinson, G. *J. Chem. Soc. A* **1968**, 348. (d) Stille, J. K.; Regan, M. T. *J. Am. Chem. Soc.* **1974**, *96*, 1508. (e) Stille, J. K.; Huang, F.; Regan, M. T. *J. Am. Chem. Soc.* **1974**, *96*, 1518. (f) Egglestone, D.; Baird, M. C. *J. Organomet. Chem.* **1976**, *113*, C25. (g) Lau, K. S. Y.; Becker, Y.; Huang, F.; Baenziger, N.; Stille, J. K. *J. Am. Chem. Soc.* **1977**, *99*, 5664. (h) Bennett, M. A.; Charles, R.; Mitchell, T. R. B.; Jeffrey, J. C. In *Fundamental Research in Homogeneous Catalysis;* Ishii, Y., Tsutsui, M., Eds.; Plenum Press: New York, 1978; Vol. 2, pp 93−100. (i) Jardine, F. H. In *Progress in Inorganic Chemistry*; Lippard, S. J., Ed.; Wiley-Interscience: New York, 1981. (j) Jardine, F. H.; Wilkinson, G. *J. Chem. Soc. C* **1967**, 270.

10.1021/om980748e CCC: $18.00
Publication on Web 03/20/1999

in organic synthesis (Q = alkyl, aryl).[10,11] Acyl inter-

$$QCHO + Rh^{I}Cl(PPh_3)_3 \rightarrow QH + \textit{trans}\text{-}Rh(CO)Cl(PPh_3)_2 \quad (1)$$

mediates formed *via* oxidative (Rh(I) → Rh(III)) addition are implicated, but these are generally very unstable with respect to reductive (Rh(III) → Rh(I)) decarbonylation. Instances of isolation and characterization of such intermediates are therefore rare.[12,13]

If decarbonylation would prevail in our reaction also, the only products would be a salicylaldimine and *trans*-$Rh(CO)Cl(PPh_3)_2$. No rhodium(I) analogue of **2** is anticipated, since the low-spin d^8 metal is already coordinatively saturated in *trans*-$Rh(CO)Cl(PPh_3)_2$. In practice, the reaction of **1** with $RhCl(PPh_3)_3$ proceeded smoothly in acidic media *without* decarbonylation, affording stable acylrhodium species incorporating motif **4**. The structure and properties of the new family of organometallics generated *via* this route are reported in this present work.

Results and Discussion

A. Synthesis. a. The Family. The title family consists of three pseudooctahedral and one distorted square pyramidal acylrhodium system. These are abbreviated as $Rh(XL_{sb})(PPh_3)_2Cl_2$ (**5**), $Rh(L_{al})(PPh_3)_2(RCO_2)$ (**6**), $Rh(L_{al})(PPh_3)_2(NO_3)$, (**7**), and $Rh(L_{al})(PPh_3)_2(Y)$ (**8**).

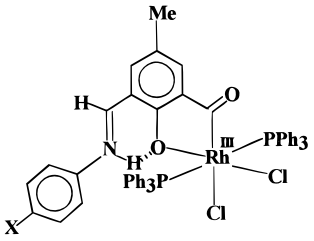

$Rh(XL_{sb})(PPh_3)_2Cl_2$

	X
5a	H
5b	Me
5c	OMe
5d	Cl

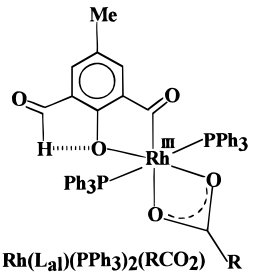

$Rh(L_{al})(PPh_3)_2(RCO_2)$

	R
6a	H
6b	Me
6c	Et
6d	Ph

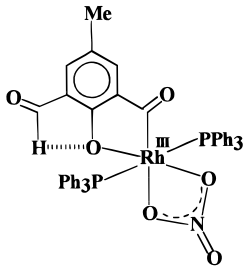

$Rh(L_{al})(PPh_3)_2(NO_3)$

7

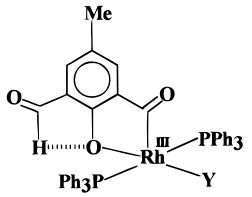

$Rh(L_{al})(PPh_3)_2(Y)$

	Y
8a	Cl
8b	NO_2

b. $Rh(XL_{sb})(PPh_3)_2Cl_2$, 5. The type **5** organometallics are afforded in excellent yields upon reacting the Schiff mono base **1** with $RhCl(PPh_3)_3$ in boiling ethanol in the presence of dilute hydrochloric acid. The reaction is shown in eq 2. The synthesis can be conveniently

$$RhCl(PPh_3)_3 + \mathbf{1} + HCl \rightarrow \mathbf{5} + PPh_3 + H_2 \quad (2)$$

carried out as a single-pot process involving **1**, $RhCl_3 \cdot 3H_2O$, and PPh_3, the last two generating $RhCl(PPh_3)_3$ and HCl *in situ*.[14,15]

In the absence of HCl the reaction of $RhCl(PPh_3)_3$ and **1** affords only *trans*-$Rh(CO)Cl(PPh_3)_2$, presumably formed *via* reductive decarbonylation of a hydridoacyl intermediate incorporating motif **9**. The acid (here HCl) is

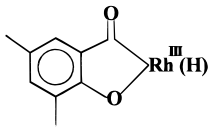

9

believed to facilitate rapid proton-assisted displacement of hydride from **9** by chloride. The acid also sustains the cationic aldiminium moiety, which helps to stabilize the system (*vide infra*). Upon using 2,6-diformyl-4-methylphenol in place of **1** in eq 2, rapid decarbonylation occurs and only *trans*-$Rh(CO)Cl(PPh_3)_2$ is isolated.

c. $Rh(L_{al})(PPh_3)_2(RCO_2)$ (6) and $Rh(L_{al})(PPh_3)_2(NO_3)$ (7). The reaction (eq 3) of $RhCl(PPh_3)_3$ with **1** in the presence of dilute carboxylic acids proceeds in a manner similar to that of eq 2 but with concomitant hydrolysis of the aldimine function affording **6** in excellent yields. Upon replacing RCO_2H by HNO_3, the

$$Rh^{I}Cl(PPh_3)_3 + \mathbf{1} + RCO_2H + H_2O \rightarrow \mathbf{6} + PPh_3 + XC_6H_4NH_2 \cdot HCl + H_2 \quad (3)$$

nitrate **7** is obtained. We have been able to isolate **6** and **7** only *via* this substitution-cum-hydrolysis route.

Use of 2,6-diformyl-4-methylphenol in place of the Schiff base **1** in eq 3 leads to decarbonylation, affording *trans*-$Rh(CO)Cl(PPh_3)_2$. This prompts us to propose that in the present synthesis the cation $[Rh(XL_{sb})(PPh_3)_2(RCO_2)]^+$ incorporating the aldiminium function is first formed in the same manner as **5** is formed in eq 2. It is, however, subject to facile nucleophilic water attack

(10) Song, L.; Arif, A. M.; Stang, P. J. *Organometallics* **1990**, *9*, 2792.
(11) Murakami, M.; Amii, H.; Shigeto, K.; Ito, Y. *J. Am. Chem. Soc.* **1996**, *118*, 8285.
(12) Suggs, J. W. *J. Am. Chem. Soc.* **1978**, *100*, 640.
(13) Acylrhodium species have, however, been isolated by using specialized multidentate ligands[13a] and *via* other synthetic routes such as carbon monoxide insertion[13b] into the Rh−C bond and addition of acid chlorides, acid anhydrides, and aldehydes to rhodium(I):[13c−j] (a) Bianchini, C.; Meli, A.; Peruzzini, M.; Vizza, F.; Bachechi, F. *Organometallics* **1991**, *10*, 820. (b) García, M. P.; Jiménez, M. V.; Cuesta, A.; Siurana, C.; Oro, L. A.; Lahoz, F. J.; Lopez, J. A. Catalán, M. P.; Tiripicchio, A.; Lanfranchi, M. *Organometallics* **1997**, *16*, 1026. (c) McGuiggan, M. F.; Doughty, D. H.; Pignolet, L. H. *J. Organomet. Chem.* **1980**, *185*, 241. (d) Bennett, M. A.; Jeffrey, J. C.; Robertson, G. B. *Inorg. Chem.* **1981**, *20*, 323. (e) Suggs, J. W.; Wovkulich, M. J.; Cox, S. D. *Organometallics* **1985**, *4*, 1101. (f) Suggs, J. W.; Wovkulich, M. J.; Williard, P. G.; Lee, K. S. *J. Organomet. Chem.* **1986,** *307*, 71. (g) Miller, J. A.; Nelson, J. A. *Organometallics* **1991**, *10*, 2958. (h) Moloy, K. G.; Wegman, R. W. *Organometallics* **1989**, *8*, 2883. (i) Egglestone, D. L.; Baird, M. C.; Lock, C. J. L.; Turner, G. *J. Chem. Soc., Dalton Trans.* **1977**, 1576. (j) Slack, D. A.; Egglestone, D. L.; Baird, M. C. *J. Organomet. Chem.* **1978**, *146*, 71.
(14) Cotton, S. A. In *Chemistry of Precious Metals;* Blackie Academic and Professional: London, 1997; pp 88−132.
(15) (a) Chatt, J.; Shaw, B. L. *J. Chem. Soc. A* **1966**, 1437. (b) Osborn, J. A.; Jardine, F. H.; Young, J. F.; Wilkinson, G. *J. Chem. Soc. A* **1966**, 1711. (c) Brown, J. M.; Lucy, A. R. *J. Chem. Soc., Chem. Commun.* **1984**, 914. (d) Duckett, S. B.; Newell, C. L.; Eisenberg, R. *J. Am. Chem. Soc.* **1994**, *116*, 10548.

furnishing electroneutral **6** *via* rapid aldiminium → aldehyde hydrolysis.

d. Rh(L_{al})(PPh_3)$_2$(Y) (8). Aldimine → aldehyde hydrolysis occurs in the case of **5** also upon boiling its solution in a dichloromethane−acetone mixture with water. The process is associated with concomitant dissociation of a chloride ligand, affording electroneutral **8a** (eq 4). In **5** the Rh−Cl bond *trans* to the acyl function

$$\mathbf{5} + H_2O \rightarrow \mathbf{8a} + XC_6H_4NH_2\cdot HCl \qquad (4)$$

is reletively weak (*vide infra*), and it is this bond that undergoes ionic dissociation. The synthesis of **8b** involves metathesis between **8a** with $NaNO_2$ (eq 5).

$$\mathbf{8a} + NaNO_2 \rightarrow \mathbf{8b} + NaCl \qquad (5)$$

e. Stability. The Rh−C(acyl) bond in the present complexes is stabilized by chelate formation involving phenolato oxygen. All members in the family **5**−**8** are indefinitely stable in the solid state and in dry halocarbon (CH_2Cl_2, $CHCl_3$) solutions. The type **5** complexes are sparingly soluble in ethanol, and dissolution in boiling ethanol is associated with reductive decarbonylation to *trans*-Rh(CO)Cl(PPh_3)$_2$. In the synthesis of **5** it is therefore necessary to optimize the reaction time so that *trans*-Rh(CO)Cl(PPh_3)$_2$ remains only a minor byproduct. In contrast to **5**, **6**−**8** have good solubility in ethanol and the solutions are thermally stable.

Internal charge balance is a crucial stabilizing factor in this family of organometallics. In this context we note the intimate relationship between the charge of the anion(s) bonded to the metal and the state of the remote side chain on the phenolato−acyl ligand. Thus, when two chloride ligands are present, electroneutrality is achieved in the form of **5**, where the side chain is in the aldiminium form. In **8** only one chloride ligand is present and the side chain becomes aldehydic (**6** and **7** are similar). We have not succeeded in isolating cationic species such as [Rh(XL_{sb})(PPh_3)$_2$(RCO_2)]$^+$, which was implicated as a hydrolytically unstable intermediate in the synthesis of **6**; neither have we been able to prepare an anionic system such as [Rh(L_{al})(PPh_3)$_2$$Cl_2$]$^-$.

The aldehyde function in **6**−**8** is a potential site of further oxidative addition to RhCl(PPh_3)$_3$. In practice, however, no reaction occurs even on prolonged boiling in ethanol. The formyl function in **6**−**8** is deactivated by the existing acyl moiety and the bulk of the neighboring Rh(PPh_3)$_2$ fragment.

B. Spectra. The colors of type **5** (orange-yellow) and type **6**−**8** (yellow) are due to MLCT($t_2 \rightarrow \pi^*$) absorption occurring near 500 and 425 nm, respectively. The acyl C═O stretch[13b,16] is observed as a strong band near 1700 cm^{-1}. Two well-separated Rh−Cl stretch (near 320 and 350 cm^{-1}) occur in **5**, consistent with the *cis*-$RhCl_2$ configuration having two Rh−Cl bonds of unequal lengths. Significantly, the single Rh−Cl stretch in **8a** is at 350 cm^{-1}. The two carboxyl vibrations[3,13e,17] in **6**, the three nitrate vibrations[4,18] in **7**. and the three nitrite vibrations[18e,19] in **8b** are consistent with the designated bonding modes.

Table 1. Ring Current Shifts (ppm)[a] of ^{1}H NMR Signals of 5b, 6b, 7, and 8b[b]

compd	3-H	5-H	4-Me	9-H	10-Me
5b	1.00 (0.90)	*c*	0.24 (0.30)		
6b	1.33 (0.90)	0.50 (0.20)	0.50 (0.20)	0.60 (0.70)	0.94 (1.35)
7	1.20 (1.40)	0.58 (0.53)	0.43 (0.45)	0.71 (0.68	
8b	0.91 (0.90)	0.29 (0.36)	0.44 (0.34)	0.83 (0.50)	

[a] Calculated shifts are in parentheses. [b] The atom-numbering scheme is the same as in X-ray structures (see Figures 1−4). [c] Not individually resolved; lies within a complex multiplet of aromatic protons (7−8 ppm).

A characteristic feature of the ^{1}H NMR spectra of the present organometallics is the significant upfield shift of several proton signals of chelated XL_{sb} and L_{al} ligands relative to **1** and 2,6-diformyl-4-methylphenol. The X-ray structural results (*vide infra*) revealed that ring currents due to phosphine phenyl rings can be the primary origin of such shifts. Using structural parameters and isoshielding $\rho-z$ plots[20] the expected shifts due to ring current have been estimated in the case of **5b**, **6b**, **7**, and **8b**. These are listed in Table 1 along with the corresponding observed shifts. The agreement is generally satisfactory. The most shifted protons are 3-H (all cases), 9-H (**6b**, **7**, **8b**), and 10-Me[21] (**6b**).

C. Structure. a. Geometrical Features. The X-ray structures of **5b** (bis(dichloromethane) adduct), **6b**, **7**, and **8b** have been determined. Molecular views are shown in Figures 1−4, and selected bond parameters are listed in Tables 2−4. To our knowledge, instances where acyl complexes have been isolated by the reaction of RhCl(PPh_3)$_3$ with aldehydes followed by X-ray structural characterization are rare, probably unknown. The present structures are of particular significance in this context. The structures of a few rhodium acyl complexes formed *via* other routes have been documented.[13a−f]

In **5b**, **6b**, and **7** the coordination spheres are severely distorted from idealized octahedral geometry. In **5b** the Rh(MeL_{sb})Cl_2 fragment defines a crystallographic plane of symmetry (x, $^1/_4$, z). The Rh(L_{al}) fragments in **6b** and **7** constitute good planes (plane A, mean deviation ≤0.05 Å), and the carboxylate (**6b**) and nitrate (**7**) chelate rings are nearly perfectly planar (plane B, mean deviation ≤0.01 Å). The dihedral angle between A and B is 11.7° in **6b** and 4.0° in **7**. Thus, the bulk of the equatorial region increases in the order **5b** < **7** < **6b**, and this is attended by a corresponding increase in the P−Rh−P angle in the same order.

(16) Coutinho, K. J.; Dickson, R. S.; Fallon, G. D.; Jackson, W. R.; Simone, T. D.; Skelton, B. W.; White, A. H. *J. Chem. Soc., Dalton Trans.* **1997**, 3193.
(17) Kavanagh, B.; Steed, J. W.; Tocher, D. A. *J. Chem. Soc., Dalton Trans.* **1993**, 327.
(18) (a) Betts, C. E.; Haszeldine, R. N.; Parish, R. V. (Dick). *J. Chem. Soc., Dalton Trans.* **1975**, 2218. (b) Steed, J. W.; Tocher, D. A. *Polyhedron* **1994**, *13*, 167. (c) Critchlow, P. B.; Robinson, S. D. *Inorg. Chem.* **1978**, *17*, 1896. (d) Critchlow, P. B.; Robinson, S. D. *Inorg. Chem.* **1978**, *17*, 1902. (e) Nakamoto, K. *Infrared and Raman Spectra of Inorganic and Coordination Compounds*, 4th ed.; Wiley: New York, 1986. (f) Heaton, B. T.; Lggo, J. A.; Jacob, C.; Blanchard, H.; Hursthouse, M. B.; Ghatak, I.; Harman, M. E.; Somerville, R. G.; Heggie, W.; Page, P. R.; Villax, I. *J. Chem. Soc., Dalton Trans.* **1992**, 2533. (g) Hursthouse, M. B.; Malik, K. M. A.; Michael, D.; Mingos, P.; Willoughby, S. D. *J. Organomet. Chem.* **1980**, *192*, 235.
(19) (a) Muccigrosso, D. A.; Mares, F.; Diamond, S. E.; Solar, J. P. *Inorg. Chem.* **1983**, *22*, 960. (b) Johnson, S. A.; Basolo, F. *Inorg. Chem.* **1962**, *1*, 925. (c) Hitchman, M. A.; Rowbottom, G. L. *Coord. Chem. Rev.* **1982**, *42*, 55.
(20) Johnson, C. E., Jr.; Bovey, F. A. *J. Chem. Phys.* **1958**, *29*, 1012.
(21) The chemical shift of the acetate methyl signal in the absence of such shielding is 1.7 ppm: Jia, G.; Rheingold, A. L.; Haggerty, B. S.; Meek, D. W. *Inorg. Chem.* **1992**, *31*, 900.

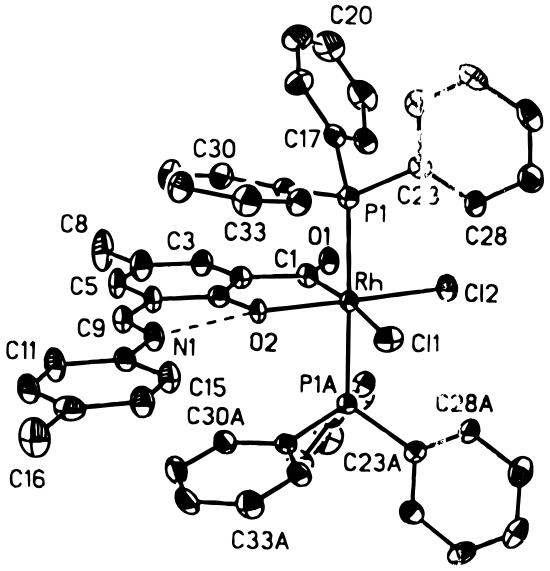

Figure 1. ORTEP plot (30% probability ellipsoids) and atom-labeling scheme for **5b**·$2CH_2Cl_2$.

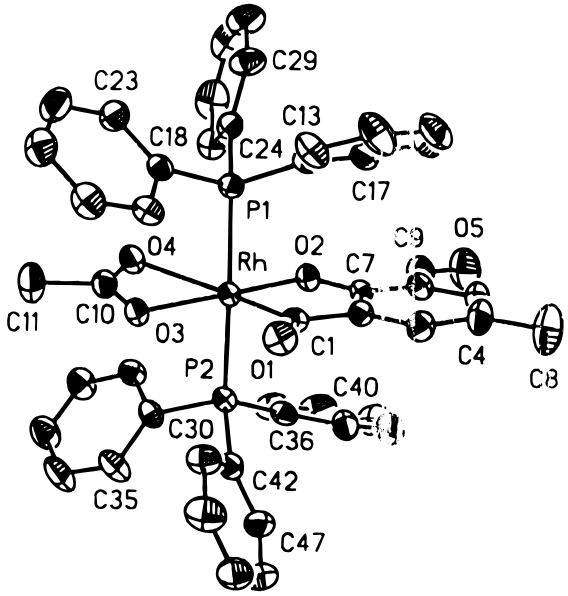

Figure 2. ORTEP plot (30% probability ellipsoids) and atom-labeling scheme for **6b**.

In **8b** the coordination sphere has distorted-square-pyramidal geometry. The donor atoms P1, P2, O2, and N1 constitute an excellent equatorial plane (mean deviation 0.02 Å), from which the metal atom is shifted by 0.15 Å toward the acyl carbon atom. The $Rh(NO_2)$ plane (mean deviation 0.02 Å) makes a dihedral angle of 86.1° with the equatorial plane and 12.8° with the $Rh(L_{al})$ plane (mean deviation 0.06 Å).

b. Bond Lengths. The observed Rh−C(acyl), C═O(acyl), and Rh−P lengths fall within reported ranges—1.94−1.99 Å,[13a−d] 1.18−1.22 Å,[13a−d] and 2.30−2.40 Å,[22] respectively. The Rh−N distance in **8b** (1.997(5) Å) is shorter than that in $Rh(NO_2)_6^{3-}$ (2.06 Å).[23]

(22) (a) Cotton, F. A.; Kang, S. J. *Inorg. Chem.* **1993**, *32*, 2336. (b) Hataya, K. O. K.; Yamamoto, T. *Inorg. Chem.* **1993**, *32*, 2360. (c) Harlow, R. L.; Thorn, D. L.; Baker, T.; Jones, N. L. *Inorg. Chem.* **1992**, *31*, 993.

(23) Gronilov, S. A.; Alekseev, V. I.; Baudina, I. A.; Kharanenko, S. P. *Russ. J. Inorg. Chem. (Engl. Transl.)* **1992**, *37*, 306.

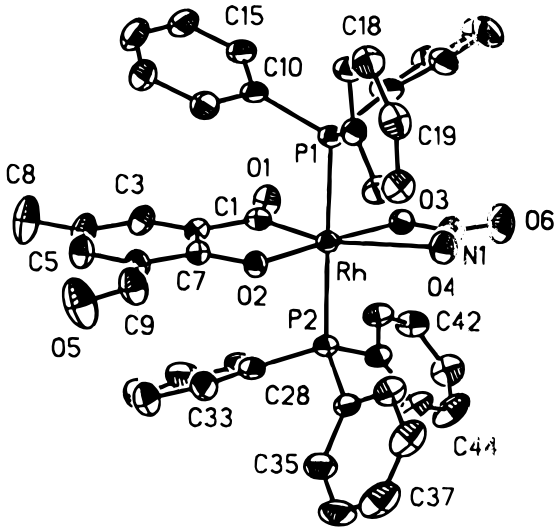

Figure 3. ORTEP plot (30% probability ellipsoids) and atom-labeling scheme for **7**.

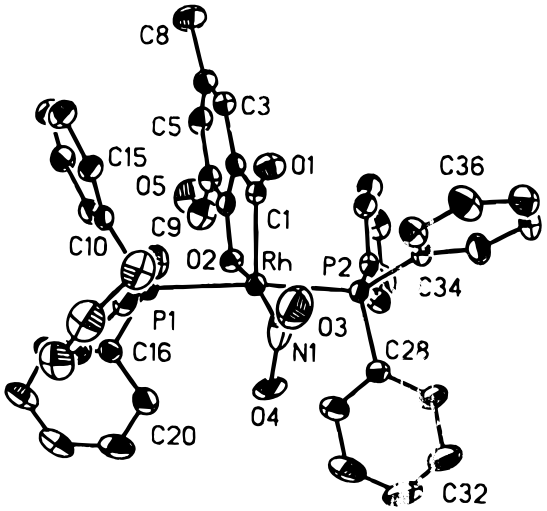

Figure 4. ORTEP plot (30% probability ellipsoids) and atom-labeling scheme for **8b**.

Table 2. Selected Bond Distances (Å) and Angles (deg) and Their Estimated Standard Deviations for 5b·$2CH_2Cl_2$

	Distances		
Rh−C1	1.983(9)	Rh−Cl2	2.365(3)
Rh−O2	2.070(6)	Rh−Pl	2.367(2)
Rh−Cl1	2.552(3)	Rh−PlA	2.367(2)
Cl−O1	1.203(11)	N1···O2	2.663(1)
	Angles		
C1−Rh−O2	83.8(3)	O2−Rh−Cl1	86.8(2)
Cl1−Rh−Cl2	96.2(1)	Cl2−Rh−Cl	93.2(3)
Pl−Rh−P1A	173.4(1)	Cl−Rh−Cl1	170.6(3)
O2−Rh−Cl2	177.0(2)	P1−Rh−Cl	92.6(1)
P1−Rh−O2	88.2(1)	P1−Rh−Cl1	87.1(1)
P1−Rh−Cl2	91.9(1)		

The structures provide an unique opportunity for observing the strong *trans* influence of the acyl function. The two Rh−Cl distances in **5b**, Rh−O(acetate) distances in **6b**, and Rh−O(nitrate) distances in **7** differ by ∼0.2, ∼0.3, and ∼0.4 Å, respectively. In each case the longer and shorter bonds lie respectively *trans* to the acyl and phenolato functions.

The C−O(acetate), N−O(nitrate), and N−O(nitrite) distances in **6b**, **7**, and **8b** are consistent with the

Table 3. Selected Bond Distances (Å) and Angles (deg) and Their Estimated Standard Deviations for 6b and 7

	6b	7		6b	7
			Distances		
Rh−C1	1.955(5)	1.965(7)	C10−O3	1.261(6)	
Rh−O2	2.045(3)	2.038(4)	C10−O4	1.237(7)	
Rh−O3	2.089(4)	2.077(4)	N1−O3		1.278(8)
Rh−O4	2.402(4)	2.495(6)	N1−O4		1.246(7)
Rh−P1	2.368(2)	2.359(2)	N1−O6		1.206(8)
Rh−P2	2.368(2)	2.370(2)	C9···O2	2.861(1)	2.860(1)
C1−O1	1.226(6)	1.194(7)			
			Angles		
C1−Rh−O2	82.7(2)	83.9(2)	P1−Rh−O2	91.0(1)	88.4(1)
O2−Rh−O4	115.2(1)	120.2(2)	P1−Rh−O4	83.0(1)	84.4(1)
O4−Rh−O3	57.3(1)	55.0(2)	P1−Rh−O3	91.6(1)	91.1(1)
O3−Rh−Cl	105.3(2)	100.9(2)	P2−Rh−Cl	91.2(1)	91.4(1)
P1−Rh−P2	178.2(1)	176.4(1)	P2−Rh−O2	90.8(1)	89.8(1)
Cl−Rh−O4	160.4(2)	155.3(2)	P2−Rh−O4	96.2(1)	93.7(1)
O2−Rh−O3	171.6(1)	175.2(2)	P2−Rh−O3	86.6(1)	90.4(1)
P1−Rh−C1	89.1(1)	91.6(1)			

Table 4. Selected Bond Distances (Å) and Angles (deg) and Their Estimated Standard Deviations for 8b

		Distances	
Rh−C1	1.975(5)	Rh−O2	2.059(3)
Rh−N1	1.997(5)	Rh−P1	2.369(2)
Rh−P2	2.376(2)	N1−O3	1.094(8)
N1−O4	1.334(7)	C1−O1	1.205(6)
		O9···O2	2.860(1)
		Angles	
C1−Rh−O2	83.3(2)	C1−Rh−N1	106.5(2)
C1−Rh−P1	90.1(1)	C1−Rh−P2	95.7(1)
O2−Rh−N1	170.1(2)	P1−Rh−P2	173.8(1)

approximate valence-bond structures **10**, **11**, and **12**, respectively. The length of the shorter N−O bond (1.094(3) Å) in **8b** approaches that of nitric oxide and the complex is thus a potentially good candidate for oxo-transfer activity.[19a,24]

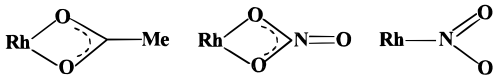

10 **11** **12**

c. Aldiminium−Phenolato and Aldehyde−Phenolato Moieties. The nonhydrogen atoms of the aldiminium−phenolato moiety **13** present in **5b** define a virtually perfect plane. The observed N1···O2 length,

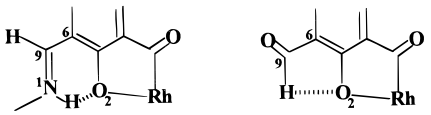

13 **14**

2.663(11) Å, is the same as that, 2.665(12) Å, in the ruthenium complex **2** (Ar = *p*-tolyl), where the iminium hydrogen was directly located.[2] The iminium N−H stretch in **5** occurs near 3400 cm^{-1},[25] and in ^1H NMR the iminium proton resonates near 14 ppm, giving rise to a relatively broad signal which disappears upon shaking with D_2O. Further, the presence of the aldiminium function in **5** is consistent with relatively high

Scheme 1

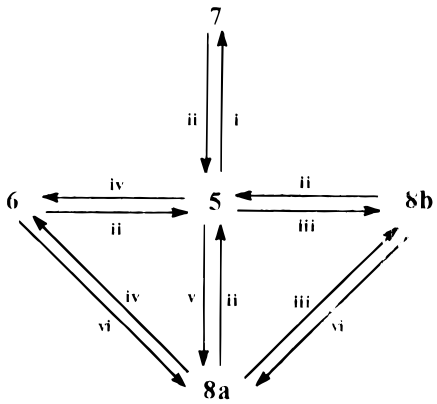

Reagents:

i = $NaNO_3$, ii = $MeArNH_2$.HCl, iii = $NaNO_2$
iv = $NaMeCO_2$, v = H_2O, vi = HCl

Reaction media:

CH_2Cl_2-Me_2CO-H_2O: i, iii, iv, v
EtOH-H_2O: ii, vi

C=N stretching frequency[25,26] (∼1635 cm^{-1}) and a high-field shift[27] of the C−H proton signal (∼7.3 ppm; 8.7 ppm in **1**).

The nearly perfectly planar aldehyde−phenolato moiety **14** is present in **6b**, **7**, and **8b**. All hydrogen atoms were resolved in difference Fourier maps in the case of **8b**. The C9···O2 distance is 2.86(1) Å in all the species. The rotameric conformations of **13** and **14** around the C6−C9 axis differ by 180°, consistent with the presence of hydrogen bonding.

d. Interconversion. (i) Species 5−8. The four groups of organometallics reported in this work are readily interconvertible upon treatment with appropriate reagents. Some of the interconversions centered around **5** are shown in Scheme 1. Thus, when **5** is reacted with excess carboxylates or free carboxylic acids, **6** is obtained in excellent yields and the reverse reaction occurs on treating **6** with $XC_6H_4NH_2$·HCl (excess) and HCl (eq 6).

$$\mathbf{5} + RCO_2H + H_2O \underset{EtOH}{\overset{CH_2Cl_2-Me_2CO-H_2O}{\rightleftharpoons}} \mathbf{6} + XC_6H_4NH_2\cdot HCl + HCl \quad (6)$$

In the conversion of **5** to the other species the reaction medium always contains water. In view of the facile nature of the reaction **5** → **8a**, it is plausible that the conversions of **5** to the other species proceed through pentacoordinated **8a**. For example, the reaction **5** → **6** can proceed *via* occupation of the vacant site by a carboxyl oxygen followed by displacement of chloride ligand and completion of chelate ligation (Scheme 2).

(ii) Comparison with Ruthenium. The pair **5** and **6** provides a contrast to the ruthenium pair **2** and **15**,

(24) Sieker, F.; Blake, A. J.; Johnson, B. F. G. *J. Chem. Soc., Dalton Trans.* **1996**, 1419.

(25) (a) Sandorfy, C.; Vocelle, D. *Mol. Phys. Chem. Biol.* **1989**, *IV*, 195. (b) Chevalier, P.; Sandorfy, C. *Can. J. Chem.* **1960**, *38*, 2524. (c) Favrot, J.; Vocelle, D.; Sandorfy, C. *Photochem. Photobiol.* **1979**, *30*, 417.

(26) Bohme, H.; Haake, M. In *Advances in Organic Chemistry*; Bohme, H., Viehe, H. G., Eds.; Interscience: New York, 1976; Part 1, Vol. 9, p 1.

(27) Sharma, G. M.; Roels, O. A. *J. Org. Chem.* **1973**, *38*, 3648.

Scheme 2

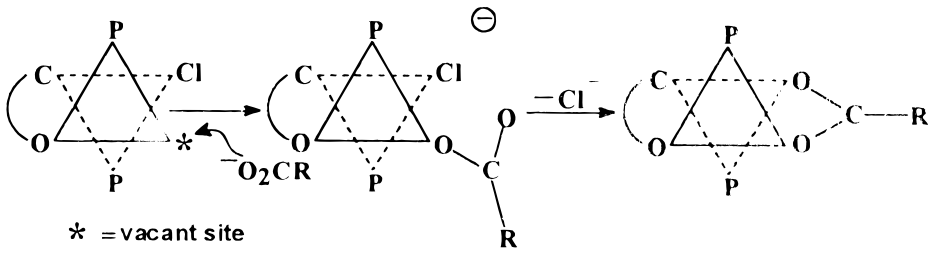

which are also interconvertible. In the **5**, **6** pair substi-

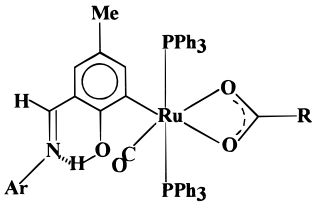

15

tution of chloride by carboxylate occurs in the ratio 2:1, but in the **2**, **15** pair this ratio is 1:1. Electroneutrality thus remains unaffected by the substitution in the latter case and there is no aldiminium hydrolysis in the conversion **2** → **15**, unlike in **5** → **6**. Chelation by RCO_2^- is accommodated in **15** by sacrificing the Ru−O(phenolato) bond present in **2**. The process is attended with aldiminium−phenolato → aldimine−phenol tautomerization and a rotameric transformation around the Ru−C(aryl) axis.[3]

The case of nitrites provides another notable rhodium−ruthenium contrast, highlighting the qualitative effect of the acyl trans influence on the binding of ligands. In the case of rhodium a pentacoordinated structure, **8b**, with a strong Rh−NO_2 bond is preferred to a hexacoordinated situation involving O,O-chelation weakened by acyl *trans* influence. For ruthenium this effect is absent and nitrite is chelating (as in **15** with RCO_2^- replaced by NO_2^-).

Concluding Remarks

Organometallics of type **5**−**7** incorporating acyl−phenolate chelation have been synthesized *via* oxidative addition of the Schiff mono base **1** to $RhCl(PPh_3)_3$ in acidic media. These are rare instances where the aldehyde−$RhCl(PPh_3)_3$ reaction gets arrested prior to reductive decarbonylation. In **5**−**7** the metal is hexacoordinated, the bond trans to the acyl function being strongly elongated (by 0.2−0.4 Å). This bond is prone to ionization, thus providing access to square-pyramidal species of type **8**. The intermediacy of pentacoordination forms a plausible basis for the observed interconversion among species of types **5**−**8**.

Internal charge balance is a crucial stabilizing factor, and there is an intimate relationship between the charge of the anion(s) bonded to the metal and the state of the remote side chain of the phenolato−acyl ligand. Thus, in **5** the side chain is aldiminium in nature and in **6**−**8** it is aldehydic. The rotameric conformations of the two functions get spontaneously adjusted to promote NH···O or CH···O hydrogen bonding.

The **5**, **6** pair provides a contrast with the ruthenium pair **2**, **15**, where chelation by RCO_2^- is accommodated by sacrificing the Ru−O(phenolato) bond. The strong *trans* influence of the acyl function promotes monodentate Rh−NO_2 bonding in **8b**, while in the nitrite analogue of **15**, NO_2^- is O,O-chelating. In view of the large asymmetry of N−O bond lengths, we are scrutinizing the possible oxo transfer behavior of **8b**.

Experimental Section

Materials. $RhCl(PPh_3)_3$ was prepared by a reported method.[28] The purification of dichloromethane was done as described before.[29] All the other chemicals and solvents were of analytical grade and were used as received. The Schiff bases **1** were prepared by reacting 2,6-diformyl-4-methylphenol with the amine $XC_6H_4NH_2$ in a 1:1 (in hot ethanol) ratio.

Physical Measurements. Electronic and IR spectra were recorded with Hitachi 330 and Perkin-Elmer 783 IR spectrophotometers. For ^1H NMR spectra a Bruker 300 MHz FT NMR spectrophotometer was used (tetramethylsilane is the internal standard). Microanalyses (C, H, N) were done by using a Perkin-Elmer 240C elemental analyzer.

Preparation of Complexes. The $Rh(XL_{sb})(PPh_3)_2Cl_2$ (**5**), $Rh(L_{al})(PPh_3)_2(RCO_2)$ (**6**), $Rh(L_{al})(PPh_3)_2(NO_3)$ (**7**), $Rh(L_{al})(PPh_3)_2$-Cl (**8a**), and $Rh(L_{al})(PPh_3)_2(NO_2)$ (**8b**) complexes were synthesized by using the same general procedures. Details are given for representative cases.

$Rh(HL_{sb})(PPh_3)_2Cl_2$ (5a). a. From $RhCl(PPh_3)_3$. To a solution of 2-formyl-4-methyl-6-((phenylimino)methyl)phenol (**1**; X = H) (13 mg, 0.05 mmol) in hot ethanol (25 mL) was added $RhCl(PPh_3)_3$ (50 mg, 0.05 mmol) and 2 N HCl (5 mL). The mixture was heated to reflux for 0.5 h. Upon cooling, a bright orange-yellow crystalline solid separated, which was collected by filtration, washed thoroughly with cold ethanol, and dried *in vacuo*. The crude product was purified by washing with benzene (30 mL), which removes the small amount of $Rh(CO)Cl(PPh_3)_2$ formed as a byproduct. Yield: 45 mg (89%). Anal. Calcd for $RhC_{51}H_{42}NO_2P_2Cl_2$: C, 65.38; H, 4.48; N, 1.49. Found: C, 65.30; H, 4.46; N, 1.50. ^1H NMR ($CDCl_3$; δ): 6.81 (s, 1H, arom), 7.13−7.86 (m, 32H arom), 7.35 (d, 2H, arom, J_{HH} = 8.7 Hz), 7.40 (d, 2H, arom, J_{HH} = 8.8 Hz), 2.16 (s, 3H, CH_3), 7.30 (s, 1H, −CH=N^+), 14.00 (s, 1H, =N^+H). IR (KBr; cm^{-1}): ν(C=N) 1630; ν(C=O(acyl)) 1680; ν(Rh−Cl) 320, 350; ν(N−H, hexachlorobutadiene) 3420. UV−vis (CH_2Cl_2; λ_{max}, nm (ϵ, M^{-1} cm^{-1})): 500 (11 600), 310 (23 300).

b. From $RhCl_3 \cdot 3H_2O$. To a solution of 2-formyl-4-methyl-6-((phenylimino)methyl)phenol (45 mg, 0.18 mmol) in hot ethanol (25 mL) was added an ethanolic solution (25 mL) of $RhCl_3 \cdot 3H_2O$ (50 mg, 0.18 mmol) and PPh_3 (100 mg, 0.38 mmol). The mixture was heated to reflux for 0.5 h. Upon cooling, a

(28) Osborn, J. A.; Wilkinson, G. *Inorg. Synth.* **1967**, *10*, 67.
(29) (a) Vogel, A. I. *Practical Organic Chemistry*, 3rd ed.; ELBS and Longman Group: Harlow, U.K., 1965; Chapter 2, pp 176−177. (b) Sawyer, D. T.; Roberts, J. L., Jr. *Experimental Electrochemistry for Chemists*; Wiley: New York, 1974; p 212.

bright orange-yellow crystalline solid separated, which was collected by filtration, washed with cold ethanol, and dried *in vacuo*. This crude product was purified by washing with benzene (30 mL). Yield: 155 mg (88%).

Rh(MeL$_{sb}$) (PPh$_3$)$_2$Cl$_2$ (5b). Yield: 89%. Anal. Calcd for $RhC_{52}H_{44}NO_2P_2Cl_2$: C, 65.68; H, 4.63; N, 1.47. Found: C, 65.62; H, 4.61; N, 1.48. ^{1}H NMR ($CDCl_3$; δ): 6.80 (s, 1H, arom), 7.14−7.86 (m, 31H, arom), 7.33 (d, 2H, arom, J_{HH} = 9.0 Hz), 7.38 (d, 2H, arom, J_{HH} = 8.9 Hz), 2.17 and 2.46 (2s, 6H, 2CH_3), 7.28 (s, 1H, −CH=N$^+$), 13.98 (s, 1H, =N$^+$H). IR (KBr; cm^{-1}): ν(C=N) 1645; ν(C=O(acyl)) 1690; ν(Rh−Cl) 320, 355; ν(N−H, hexachlorobutadiene) 3440. UV−vis (CH_2Cl_2; λ_{max}, nm (ϵ, M^{-1} cm^{-1})): 500 (11 300), 310 (22 600).

Rh(MeOL$_{sb}$) (PPh$_3$)$_2$Cl$_2$ (5c). Yield: 90%. Anal. Calcd for $RhC_{52}H_{44}NO_3P_2Cl_2$: C, 64.59; H, 4.55; N, 1.44. Found: C, 64.61; H, 4.57; N, 1.42. ^{1}H NMR ($CDCl_3$; δ): 6.75 (s, 1H, arom), 7.11−7.81 (m, 31H, arom), 6.93 (d, 2H, arom, J_{HH} = 8.7 Hz), 7.15 (d, 2H, arom, J_{HH} = 7.3 Hz), 2.13 (s, 3H, CH_3), 3.84 (s, 3H, OCH_3), 7.28 (s, 1H, −CH=N$^+$), 14.02 (s, 1H, =N$^+$H). IR (KBr; cm^{-1}): ν(C=N) 1635; ν(C=O(acyl)) 1680; ν(Rh−Cl) 315, 350; ν(N−H, hexachlorobutadiene) 3440. UV−vis (CH_2Cl_2; λ_{max}, nm (ϵ, M^{-1} cm^{-1})): 505 (10 800), 315 (21 900).

Rh(ClL$_{sb}$) (PPh$_3$)$_2$Cl$_2$ (5d). Yield: 91%. Anal. Calcd for $RhC_{51}H_{41}NO_2P_2Cl_3$: C, 63.06; H, 4.22; N, 1.44. Found: C, 63.10; H, 4.24; N, 1.45. ^{1}H NMR ($CDCl_3$; δ): 6.82 (s, 1H, arom), 7.13−7.83 (m, 31H, arom), 7.19 (d, 2H, arom, J_{HH} = 7.2 Hz), 7.42 (d, 2H, arom, J_{HH} = 8.7 Hz), 2.17 (s, 3H, CH_3), 7.34 (s, 1H, −CH=N$^+$), 14.01 (s, 1H, =N$^+$H). IR (KBr; cm^{-1}): ν(C=N) 1630; ν(C=O(acyl)) 1685; ν(Rh−Cl) 310, 350; ν(N−H, hexachlorobutadiene) 3440. UV−vis (CH_2Cl_2; λ_{max}, nm (ϵ, M^{-1} cm^{-1})): 510 (11 600), 320 (22 400).

Rh(LaI)(PPh$_3$)$_2$(HCO$_2$) (6a). To a solution of 2-formyl-4-methyl-6-((*p*-tolylimino)methyl)phenol (20 mg, 0.07 mmol) in hot ethanol (25 mL) was added $RhCl(PPh_3)_3$ (50 mg, 0.05 mmol) and 0.3 N HCOOH (10 mL). The mixture was heated to reflux for 1.5 h, affording a yellow solution. The solvent was removed under reduced pressure, leaving a yellow residue. This was isolated by filtration and washed with water and dried *in vacuo*. Yield: 41 mg (92%). Anal. Calcd for $RhC_{46}H_{37}O_5P_2$: C, 66.18; H, 4.43. Found: C, 66.02; H, 4.32. ^{1}H NMR ($CDCl_3$; δ): 6.876 (d, 1H, arom, J_{HH} = 1.7 Hz), 7.01 (d, 1H, arom, J_{HH} = 1.9 Hz), 7.34−7.61 (m, 31H, arom and HCO_2), 1.93 (s, 3H, CH_3), 9.50 (s, 1H, −CHO). IR (KBr; cm^{-1}): ν(C=O(acyl, formyl)) 1670; ν(OCO) 1455 (sym), 1545 (asym). UV−vis (CH_2Cl_2; λ_{max}, nm (ϵ, M^{-1} cm^{-1})): 435 (6450).

Rh(L$_{al}$)(PPh$_3$)$_2$(MeCO$_2$) (6b). Yield: 93%. Anal. Calcd for $RhC_{47}H_{39}O_5P_2$: C, 66.50; H, 4.59. Found: C, 66.40; H, 4.61. ^{1}H NMR ($CDCl_3$; δ): 6.52 (d, 1H, arom, J_{HH} = 1.8 Hz), 7.01 (d, 1H, arom, J_{HH} = 2.0 Hz), 7.31−7.56 (m, 30H, arom), 1.91 and 0.76 (2s, 6H, 2CH_3), 9.89(s, 1H, −CHO). IR (KBr; cm^{-1}): ν(C=O(acyl, formyl)) 1670; ν(OCO) 1450 (sym), 1550 (asym). UV−vis (CH_2Cl_2; λ_{max}, nm (ϵ, M^{-1} cm^{-1})): 430 (6830).

Rh(L$_{al}$)(PPh$_3$)$_2$(EtCO$_2$) (6c). Yield: 94%. Anal. Calcd for $RhC_{48}H_{41}O_5P_2$: C, 66.82; H, 4.75. Found: C, 66.92; H, 4.82. ^{1}H NMR ($CDCl_3$; δ): 6.48 (d, 1H, arom, J_{HH} = 1.8 Hz), 6.98 (d, 1H, arom, J_{HH} = 2.1 Hz), 7.32−7.55 (m, 30H, arom), 0.96 (q, 2H, Et), 0.17 (t, 3H, Et), 1.90 (s, 3H, CH_3), 9.88 (s, 1H, −CH=O). IR (KBr; cm^{-1}): ν(C=O(acyl, formyl)) 1665; ν(OCO) 1450 (sym), 1550 (asym). UV−vis (CH_2Cl_2; λ_{max}, nm (ϵ, M^{-1} cm^{-1})): 430 (6520).

Rh(L$_{al}$)(PPh$_3$)$_2$(PhCO$_2$) (6d). Yield: 94%. Anal. Calcd for $RhC_{52}H_{41}O_5P_2$: C, 68.57; H, 4.50. Found: C, 68.63; H, 4.61. ^{1}H NMR ($CDCl_3$; δ): 6.52 (d, 1H, arom, J_{HH} = 1.8 Hz), 7.02 (d, 1H, arom, J_{HH} = 2.0 Hz), 7.11−7.58 (m, 31H, arom), 6.66 (d, 2H, arom, J_{HH} = 7.8 Hz), 6.93 (t, 2H, arom, J_{HH} = 6.7 Hz), 1.91 (s, 3H, CH_3), 9.96 (s, 1H, −CH=O). IR (KBr; cm^{-1}): ν(C=O(acyl, formyl)) 1670; ν(OCO) 1457 (sym), 1555 (asym). UV−vis (CH_2Cl_2;, λ_{max}, nm (ϵ, M^{-1} cm^{-1})): 430 (7200).

Rh(L$_{al}$)(PPh$_3$)$_2$(NO$_3$) (7). To a solution of 2-formyl-4-methyl-6-((*p*-tolylimino)methyl)phenol (20 mg, 0.07 mmol) in hot ethanol (25 mL) was added $RhCl(PPh_3)_3$ (50 mg, 0.05 mmol) and 0.4 N HNO_3 (10 mL). The mixture was heated to reflux for 1 h, affording a yellow solution. The solvent was removed under reduced pressure, leaving a yellow residue. This was isolated by filtration, washed with water, and dried *in vacuo*. Yield: 42 mg (92%). Anal. Calcd for $RhC_{45}H_{36}NO_6P_2$: C, 63.45; H, 4.23. Found: C, 63.48; H, 4.19; N, 1.62. ^{1}H NMR ($CDCl_3$; δ): 6.65 (d, 1H, arom, J_{HH} = 3 Hz), 6.93 (d, 1H, arom, J_{HH} = 3 Hz), 7.33−7.51 (m, 30H, arom), 1.97 (s, 3H, CH_3), 9.84 (s, 1H, −CHO). IR (KBr; cm^{-1}): ν(C=O(acyl)) 1705; ν(C=O(formyl)) 1670; ν(N=O) 1500; ν(NO_2) 1000 (sym), 1200 (asym). UV−vis (CH_2Cl_2; λ_{max}, nm (ϵ, M^{-1} cm^{-1})): 420 (4250).

Rh(L$_{al}$)(PPh$_3$)$_2$Cl (8a). To a solution of Rh(MeL$_{sb}$)(PPh$_3$)$_2$-Cl_2 (50 mg, 0.05 mmol) in dichloromethane (20 mL) and acetone (20 mL) was added water (15 mL). The heterogeneous mixture was then heated to reflux for 0.5 h, affording a yellow solution. The organic solvents were removed under reduced pressure, leaving a suspension of the yellow residue in water. The solid was isolated by filtration, washed with water, and dried *in vacuo*. Yield: 40 mg (93%). Anal. Calcd for $RhC_{45}H_{36}O_3$-ClP_2: C, 65.49; H, 4.36. Found: C, 65.51; H, 4.38. ^{1}H NMR ($CDCl_3$, δ): 6.87 (d, 1H, arom, J_{HH} = 2.1 Hz), 7.01 (d, 1H, arom, J_{HH} = 2.1 Hz), 7.33−7.51 (m, 30H, arom), 2.00 (s, 3H, CH_3), 9.51 (s, 1H, −CHO). IR (KBr; cm^{-1}): ν(C=O(acyl)) 1705; ν(C=O(formyl)) 1675; ν(Rh−Cl) 350. UV−vis (CH_2Cl_2; λ_{max}, nm (ϵ, M^{-1} cm^{-1})): 425 (5200).

Rh(L$_{al}$)(PPh$_3$)$_2$(NO$_2$) (8b). To a stirred solution of Rh-(MeL$_{sb}$)(PPh$_3$)$_2$Cl$_2$ (50 mg, 0.005 mmol) in dichloromethane−acetone (1:1) (30 mL) was added an aqueous solution of $NaNO_2$ (40 mg, 0.57 mmol). Stirring was continued for 0.5 h, and the orange color of the solution changed to yellow. The resulting solution was evaporated under reduced pressure. A yellow suspension of the complex was obtained, which was isolated by filtration and then washed repeatedly with water. The crystalline solid was dried *in vacuo*. Yield: 41 mg (94%). Anal. Calcd for $RhC_{45}H_{36}NO_5P_2$: C, 64.67; H, 4.31; N, 1.67. Found: C, 64.61; H, 4.40; N, 1.65. ^{1}H NMR ($CDCl_3$; δ): 6.94 (d, 1H, arom, J_{HH} = 3.2 Hz), 7.22 (d, 1H, arom, J_{HH} = 2.8 Hz), 7.37−7.65 (m, 30H, arom), 1.96 (s, 3H, CH_3), 9.72 (s, 1H, −CHO). IR (KBr; cm^{-1}): ν(C=O(acyl)) 1705; ν(C=O(formyl)) 1670; ν(N−O) 1280 (sym), 1310 (asym); ν(O−N−O) 830. UV−vis (CH_2-Cl_2; λ_{max}, nm (ϵ, M^{-1} cm^{-1})): 420 (5120).

Interconversions. a. Rh(MeL$_{sb}$)(PPh$_3$)$_2$Cl$_2$ (5b) to Rh-(L$_{al}$)(PPh$_3$)$_2$(MeCO$_2$) (6b). To a stirred solution of Rh-(MeL$_{sb}$)(PPh$_3$)$_2$Cl$_2$ (50 mg, 0.05 mmol) in 1:1 dichloromethane−acetone (40 mL) was added an aqueous solution of $NaCO_2Me$·$3H_2O$ (50 mg, 0.36 mmol). The solution instantly changed from orange to yellow. Stirring was continued for 0.5 h. The organic solvents were removed under reduced pressure, leaving an aqueous suspension of a yellow residue of **6b**. This was isolated by filtration, washed with water, and dried *in vacuo*. Yield: 93%.

b. Rh(L$_{al}$)(PPh$_3$)$_2$(MeCO$_2$) (6b) to Rh(MeL$_{sb}$)(PPh$_3$)$_2$Cl$_2$ (5b). To a stirred solution of Rh(L$_{al}$)(PPh$_3$)$_2$(MeCO$_2$) (10 mg) in ethanol (5 mL) were added MeArNH$_2$·HCl (10 mg) and 0.3 N HCl solution (2 mL). The solution immediately changed from yellow to orange. Stirring was continued for another 15 min. The solvent was then removed under reduced pressure, and water was added to the orange residue of **5b**. The suspension was stirred, and the orange solid was collected by filtration, washed with water, and dried *in vacuo*. Yield: 79%.

c. Rh(L$_{al}$)(PPh$_3$)$_2$Cl (8a) to Rh(MeL$_{sb}$)(PPh$_3$)$_2$Cl$_2$ (5b). To a stirred solution of Rh(L$_{al}$)(PPh$_3$)$_2$Cl (10 mg) in ethanol (20 mL) was added $MeC_6H_4NH_2$·HCl (10 mg) and 0.3 N HCl solution (5 mL). Stirring was continued for 0.5 h. After the organic solvent was evaporated, the residue of **5b** was washed with ethanol dried *in vacuo*. Yield :94%.

d. Rh(L$_{al}$)(PPh$_3$)$_2$Cl (8a) to Rh(L$_{al}$)(PPh$_3$)$_2$(RCO$_2$) (6b). To a stirred solution of Rh(L$_{al}$)(PPh$_3$)$_2$Cl (50 mg, 0.06 mmol) in a 1:1 dichloromethane−acetone mixture (25 mL) was added an aqueous solution of $NaCO_2Me$ (30 mg, 0.24 mmol). Stirring was continued for 0.5 h. After the organic solvents were

Table 5. Crystal, Data Collection, and Refinement Parameters for 5b·2CH_2Cl_2, 6b, 7, and 8b

	5b·2CH_2Cl_2	**6b**	**7**	**8b**
mol formula	$C_{54}H_{49}Cl_6NO_2P_2Rh$	$C_{47}H_{39}O_5P_2Rh$	$C_{45}H_{36}NO_6P_2Rh$	$C_{45}H_{36}NO_5P_2Rh$
mol wt	1121.5	848.6	851.6	835.6
cryst syst	orthorhombic	monoclinic	monoclinic	monoclinic
space group	*Pnma* (No. 62)	$P2_1/c$ (No. 14)	$P2_1/n$ (No. 14)	$P2_1/c$ (No. 14)
a, Å	18.560(7)	10.967(4)	21.086(10)	17.885(10)
b, Å	18.230(6)	31.117(16)	10.216(6)	9.930(3)
c, Å	15.182(4)	11.698(6)	21.309(7)	22.060(9)
β, deg		93.02(4)	118.70(3)	94.43(4)
V, Å^3	5137(3)	3987(3)	4026(3)	3904(3)
Z	4	4	4	4
λ, Å	0.710 73	0.710 73	0.710 73	0.710 73
μ, cm^{-1}	7.49	5.56	5.54	5.67
D_{calcd}, g cm^{-3}	1.450	1.414	1.408	1.422
temp, °C	22	22	22	22
R,[a] %	3.79	4.10	4.12	3.63
R,[b] %	4.36	4.99	4.58	4.22
GOF[c]	1.29	1.32	1.06	1.03

[a] $R = \sum||F_o| - |F_c||/\sum|F_o|$. [b] $R_w = [\sum w(||F_o| - |F_c|)^2/\sum w|F_o|^2]^{1/2}$; $w^{-1} = \sigma^2|F_o| + g|F_o|^2$. $g = 0.004$ for **5b**·2CH_2Cl_2, 0.002 for **6b**, 0.0002 for **7**, and 0.0003 for **8b**. [c] The goodness of fit is defined as $[\sum w(|F_o| - |F_c|)^2/(n_o - n_v)]^{1/2}$, where n_o and n_v denote the numbers of data and variables, respectively.

evaporated. the yellow aqueous suspension of **6b** was filtered, washed with water, and dried *in vacuo*. Yield: 98%.

e. Rh(L_{al})(PPh_3)$_2$Cl (8a) to Rh(L_{al})(PPh_3)$_2$(NO_3) (7). Use of $NaNO_3$ instead of $NaCO_2Me$ in the above procedure afforded **7**. Yield: 94%.

f. Rh(L_{al})(PPh_3)$_2$Cl (8a) to Rh(L_{al})(PPh_3)$_2$(NO_2) (8b). Use of $NaNO_2$ in place of $NaCO_2Me$ in procedure **d** above furnished **8b**. Yield: 98%.

g. Rh(L_{al})(PPh_3)$_2$(NO_2) (8b) to Rh(L_{al})(PPh_3)$_2$Cl (8a). To a stirred solution of Rh(L_{al})(PPh_3)$_2$(NO_2) (50 mg, 0.05 mmol) in ethanol (20 mL) was added 0.3 N aqueous HCl (5 mL). The stirring was continued for 0.5 h. After the organic solvent was evaporated, the residue **8a** was extracted with water and finally isolated by filtration. It was washed repeatedly with water and dried *in vacuo*. Yield: 95%.

h. Rh(L_{al})(PPh_3)$_2$($MeCO_2$) (6b) to Rh(L_{al})(PPh_3)$_2$Cl (8a). This was achieved by using Rh(L_{al})(PPh_3)$_2$($MeCO_2$) in place of Rh(L_{al})(PPh_3)$_2$(NO_2) in procedure **g**. Yield: 97%.

i. Rh(L_{al})(PPh_3)$_2$(NO_3) (7) to Rh(L_{al})(PPh_3)$_2$Cl (8a). Rh(L_{al})(PPh_3)$_2$(NO_3) was used instead of Rh(L_{al})(PPh_3)$_2$(NO_2) in procedure **g**. Yield: 98%.

Reaction of 1 (X = OMe) with $RhCl(PPh_3)_3$ in the Absence of HCl. To a solution of 2-formyl-4-methyl-6-((*p*-methoxyimino)methyl)phenol (22 mg, 0.08 mmol) in hot ethanol (25 mL) was added $RhCl(PPh_3)_3$ (50 mg, 0.05 mmol). The mixture was heated to reflux for 0.5 h. Upon cooling, bright yellow crystalline *trans*-Rh(CO)Cl(PPh_3)$_2$ separated out. It was collected by filtration, washed thoroughly with cold ethanol, and dried *in vacuo*. Yield: 36 mg (98%). The same result was obtained irrespective of the X substituent.

X-ray Structure Determinations. Single crystals of **5b**·2CH_2Cl_2 (0.40 × 0.30 × 0.25 mm^3) and **6b** (0.50 × 0.40 × 0.35 mm^3), **7** (0.20 × 0.30 × 0.30 mm^3), and **8b** (0.20 × 0.20 × 0.35 mm^3) were grown by slow diffusion of hexane into dichloromethane and benzene solutions, respectively. To avoid loss of solvent and crystallinity **5b**·2CH_2Cl_2 was mounted in a sealed capillary over mother liquor. Cell parameters were determined by a least-squares fit of 30 machine-centered reflections (2θ = 15−30°). Data were collected by the ω-scan technique in the ranges 3° ≤ 2θ ≤ 46° for **5b**·2CH_2Cl_2, 3° ≤ 2θ ≤ 45° for **6b**, 3° ≤ 2θ ≤ 48° for **7**, and 3° ≤ 2θ ≤ 45° for **8b** on a Siemens R3m/V four-circle diffractometer with graphite-monochromated Mo Kα radiation (λ = 0.710 73 Å). Two check reflections measured after every 198 reflections showed no significant intensity reduction in all cases. All data were corrected for Lorentz−polarization effects, and an empirical absorption correction[30] was done on the basis of an azimuthal scan of six reflections for each crystal.

In each case the metal atom was located from a Patterson map; the rest of the non-hydrogen atoms emerged from successive Fourier synthesis. The structures were refined by full-matrix least-squares procedures. All the non-hydrogen atoms were refined anisotropically, and the hydrogen atoms of **5b**·2CH_2Cl_2, **6b**, and **7** were added at calculated positions with fixed U = 0.08 Å^2. All the hydrogen atoms of **8b** were located by difference Fourier maps and refined with a fixed U = 0.08 Å^2 using a riding model. The highest residuals were 0.33 e Å^{-3} (**5b**·2CH_2Cl_2), 0.92 e Å^{-3} (**6b**), 0.94 e Å^{-3} (**7**), and 0.50 e Å^{-3} (**8b**) near the metal atom. All calculations were done on a MicroVax II computer using the SHELXTL-PLUS program package.[31] Significant crystal data are listed in Table 5.

Computation of Chemical Shift Due Ring Currents. The parameters taken from the crystallographic data of **5b**·2CH_2Cl_2, **6b, 7**, and **8b** are (i) distance of the concerned proton from the centroid (G) of each PPh_3 phenyl ring and (ii) the angle between each distance vector and the normal to the plane of the phenyl ring at G. From these parameters the cylindrical coordinates[32] ρ and z of the proton involved were calculated in units of the radius of the benzene hexagon. With the help of isoshielding plots[20] and ρ, z values the shifts were calculated. The net shifts were obtained after summation of the individual contributions. Further details are given in a dissertation.[33]

Acknowledgment. We are thankful to the Indian National Science Academy, New Delhi, India, the Department of Science and Technology, New Delhi, India, and the Council of Scientific and Industrial Research, New Delhi, India, for financial support. Affiliation with the Jawaharlal Nehru Centre for Advanced Scientific Research, Bangalore, India, is acknowledged.

Supporting Information Available: For Rh(MeL_{sb})(PPh_3)$_2$-Cl_2·2CH_2Cl_2 (**5b**·2CH_2Cl_2), Rh(L_{al})(PPh_3)$_2$($MeCO_2$) (**6b**), Rh(L_{al})(PPh_3)$_2$(NO_3) (**7**), and Rh(L_{al})(PPh_3)$_2$(NO_2) (**8b**) all bond distances (Tables S1, S6, S11, and S16) and angles (Tables

(30) North, A. C. T.; Phillips, D. C.; Mathews, F. A. *Acta Crystallogr., Sect. A* **1968**, *A24*, 351.
(31) Sheldrick, G. M. SHELXTL-Plus Structure Determination Software Programs; Siemens Analytical X-ray Instruments Inc., Madison, WI, 1990.
(32) Margenan, H.; Murphy, G. M. *The Mathematics of Physics and Chemistry*; Van Nostrand: Princeton, NJ, 1956.
(33) Pattanayak, S. Chemistry of New Coordination and Organometallic Compounds of d-Block Elements. Ph.D. Thesis, Jadavpur University, Calcutta, India, 1998.

S2, S7, S12, and S17), anisotropic thermal parameters (Tables S3, S8, S13, and S18), hydrogen atom positional parameters (Tables S4, S9, S14, and S19), and non-hydrogen atomic coordinates and *U* values (Tables S5, S10, S15, and S20). This material is available free of charge via the Internet at http://pubs.acs.org.

OM980748E

Metallacycle Expansion by Alkyne Insertion. Chemistry of a New Family of Ruthenium Organometallics

Kaushik Ghosh, Sujay Pattanayak, and Animesh Chakravorty*

Department of Inorganic Chemistry, Indian Association for the Cultivation of Science, Calcutta 700 032, India

Received October 21, 1997

Acetylene and phenylacetylene reacts with carbonylchloro[4-methyl-6-((R-imino)methyl)-phenolato-*C*,*O*]bis(triphenylphosphine)ruthenium(II), $Ru(RL^1)(PPh_3)_2(CO)Cl$ (**3**), affording the inserted product carbonylchloro[2-vinyl-4-methyl-6-((R-imino)methyl)phenolato-*C*,*O*]bis-(triphenylphosphine)ruthenium(II), $Ru(RL^2,X)(PPh_3)_2(CO)Cl$ (**4**), in virtually quantitative yield. The X-ray structures of **4b** (R = X = Ph) and **4g** (R = Et, X = H) have revealed the presence of distorted-octahedral RuC_2P_2ClO coordination spheres. In the conversion **3** → **4**, the Ru(C,O) chelate ring expands from four-membered to six-membered. The insertion of phenylacetylene is regiospecific, and a reaction model implicating initial Ru−O cleavage and steric control is proposed. The Ru−O bond in **4** is significantly shorter (by ∼0.14 Å) and stronger than that in **3**. This is reflected in the lowering of the ruthenium(III)−ruthenium(II) reduction potential by ∼200 mV. The uncoordinated Schiff base moiety in **4** is present in the hydrogen-bonded iminium−phenolato zwitterionic form, as revealed by the N···O distance as well as by IR and NMR data.

Introduction

The insertion of atoms and small unsaturated molecules into metal−carbon bonds is of abiding interest in chemical research. In the particular case of alkyne insertion—a reaction first observed in the form of metal-promoted oligomerization[1,2]—the net outcome of the primary process and secondary reactions that frequently follow is the formation of new metal−carbon, carbon−carbon, and/or carbon−nonmetal bonds. This makes alkyne insertion a potentially versatile tool for organometallic and organic synthesis.[3−8]

The concern of the present work is alkyne insertion into ruthenium−carbon bonds, several instances of which are known.[2,3d,9−13] Herein we describe the new insertion reaction stated in eq 1, where the four-membered metallacycle **1** is expanded to the six-membered type **2**. The structure and properties of a family of hitherto unknown organometallics incorporating **2** are reported. The pathway of the reaction of eq 1 is scrutinized.

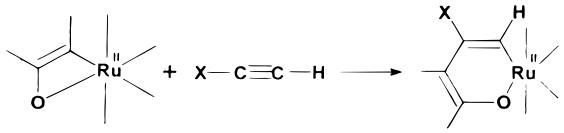

(1)

1 **2**

Results and Discussion

The New Family. The precursor complexes incorporating the chelate ring **1** are of the type $Ru(RL^1)(PPh_3)_2(CO)Cl$ (**3**), formed by decarbonylative metalation of 4-methyl-2,6-diformylphenol by $Ru(PPh_3)_3Cl_2$ in the

(1) (a) Keim, W. *J. Organomet. Chem*. **1969**, *16*, 191. (b) Ricci, J. S.; Ibers, J. A. *J. Organomet. Chem*. **1971**, *27*, 261. (c) Maitlis, P. M. *Acc. Chem. Res*. **1976**, *9*, 93. (d) Mague, J. T.; Wilkinson, G. *Inorg. Chem*. **1968**, *7*, 542.

(2) (a) Bruce, M.; Gardner, R. C. F.; Stone, F. G. A. *J. Chem. Soc., Dalton Trans*. **1976**, 81. (b) Bruce, M. I.; Gardner, R. C. F.; Howard, J. A. K.; Stone, F. G. A.; Welling, M.; Woodward, P. *J. Chem. Soc., Dalton Trans*. **1977,** 621. (c) Bruce, M. I.; Gardner, R. C. F.; Stone, F. G. A. *J. Chem. Soc., Dalton Trans*. **1979**, 906.

(3) Some representative examples are cited in refs 3−7 according to the metal in the M−C bond undergoing insertion. Pd−C: (a) Tao, W.; Silverberg, L. J.; Rheingold, A. L.; Heck, R. F. *Organometallics* **1989**, *8*, 2550. (b) Larock, R. C.; Doty, M. J.; Cacchi, S. *J. Org. Chem*. **1993**, *58*, 4579. (c) Vicente, J.; Abad, J. A.; Gil-Rubio, J. *Organometallics* **1996**, *15*, 3509. (d) Spencer, J.; Pfeffer, M.; Kyritsakas, N.; Fischer, J. *Organometallics* **1995**, *14*, 2214. (e) Pfeffer, M. *Pure Appl. Chem*. **1992**, *64*, 335. (f) Bahsoun, A.; Dehand, J.; Pfeffer, M.; Zinsius, M.; Bouaoud, S.-E.; Borgne, G. L. *J. Chem. Soc., Dalton Trans*. **1979,** 547. (g) Arlen, C.; Pfeffer, M.; Bars, O.; Grandjean, D. *J. Chem. Soc., Dalton Trans*. **1983**, 1535. (h) Ossor, H.; Pfeffer, M.; Jastrzebski, J. T. B. H.; Stam, C. H. *Inorg. Chem*. **1987**, *26*, 1169.

(4) V−C: (a) Buijink, J. K. F.; Kloeststra, K. R.; Meetsma, A.; Teuben, J. H.; Smeets, W. J. J.; Spek, A. L. *Organometallics* **1996**, *15*, 2523. (b) Moore, M.; Gambarotta, S.; Yap, G.; Liable-Sands, L. M.; Rheingold, A. L. *J. Chem. Soc., Chem. Commun*. **1997**, 643.

(5) Mn−C: (a) Liebeskind, L. S.; Gasdaska, J. R.; McCallum, J. S.; Tremont, S. J. *J. Org. Chem*. **1989**, *54*, 669. (b) Grigsby, W. J.; Main, L.; Nicholson, B. K. *Organometallics* **1993**, *12*, 397.

(6) Fe−C: Butler, I. R. *Can. J. Chem*. **1990**, *68*, 1979.

(7) Ni−C: (a) Yang, K.; Bott, S. G.; Richmond, M. G. *Organometallics* **1994**, *13*, 3767. (b) Carmona, E.; Gutierrez-Puebla, E.; Monge, A.; Marin, J. M.; Paneque, M.; Poveda, M. L. *Organometallics* **1989**, *8*, 967. (c) Martinez, M.; Muller, G.; Panyella, D.; Rocamora, M.; Solans, X.; Font-Bardia, M. *Organometallics* **1995**, *14*, 5552. (d) Arlen, C.; Pfeffer, M.; Fischer, J.; Mitschler, A. *J. Chem. Soc., Chem. Commun*. **1983**, 928.

(8) Schore, N. E. *Chem. Rev*. **1988**, *88*, 1081.

(9) Burns, R. M.; Hubbard, J. L. *J. Am. Chem. Soc*. **1994**, *116*, 9514.

(10) Garn, D.; Knoch, F.; Kish, H. *J. Organomet. Chem*. **1993**, *444*, 155.

(11) Ferstl, W.; Sakodinskaya, I. K.; Beydoun-Sutter, N.; Borgne, G. L.; Pfeffer, M.; Ryabov, A. D. *Organometallics* **1997**, *16*, 411.

(12) Bruce, M. I.; Catlow, A.; Cifuentes, M. P.; Snow, M. R.; Tiekink, E. R. T. *J. Organomet. Chem*. **1990**, *397*, 187.

(13) Lutsenko, Z. L.; Aleksandrov, G. G.; Petrovskii, P. V.; Shubina, E. S.; Andrianov, V. G.; Struchkov, Yu. T.; Rubezhov, A. Z. *J. Organomet. Chem*. **1985**, *281*, 349.

S0276-7333(97)00917-5 CCC: $15.00
Publication on Web 04/15/1998

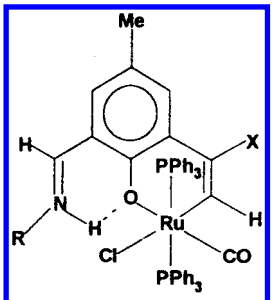

	R	X
4a	Me	H
4b	Et	H
4c	p-MeC$_6$H$_4$	H
4d	p-ClC$_6$H$_4$	H
4e	Me	Ph
4f	Et	Ph
4g	Ph	Ph
4h	p-MeC$_6$H$_4$	Ph

Figure 1. Alkyne-inserted organometallics synthesized in the present work.

presence of primary amines (RNH_2).[14] The four-

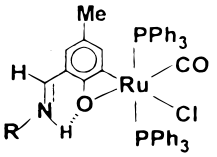

$Ru(RL^1)(PPh_3)_2(CO)Cl$

3

membered ring in **3** is known to undergo facile cleavage by ligands,[15,16] and this prompted us to explore the possible reactivity of **3** toward alkynes. A smooth and virtually quantitative reaction is indeed observed (eq 2) in a boiling dichloromethane-methanol mixture,

$$\underset{\mathbf{3}}{Ru(RL^1)(PPh_3)_2(CO)Cl} + HC{\equiv}CX \rightarrow \underset{\mathbf{4}}{Ru(RL^2,X)(PPh_3)_2(CO)Cl} \quad (2)$$

$$X = H, Ph$$

affording the insertion product $Ru(RL^2,X)(PPh_3)_2(CO)Cl$ (**4**), which incorporates ring **2**. The alkynes used are acetylene and phenylacetylene. The eight species of type **4** (**4a**−**h**) are listed in Figure 1.

In previous studies only substituted acetylenes have been inserted into ruthenium−carbon bonds.[2,3d,9−13] Acetylene itself is successfully employed here (eq 2, X = H) for the first time.[17] The reaction of eq 2 also

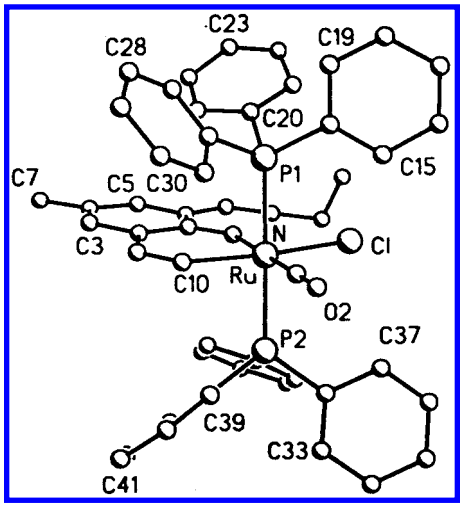

Figure 2. Perspective view and atom-labeling scheme for **4b**·CH_2Cl_2 (excluding CH_2Cl_2).

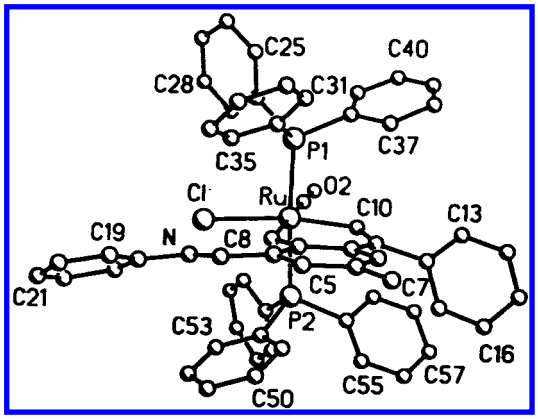

Figure 3. Perspective view and atom-labeling scheme for **4g**.

represents a rare[11] example of straightforward two-carbon metallacycle expansion uncomplicated by subsequent reactions.

The type **4** species are diamagnetic and soluble in halocarbon solvents, affording green (R = aryl) or pink (R = alkyl) solutions. An allowed band in the 500−600 nm range (the range for the corresponding band in **3** is 480−540 nm[14]) is assigned to a $t_2 \rightarrow \pi^*$ MLCT transition which is blue shifted by ~60 nm on going from R = aryl to R = alkyl. In ^1H NMR the olefinic C=CH(Ru) protons resonate in the range δ 6.0−6.4 ($J_{HH} \approx 9$ Hz for X = H).

Structure. The X-ray structures of two representative compounds, viz. **4b**·CH_2Cl_2 and **4g**, have been determined, authenticating the insertion process. Molecular views are shown in Figures 2 and 3, and bond parameters are listed in Table 1. The RuC_2P_2ClO coordination sphere is distorted octahedral. The corresponding bond parameters of the two complexes are similar. The (σ-vinyl)phenolato chelate ring along with the benzene ring and the aldimine function (R and Me excluded), constitutes a good plane (mean deviation: **4b**·CH_2Cl_2, 0.03 Å; **4g**, 0.06 Å). The aryl rings at C9 and N in **4g** make dihedral angles of 122.5 and 24.8°, respectively, with the above plane.

The average Ru−C10 distance (2.034(10) Å) is slightly shorter than the usual Ru−C(σ-vinyl) lengths (~2.1 Å). The Ru−P, Ru−Cl, and Ru−C(carbonyl) lengths lie close

(14) (a) Ghosh, P.; Bag, N.; Chakravorty, A. *Organometallics* **1996**, *15*, 3042. (b) Bag, N.; Choudhury, S. B.; Pramanik, A.; Lahiri, G. K.; Chakravorty, A. *Inorg. Chem.* **1990**, *29*, 5013. (c) Bag. N.; Choudhury, S. B.; Lahiri, G. K.; Chakravorty, A. *J. Chem. Soc., Chem. Commun.* **1990**, 1626.

(15) Ghosh, P.; Pramanik, A.; Chakravorty, A. *Organometallics* **1996**, *15*, 4147.

(16) (a) Ghosh, P.; Chakravorty, A. *Inorg. Chem.* **1997**, *36*, 64. (b) Pramanik, K.; Ghosh, P.; Chakravorty, A. *J. Chem. Soc., Dalton Trans.*, in press.

(17) Acetylene has however been inserted into the Ru−Si bond: Maddock, S. M.; Rickard, C. E. F.; Roper, W. R.; Wright, L. J. *Organometallics* **1996**, *15*, 1793.

Table 1. Selected Bond Distances (Å) and Angles (deg) and Their Estimated Standard Deviations for $Ru(EtL^2,H)(PPh_3)_2(CO)Cl\cdot CH_2Cl_2$ ($4b\cdot CH_2Cl_2$) and $Ru(PhL^2,Ph)(PPh_3)_2(CO)Cl$ (4g)

	$4b\cdot CH_2Cl_2$	4g
	Distances	
Ru−Cl	2.536(3)	2.540(3)
Ru−C10	2.040(9)	2.029(10)
Ru−P1	2.372(3)	2.372(3)
Ru−P2	2.372(3)	2.396(3)
Ru−O1	2.095(7)	2.100(7)
Ru−C11	1.809(10)	1.803(11)
O1−C1	1.287(12)	1.292(12)
O2−C11	1.149(12)	1.175(14)
N−C8	1.236(21)	1.323(15)
C9−C10	1.352(13)	1.346(13)
O1...N	2.556(12)	2.639(13)
	Angles	
Cl−Ru−P1	92.7(1)	95.2(1)
Cl−Ru−C10	163.4(3)	167.0(3)
P1−Ru−C11	88.8(3)	88.9(4)
Cl−Ru−O1	77.5(2)	81.5(2)
P1−Ru−C10	88.0(3)	90.5(3)
P1−Ru−P2	175.8(1)	176.0(1)
Cl−Ru−C11	101.2(3)	98.8(4)
C10−Ru−C11	95.3(4)	93.0(5)
P1−Ru−O1	91.0(2)	90.9(2)
O1−Ru−C10	85.9(3)	86.8(3)
O1−Ru−C11	178.7(4)	179.7(5)
Ru−C11−O2	179.5(7)	175.9(10)

to those in type **3** precursor complexes.[14] On the other hand, the average Ru−O1 length (2.098(7) Å) in $\mathbf{4b}\cdot CH_2Cl_2$ and **4g** is significantly shorter than that in the type **3** complex $Ru(MeC_6H_4L^1)(PPh_3)_2(CO)Cl$ (2.235(4) Å).[14b] Evidently the four-membered chelate ring of **3** is quite strained. Ring expansion via alkyne insertion increases the chelate bite angle from ~64° to ~87°, and the Ru−O(phenolato) bond becomes correspondingly shorter and stronger.

The Zwitterionic Iminium−Phenolato Function. The N···O1 lengths in $\mathbf{4b}\cdot CH_2Cl_2$ and **4g** (2.56(12) and 2.64(13) Å, respectively) are indicative of hydrogen bonding. The presence of the zwitterionic fragment **5**

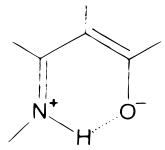

5

is consistent with IR and ^1H NMR data. The N^+-H stretch occurs as a broad band of medium intensity in the region 3400−3440 cm^{-1}, suggesting the presence of relatively weak hydrogen bonding.[14,18] The C=N stretching frequency is relatively high (1620−1640 cm^{-1}), and this is consistent with the protonation of nitrogen.[14,18,19]

In compounds with R = aryl the iminium (δ 11.9−12.6; the signal disappears upon shaking with D_2O) and the azomethine (δ 6.9−7.4) ^1H signals are mutually split into well-resolved doublets, the coupling constant (~20 Hz) corresponding to trans disposition of the protons as in **5**. For R = alkyl species, the azomethine hydrogen is still a doublet but the N^+-H signal is broadened, presumably due to additional coupling with alkyl protons (on α-carbon).

Regiospecificity: A Reaction Model. The reaction of eq 2 is not hindered by the presence of large excesses (10- to 50-fold) of either chloride ($LiCl/Et_4NCl$) or PPh_3 in the reaction solution. Therefore, the reaction does not appear to proceed via equilibrium dissociation of halide or phosphine ligands. Another crucial feature of the reaction is that phenylacetylene inserts regiospecifically, the ≡CPh and ≡CH carbons adding respectively to the carbon and metal ends of the Ru−C bond of **3**. In this manner the Ph group gets positioned anti to the metal site in **4** and is distanced from both PPh_3 and Cl. Interestingly, diphenylacetylene fails to insert into **3** under the conditions used for acetylene and phenylacetylene. These findings are indicative of a dominant steric control of the reaction path.

The Ru−O(phenolato) bond in **3** is known to be long (~2.24 Å),[9] being subject to facile reversible cleavage by ligands.[14−16,20] The initial π-anchoring of the alkyne to the metal is believed to be attended with Ru−O cleavage, as in **6**.[20] Subsequent 2 + 2 alkyne addition to the Ru−C bond is subject to steric crowding from the Cl and PPh_3 ligands (see **7**).[21,22]

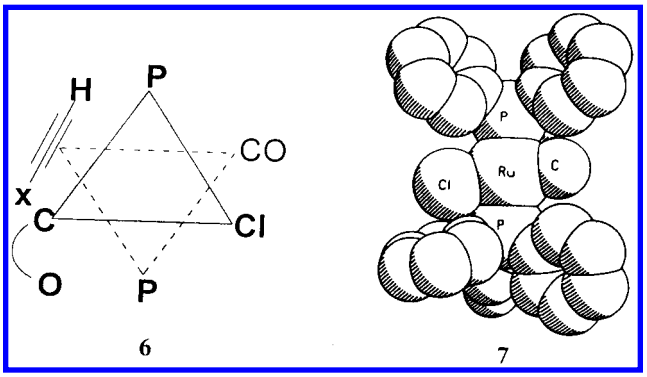

6 **7**

The bulky ≡CPh end of phenylacetylene therefore adds to the carbon site. After insertion, the Ru−O bond is reestablished as in **4**. The inertness of diphenylacetylene to insertion is consistent with this model.

Oxidized Species. Organometallics incorporating trivalent ruthenium are scarce,[23] and this prompted us to explore the feasibility of generating ruthenium(III) congeners of **4**. In dichloromethane solution **4** was indeed found to display a quasireversible one-electron cyclic voltammetric response (eq 3) with $E_{1/2}$ in the range 0.3−0.4 V vs SCE (Table 2).

The $E_{1/2}$ values for X = Ph species are lower by 20−30 mV than those of the corresponding X = H species, as expected. Significantly, the $E_{1/2}$ values are much lower (by ~200 mV) than those of the corresponding

(18) (a) Sandorfy, C.; Vocelle, D. *Mol. Phys., Chem., Biol.* **1989**, *4*, 195. (b) Chevalier, P.; Sandorfy, C. *Can. J. Chem.* **1960**, *38*, 2524. (c) Favrot, J.; Vocelle, D.; Sandorfy, C. *Photochem. Photobiol.* **1979**, *30*, 417.

(19) Bohme, H.; Haake, M. In *Advances in Organic Chemistry*; Bohme, H., Viehe, H. G., Eds.; Interscience: New York, 1976; Part 1, Vol. 9, p 1.

(20) To exclude steric repulsion between the entering ligand and the displaced phenolic oxygen, the cleavage process is associated with a 180° rotation of the RL^1 ligand around the Ru−C bond,[15,16] as implied in **6**.

(21) Diagram **7** was generated using coordinates of solved structures[9] of type **3** using the programs of SHELXTL-Plus.[22]

(22) Sheldrick, G. M. SHELXTL-Plus Structure Determination Software Programs; Siemens Analytical X-ray Instruments Inc., Madison, WI, 1990.

(23) Ghosh, P.; Pramanik, A.; Bag, N.; Lahiri, G. K.; Chakravorty, A. *J. Organomet. Chem.* **1993**, *454*, 237 and references therein.

Table 2. Cyclic Voltammetric Reduction Potentials[a] at 298 K

compd	$E_{1/2}$[M(III)−M(II)],[b] V (ΔE_p, mV)	compd	$E_{1/2}$[M(III)−M(II)],[b] V (ΔE_p, mV)
4a	0.35 (120)	**4e**	0.32 (100)
4b	0.34 (100)	**4f**	0.31 (170)
4c	0.37 (100)	**4g**	0.38 (160)
4d	0.39 (130)	**4h**	0.35(140)

[a] Conditions: solvent, dichloromethane; supporting electrolyte, TEAP (0.1 M); working electrode, platinum; reference electrode, SCE; solute concentration, $\sim 10^{-3}$ M. [b] $E_{1/2} = 0.5(E_{pa} + E_{pc})$ at scan rate 50 mV s^{-1}, where E_{pa} and E_{pc} are anodic and cathodic peak potentials, respectively; $\Delta E_p = E_{pa} - E_{pc}$.

$$Ru^{III}(RL^2,X)(PPh_3)_2(CO)Cl^+ + e^- \rightleftharpoons Ru^{II}(RL^2,X)(PPh_3)_2(CO)Cl \quad (3)$$

couples of complexes of type **3**.[14a] Coordination by the phenolato group, a hard donor, has been documented to stabilize trivalent ruthenium.[23,24] The lowering of $E_{1/2}$ values of **4** compared to those of **3** is associated with the strengthening of the Ru−O(phenolato) bond and formation of the Ru−C(vinyl) bond on going from **3** to **4**. The oxidized species in eq 3 were however found to be still too unstable for isolation via coulometry.

Concluding Remarks

The four-membered chelate ring of **3** smoothly expands by two carbon atoms upon insertion of acetylene/phenylacetylene, affording the new organometallic family **4**. The regiospecificity of phenylacetylene insertion and the inertness of diphenylacetylene are of steric origin. This work has provided the first examples of the insertion of unsubstituted acetylene into the Ru−C bond.

The hydrogen-bonded zwitterionic iminium-phenolato function is retained on going from **3** to **4**, even though during the insertion process the Ru−O bond is believed to be temporarily cleaved for initial anchoring of the alkyne. The Ru−O bond length and the $t_2 \rightarrow \pi^*$ MLCT exitation energy as well as the ruthenium(III)−ruthenium(II) reduction potential systematically decrease on going from **3** to **4**.

The RL^2 ligand in **4** is new, and we are trying to liberate it from **4** via demetalation with the objective of developing its organometallic chemistry with other transition metals.

Experimental Section

Materials. The starting materials $Ru(PPh_3)_3Cl_2$[25] and $Ru(RL^1)(PPh_3)_2(CO)Cl$[14] were prepared by reported methods. Phenylacetylene was obtained from Aldrich. The purification of dichloromethane and the preparation of tetraethylammonium perchlorate (TEAP) for electrochemical work were done as described before.[26] All other chemicals and solvents were of analytical grade and were used as received.

Physical Measurements. Electronic and IR spectra were recorded with Hitachi 330 and Perkin-Elmer 783 IR spectrophotometers. For ^{1}H NMR spectra a Bruker 300 MHz FT NMR spectrophotometer was used (tetramethylsilane is the internal standard). Magnetic properties were examined using a PAR 155 vibrating-sample magnetometer fitted with a Walker Scientific magnet. Microanalyses (C,H,N) were done by using a Perkin-Elmer 240C elemental analyzer. Electrochemical measurements were performed under a nitrogen atmosphere using a PAR 370-4 electrochemistry system. All potentials reported in this work are uncorrected for junction contribution.

Preparation of Complexes. The $Ru(RL^2,X)(PPh_3)_2(CO)Cl$ (**4**) complexes were synthesized in nearly quantitative yields by reacting $Ru(RL^1)(PPh_3)_2(CO)Cl$ with alkynes. Details are given for representative cases only.

[Ru(MeL^2,H)(PPh$_3$)$_2$(CO)Cl] (4a). The orange solution of $Ru(MeL^1)(PPh_3)_2(CO)Cl$ (50 mg, 0.06 mmol) in a warm 1:4 mixture (50 mL) of dichloromethane and methanol was first purged with acetylene gas, and then the solution was heated to reflux for 5 h in an acetylene atmosphere with the help of a balloon filled with acetylene. The solution turned pink, and upon concentrating and cooling a pink crystalline solid separated, which was collected, washed thoroughly with methanol, and dried in vacuo. Yield: 51 mg (99%). Anal. Calcd for $RuC_{48}H_{42}NO_2P_2Cl$: C, 66.78; H, 4.87; N, 1.62. Found: C, 66.82; H, 4.80; N, 1.59. ^{1}H NMR ($CDCl_3$, δ): 6.17 (s, 1H arom), 6.52 (s,1H arom), 7.14−7.62 (m, 30H arom and 1H, CH=C(Ru)), 2.04 (s, 3H, CH_3), 6.06 (d, 1H, C=CH(Ru), J_{HH} 9.0 Hz), 12.15 (s, 1H, $=N^+H$), 6.93 (d, 1H, $-CH=N^+$, J_{HH} 11.8), 2.62 (d, 3H, NCH_3, J_{HH} 6.0). IR (KBr, cm^{-1}): ν(C=N) 1640; ν(C≡O) 1900; ν(N−H, hexachlorobutadiene) 3400. UV−vis (CH_2Cl_2, λ_{max}, nm (ϵ, M^{-1} cm^{-1})): 520 (2850), 370 (3880), 310 (9830). Complexes **4b**−**d** were prepared using the same procedure as above.

[Ru(EtL^2,H)(PPh$_3$)$_2$(CO)Cl] (4b). Using $Ru(EtL^1)(PPh_3)_2(CO)Cl$ (50 mg, 0.058 mmol) a pink crystalline solid of **4b** was obtained. Yield: 50 mg (98%). Anal. Calcd for $RuC_{49}H_{44}NO_2P_2Cl$: C, 67.08; H, 5.01; N, 1.59. Found: C, 66.98; H, 4.99; N, 1.63. ^{1}H NMR ($CDCl_3$, δ): 6.22 (s, 1H arom), 6.55 (s, 1H arom), 7.17−7.61 (m, 30H arom and 1H, −CH=C(Ru)), 2.06 (s, 3H, CH_3), 6.08 (d, 1H, C=CH(Ru), J_{HH} 8.9 Hz), 12.25 (s, 1H, $=N^+H$), 6.95 (d, 1H, $CH=N^+$, J_{HH} 11.2), 2.89 (q, 2H, NEt), 1.01 (t, 3H, NEt). IR (KBr, cm^{-1}): ν(C=N) 1640; ν(C≡O) 1895; ν(N−H, hexachlorobutadiene) 3400. UV−vis (CH_2Cl_2, λ_{max}, nm (ϵ, M^{-1} cm^{-1})): 520 (3240), 370 (3840), 310 (9490).

[Ru(MeC$_6$H$_4$L^2,H)(PPh$_3$)$_2$(CO)Cl] (4c). Using $Ru(MeC_6H_4L^1)(PPh_3)_2(CO)Cl$ (50 mg, 0.054 mmol) a green crystalline solid of **4c** was obtained. Yield: 50 mg (98%). Anal. Calcd for $RuC_{54}H_{46}NO_2P_2Cl$: C, 69.05; H, 4.90; N, 1.49. Found: C, 68.98; H, 4.96; N, 1.53. ^{1}H NMR ($CDCl_3$, δ): 6.25 (s, 1H arom), 6.52 (s, 1H arom), 7.09−7.65 (m, 34H arom and 1H, CH=C-(Ru)), 2.06 and 2.30 (2s, 6H, $2CH_3$), 6.13 (d, 1H, C=CH(Ru), J_{HH} 9.1 Hz), 12.87 (d, 1H, $=N^+H$, J_{HH} 21.0), 7.37 (d, 1H, $-CH=N^+$, J_{HH} 20.9). IR (KBr, cm^{-1}): ν(C=N) 1620; ν(C≡O) 1990; ν(N−H, hexachlorobutadiene) 3430. UV−vis (CH_2Cl_2, λ_{max}, nm (ϵ, M^{-1} cm^{-1})): 580 (3560), 428 (7010), 320 (10 460).

[Ru(ClC$_6$H$_4$L^2,H)(PPh$_3$)$_2$(CO)Cl] (4d). Using $Ru(ClC_6H_4L^1)(PPh_3)_2(CO)Cl$ (50 mg, 0.053 mmol) a green crystalline solid of **4d** was obtained. Yield: 50.5 mg (99%). Anal. Calcd for $RuC_{53}H_{43}NO_2P_2Cl_2$: C, 66.32; H, 4.48; N, 1.45. Found: C, 66.29; H, 4.50; N, 1.48. ^{1}H NMR ($CDCl_3$, δ): 6.25 (s, 1H arom), 6.58 (s, 1H arom), 7.13−7.76 (m, 34H arom and 1H, CH=C-(Ru)), 2.06 (s, 3H, CH_3), 6.12 (d, 1H, C=CH(Ru), J_{HH} 9.0 Hz), 12.82 (d, 1H, $=N^+H$, J_{HH} 20.9), 7.36 (d, 1H, $-CH=N^+$, J_{HH} 20.7). IR (KBr, cm^{-1}): ν(C=N) 1620; ν(C≡O) 1990; ν(N−H, hexachlorobutadiene) 3430. UV−vis (CH_2Cl_2, λ_{max}, nm (ϵ, M^{-1} cm^{-1})): 585 (3610), 430 (7380), 320 (12 950).

[Ru(MeL^2,Ph)(PPh$_3$)$_2$(CO)Cl] (4e). To a solution of $Ru(MeL^1)(PPh_3)_2(CO)Cl$ (50 mg, 0.06 mmol) in a warm 1:4 mixture (50 mL) of dichloromethane and methanol was added phenylacetylene (30 mg, 0.30 mmol). The reaction mixture was heated to reflux for 1.0 h. Upon concentrating and cooling, a pink colored crystalline solid separated, which was collected,

(24) Lahiri, G. K.; Bhattacharya, S.; Mukherjee, M.; Mukherjee, A. K.; Chakravorty, A. *Inorg. Chem.* **1987**, *26*, 3359.
(25) Stephenson, T. A.; Wilkinson, G. *J. Inorg. Nucl. Chem.* **1966**, *28*, 945.
(26) (a) Vogel, A. I. *Practical Organic Chemistry*, 3rd ed.; ELBS and Longman Group: Harlow, England, 1965; Chapter 2, pp 176−177. (b) Sawyer, D. T.; Roberts, J. L., Jr. *Experimental Electrochemistry for Chemists*; Wiley: New York, 1974; p 212.

washed thoroughly with methanol, and dried in vacuo. Yield: 56 mg (99%). Anal. Calcd for $RuC_{54}H_{46}NO_2P_2Cl$: C, 69.04; H, 4.90; N, 1.49. Found: C, 68.90; H, 4.93; N, 1.51. ^{1}H NMR ($CDCl_3$, δ): 6.35 (s, 1H arom), 6.89 (s, 1H arom), 7.00−7.60 (m, 33H arom), 1.93 (s, 3H, CH_3), 6.27 (s, 1H, C═CH(Ru)), 11.87 (s, 1H, ═N^+H), 6.95 (d, 1H, −CH═N^+, J_{HH} 11.7 Hz), 2.49 (d, 3H, NCH_3, J_{HH} 6.0), IR (KBr, cm^{-1}): ν(C═N) 1640; ν(C≡O) 1885; ν(N−H, hexachlorobutadiene) 3400. UV−vis (CH_2Cl_2, λ_{max}, nm (ϵ, M^{-1} cm^{-1})): 520 (3940), 360 (5150), 310 (11 200). The following complexes (**4f**−**h**) were prepared using the same procedure as above.

[Ru(EtL^2,Ph)(PPh$_3$)$_2$(CO)Cl] (4f). Using Ru(EtL^1)(PPh$_3$)$_2$(CO)Cl (50 mg, 0.058 mmol), a pink crystalline solid of **4f** was obtained. Yield: 55 mg (99%). Anal. Calcd for $RuC_{55}H_{48}NO_2P_2Cl$: C, 69.29; H, 5.03; N, 1.46. Found: C, 69.31; H, 5.06; N, 1.45. ^{1}H NMR ($CDCl_3$, δ): 6.38 (s, 1H arom), 6.92 (s, 1H arom), 6.99−7.60 (m, 33H arom), 1.94 (s, 3H, CH_3), 6.32 (s, 1H, C═CH(Ru)), 12.01 (s, 1H, ═N^+H), 6.98 (d, 1H, −CH═N^+, J_{HH} 11.0 Hz), 2.77 (q, 2H, NEt), 0.90 (t, 3H, NEt), 5.84 (d, 2H arom, J_{HH} 6.0 Hz). IR (KBr, cm^{-1}): ν(C═N) 1640; ν(C≡O) 1885; ν(N−H, hexachlorobutadiene) 3400. UV−vis (CH_2Cl_2, λ_{max}, nm (ϵ, M^{-1} cm^{-1})): 520 (3760), 360 (5060), 310 (10 890).

[Ru(PhL^2,Ph)(PPh$_3$)$_2$(CO)Cl] (4g). Using Ru(PhL^1)(PPh$_3$)$_2$(CO)Cl (50 mg, 0.055 mmol) a green crystalline solid of **4g** was obtained. Yield: 54 mg (98%). Anal. Calcd for $Ru_{59}H_{48}NO_2P_2Cl$: C, 70.76; H, 4.79; N, 1.39. Found: C, 70.71; H, 4.82; N, 1.41. ^{1}H NMR ($CDCl_3$, δ): 6.42 (s, 1H arom), 7.00 (s, 1H arom), 7.02−7.70 (m, 38H arom), 1.94 (s, 3H, CH_3), 6.34 (s, 1H, C═CH(Ru)), 12.63 (d, 1H, ═N^+H, J_{HH} 21.03 Hz), 7.37 (d, 1H, −CH═N^+, J_{HH} 15.0), 5.95 (d, 2H arom, J_{HH} 6.0). IR (KBr, cm^{-1}): ν(C═N) 1620; ν(C≡O) 1920; ν(N−H, hexachlorobutadiene) 3440. UV−vis (CH_2Cl_2, λ_{max}, nm (ϵ, M^{-1} cm^{-1})): 585 (4330), 425 (8400), 320 (12 600).

[Ru(MeC$_6$H$_4$L^2,Ph)(PPh$_3$)$_2$(CO)Cl] (4h). Using Ru(MeC$_6$H$_4$L^1)(PPh$_3$)$_2$(CO)Cl (50 mg, 0.054 mmol) a green crystalline solid of **4h** was obtained. Yield: 54 mg (98%). Anal. Calcd for $RuC_{60}H_{50}NO_2P_2Cl$: C, 70.97; H, 4.92; N, 1.37. Found: C, 71.10; H, 4.96; N, 1.41. ^{1}H NMR ($CDCl_3$, δ): 6.41 (s, 1H arom), 7.01 (s, 1H arom), 7.02−7.68 (m, 37H arom), 1.93 and 2.30 (2s, 6H, $2CH_3$), 6.33 (s, 1H, C═CH(Ru)), 12.64 (d, 1H, ═N^+H, J_{HH} 20.1 Hz), 7.35 (d, 1H, −CH═N^+, J_{HH} 13.1), 5.96 (d, 2H arom, J_{HH} 6.0). IR (KBr, cm^{-1}): ν(C═N) 1620; ν(C≡O) 1900; ν(N−H, hexachlorobutadiene) 3440. UV−vis (CH_2Cl_2, λ_{max}, nm (ϵ, M^{-1} cm^{-1})): 585 (4040), 425 (8170), 320 (12 960).

Attempted Reaction between [Ru(MeC$_6$H$_4$L^1)(PPh$_3$)$_2$(CO)Cl] and Diphenylacetylene. To a solution of Ru(MeC$_6$H$_4$L^1)(PPh$_3$)$_2$(CO)Cl (50 mg, 0.06 mmol) in a warm 1:4 mixture of dichloromethane and methanol was added diphenylacetylene (107 mg, 0.60 mmol). The reaction mixture was heated to reflux up to 3.0 h. No green coloration appeared, and the reaction mixture consisted of starting materials only.

X-ray Structure Determination. The single crystals of Ru(EtL^2,H)(PPh$_3$)$_2$(CO)Cl.CH_2Cl_2 (**4b**·CH_2Cl_2; 0.20 × 0.40 × 0.40 mm^3) and Ru(PhL^2, Ph)(PPh$_3$)$_2$(CO)Cl (**4g**; 0.25 × 0.20 × 0.30 mm^3) were grown (at 298 K) by slow diffusion of hexane into dichloromethane solution followed by evaporation. Cell parameters were determined by a least-squares fit of 30 machine-centered reflections (2θ = 15−30°). Data were collected by the ω-scan technique in the range $3^o \le 2\theta \le 45°$ on a Siemens R3m/V four-circle diffractometer with graphite-monochromated Mo Kα radiation (λ = 0.710 73 Å). Two check reflections measured after every 198 reflections showed no significant intensity reduction in any cases. All data were corrected for Lorentz-polarization effects, and an empirical absorption correction[27] was done on the basis of an azimuthal scan of six reflections for each crystal.

Table 3. Crystal, Data Collection, and Refinement Parameters for 4b·CH_2Cl_2 and 4g

	4b·CH_2Cl_2	**4g**
mol formula	$C_{50}H_{46}Cl_3NO_2P_2Ru$	$C_{59}H_{48}ClNO_2P_2Ru$
mol wt	962.2	1001.4
cryst syst	monoclinic	monoclinic
space group	$P2_1/n$	$P2_1/c$
a, Å	12.129(4)	14.845(6)
b, Å	28.336(9)	15.010(4)
c, Å	13.349(5)	22.003(7)
β, deg	90.29(3)	93.57(3)
V, Å^3	4587(3)	4922(3)
Z	4	4
λ, Å	0.710 73	0.710 73
μ, cm^{-1}	6.28	4.84
F(000)	1976	2064
D_{calcd}, g cm^{-3}	1.396	1.356
temp, ^{o}C	22	22
R,[a] %	6.36	6.02
R,[b] %	7.30	6.94
GOF[c]	1.27	1.30

[a] $R = \sum||F_o| - |F_c||/\sum|F_o|$. [b] $R_w = [\sum w(||F_o| - |F_c|)^2/\sum w|F_o|^2]^{1/2}$; $w^{-1} = \sigma^2|F_o| + g|F_o|^2$; g = 0.0005 for **4b**·CH_2Cl_2 and 0.0003 for **4g**. [c] The goodness of fit is defined as $[\sum w(|F_o| - |F_c|)^2/(n_o - n_v)]^{1/2}$, where n_o and n_v denote the numbers of data and variables, respectively.

In each case the metal atom was located from a Patterson map and the rest of the non-hydrogen atoms emerged from successive Fourier synthesis. The structures were refined by full-matrix least-squares procedures. The NEt group in **4b**·CH_2Cl_2 is disordered. All non-hydrogen atoms except for the NEt group in **4b**·CH_2Cl_2 were refined anisotropically, and hydrogen atoms were added at calculated positions with fixed U = 0.08 Å^2. The highest residuals were 1.43 e Å^{-3} (**4b**·CH_2Cl_2) and 1.07 e Å^{-3} (**4g**). All calculations were done on a Micro Vax II computer using the SHELXTL-PLUS program package.[22] Significant crystal data are listed in Table 3.

Acknowledgment. We are grateful to the Department of Science and Technology, New Delhi, India, the Indian National Science Academy, New Delhi, India, and The Council of Scientific and Industrial Research, New Delhi, India, for financial support. Affiliation with the Jawharlal Nehru Centre for Advanced Scientific Research, Bangalore, India, is acknowledged.

Supporting Information Available: For Ru(EtL^2,H)(PPh$_3$)$_2$(CO)Cl·CH_2Cl_2 (**4b**·CH_2Cl_2) and Ru(PhL^2,Ph)(PPh$_3$)$_2$(CO)Cl (**4g**) tables of all bond distances (Tables S1 and S6) and angles (Tables S2 and S7), anisotropic thermal parameters (Tables S3 and S8), hydrogen atom positional parameters (Tables S4 and S9), and non-hydrogen atomic coordinates and U values (Tables S5 and S10) (13 pages). Ordering information is given on any current masthead page.

OM970917F

(27) North, A. C. T.; Phillips, D. C.; Mathews, F. A. *Acta Crystallogr., Sect. A* **1968**, *A24*, 351.

Pergamon

PII: S0277-5387(97)00057-0

Polyhedron Vol. 16, No. 17, pp. 2951–2956, 1997

0277-5387/97 $17.00+0.00

Valence specific chelation of ruthenium to Schiff mono-bases of 2,6-diformyl-4-methylphenol: synthesis and structure of trivalent salicylaldiminato species of coordination type RuN_2O_2PCl

Sujay Pattanayak, Kausikisankar Pramanik, Nilkamal Bag, Prasanta Ghosh and Animesh Chakravorty*

Department of Inorganic Chemistry, Indian Association for the Cultivation of Science, Calcultta 700 032, India

(Received 18 December 1996; accepted 29 January 1997)

Abstract—The reaction of Schiff mono-bases, HRL (R = Me, Et), of 2,6-diformyl-4-methylphenol with $K_2RuCl_5(H_2O)$ has afforded $Ru^{III}(RL)_2(PPh_3)Cl$. The X-ray structure of the R = Et complex has revealed metal chelation at the salicylaldimine segment of RL^-, the two phenolic oxygen and azomethine nitrogen atoms lying in mutually *trans* and *cis* positions, respectively. The trivalent state of the metal is stabilized in $Ru(RL)_2(PPh_3)Cl$, the ruthenium(III)/ruthenium(II) $E_{1/2}$ being ~0.40 V *vs* SCE. These distorted low-spin (t_2^5) complexes display rhombic EPR spectra and are characterized by a pair of ligand field transitions (in the near-IR region) within the split t_2 shell. The complexes provide a striking contrast with the ruthenium(II) organometallics arising from the reaction of HRL with $Ru^{II}(PPh_3)_3Cl_2$. © 1997 Elsevier Science Ltd

Keywords: trivalent ruthenium salicylaldimines; valence specific chelation.

The Schiff mono-base of 2,6-diformyl-4-methylphenol (**1**) is a potentially ambidentate chelate ligand with two possible binding sites: the salicylaldehyde site, A, and salicylaldimine site, B, the phenolic group being common to both. In the reaction of **1** with $Ru(PPh_3)_3Cl_2$, chelation associated with decarbonylation, is known to occur [1,2] at the A site as in motif **2**. We now report that it is the B site that is utilized, motif **3**, when **1** chelates ruthenium(III) in the presence of PPh_3. A remarkable valence specificity of the chelation mode of **1** is thus revealed. The synthesis as well as X-ray and electronic structures of complexes incorporating **3** are described. We have here the first structural characterization of a ruthenium(III) salicylaldiminate.

* Author to whom correspondence should be addressed.

EXPERIMENTAL

Materials

The starting materials $K_2RuCl_5(H_2O)$ [3] and 2,6-diformyl-4-methylphenol [4] were prepared by reported procedures. The purification of dichloromethane and preparation of tetraethylammonium perchlorate (TEAP) for electrochemical work were carried out as before [5]. All other chemicals and solvents were of analytical grade and used without further purification.

Preparation of complexes

The two $Ru(RL)_2(PPh_3)Cl$ complexes were prepared by the same procedure. Details are given below for the R = Et complex.

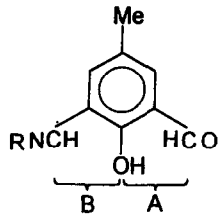

1

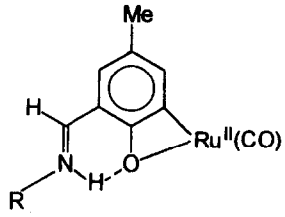

2

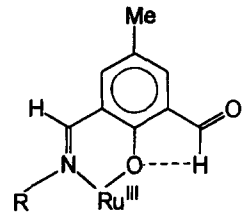

3

Chloro-bis[4-*methyl*-6-*formyl*-2-(N-*ethyl*(*imino-methyl*)*phenolato*-N,O)]*triphenylphosphineruthenium* (III), $Ru(EtL)_2(PPh_3)Cl$. To a hot solution of 2,6-diformyl-4-methylphenol (54 mg, 0.33 mmol) in dehydrated ethanol (25 cm^3) was added a 50% aqueous solution of ethylamine (30 mg, 0.33 mmol $EtNH_2$). The mixture was heated for 20 min. To this hot yellow Schiff mono-base solution was successively added $K_2RuCl_5(H_2O)$ (50 mg, 0.13 mmol) and PPh_3 (41 mg, 0.15 mmol). The reaction mixture was then heated to reflux until ($\sim$5 h) a deep green solution resulted. The ethanol solvent was removed under low pressure and the residue was purified by column chromatography on neutral Al_2O_3. The green $Ru(EtL)_2(PPh_3)Cl$ complex was eluted with 1 : 1 benzene : acetonitrile. Yield: 70 mg [67% on the basis of $K_2RuCl_5(H_2O)$]. Found: C, 61.7; H, 5.1; N, 3.5. Calc. for $C_{40}H_{39}N_2O_4PClRu$: C, 61.6; H, 5.0; N, 3.6%.

Chloro-bis[4-*methyl*-6-*formyl*-2-(N-*methyl*(*imino-methyl*)*phenolato*-N,O)]*triphenylphosphineruthenium* (III), $Ru(MeL)_2(PPh_3)Cl$. This was similarly prepared using $MeNH_2$ in place of $EtNH_2$ in the above procedure. Yield: 65%. Found: C, 60.7; H, 4.7; N, 3.7. Calc. for $C_{38}H_{35}N_2O_4PClRu$: C, 60.7; H, 4.7; N, 3.7%.

Physical measurements

IR (4000–200 cm^{-1}) spectra (as KBr discs) were recorded on a Perkin–Elmer 783 spectrometer and electronic spectral measurements were made with a Hitachi 330 spectrophotometer. Magnetic susceptibilities were measured on a PAR 155 vibrating sample magnetometer and EPR spectra were obtained on a Varian model 109C E-line X-band spectrometer fitted with a quartz Dewar for measurements at 77 K (liquid nitrogen). Spectra were calibrated with diphenylpicrylhydrazyl (DPPH), g = 2.0037. Electrochemical measurements were performed under nitrogen atmosphere on a PAR model 370-4 electrochemistry apparatus as reported earlier [5]. Microanalyses (C,H,N) were carried out with a Perkin–Elmer 240C elemental analyser. Solution ($\sim 10^{-3}$ M) electrical conductivities were measured with the help of a Philips PR 9500 bridge.

X-ray structure determination of $Ru(EtL)_2(PPh_3)Cl$

A single crystal of $0.24 \times 0.36 \times 0.22$ mm^3 grown (at 298 K) by slow diffusion of hexane into dichloromethane solution was used. Cell parameters were determined by least-squares fit of 30 machine-centered reflections (2θ = 14–28°). Data were collected by the ω-scan technique in the angle $3 \leqslant 2\theta \leqslant 48°$ on a Siemens R3m/V four-circle diffractometer with the graphite-monochromated Mo-K_α radiation (λ = 0.71073 Å). Two check reflections measured after every 98 reflections showed no significant intensity reduction. All data were corrected for Lorentz–polarization effects and an empirical absorption correction was done on the basis of azimuthal scan of five reflections [6].

Systematic absences led to the space group $P2_1/n$. The metal atom was located from Patterson maps and the remaining non-hydrogen atoms emerged from successive Fourier synthesis. The structure was refined by full-matrix least-square procedure. All non-hydrogen atoms except PPh_3 carbons were refined anisotropically. The methyl carbon [C(29)] of the N(1)Et substituent shows two fold disorderness around the C(28)–C(29) bond. A number of hydrogen atoms [H(21), H(23), H(26), H(27), H(32), H(34) and H(37)] were directly located from difference-Fourier maps and others were added at calculated positions with fixed U = 0.08 $Å^2$. The aldehydic hydrogens [H(26) and H(37)] were refined isotropically. The highest residual was 0.43 e $Å^{-3}$. All calculations were done on a Micro VaxII computer using the SHELXTL-PLUS program package [7]. Significant crystal data are listed in Table 1.

Tables of atomic coordinates, anisotropic thermal parameters, full listings of bond lengths and angles, and observed and calculated structure factors are available as supplementary materials from the Editor.

RESULTS AND DISCUSSION

Synthesis and valence specificity of chelation

Two Schiff bases of type **1** abbreviated as HRL (R = Me, Et), have been used. The most convenient ruthenium(III) salt for synthesis has been found to be

Table 1. Crystal data collection and refinement parameters for $Ru(EtL)_2(PPh_3)Cl$

Molecular formula	$C_{40}H_{39}N_2O_4PClRu$
Molecular weight	778.84
Crystal system	Monoclinic
Space group	$P2_1/n$
a (Å)	18.194(10)
b (Å)	9.164(4)
c (Å)	23.697(12)
β (°)	106.24(4)
V (Å^3)	3793(3)
Z	4
D_c (g cm^{-3})	1.364
μ (Mo-K_α) (cm^{-1})	5.67
Temperature (°C)	22
Transmission coefficient	0.8052–0.9122
Total no. of reflections	6833
No. of unique reflections	6159
No. of observed reflections $[I > 3.0\sigma(I)]$	2216
No. of parameters refined	368
Final R^a	0.0538
Final $R_w{}^b$	0.0571
Goodness of fit (GOF)^c	1.12

^{a} $R = \Sigma \| F_o| - |F_c\| / \Sigma |F_o|$.
^{b} $R_w = [\Sigma w(\| F_o| - |F_c\|)^2 / \Sigma w |F_o|^2]^{1/2}$.
$w^{-1} = \sigma^2 |F_o| + g|F_o|^2$, $g = 0.0008$.
^{c} The GOF is defined as $[\Sigma w(|F_o| - |F_c|)^2/(n_o - n_v)]^{1/2}$, where n_o and n_v denote the number of data and variables, respectively.

$K_2RuCl_5(H_2O)$. It reacts with HRL in the presence of PPh_3 affording deep green $Ru^{III}(RL)_2(PPh_3)Cl$ in good yield. The complexes display C=O, C=N an Ru—Cl stretches at 1670, 1540 and 325 cm^{-1} respectively.

The reaction of $Ru^{II}(PPh_3)_3Cl_2$ with **1** proceeds *via* oxidative addition, the probable intermediate being **4**, which is subject to rearrangement and reductive proton elimination affording motif **2** [1,2]. When the starting material is $K_2Ru^{III}Cl_5(H_2O)$, the trivalent metal is unsuitable for oxidative addition and instead gets O,N-chelated at the salicylaldimine site. The salicylaldehyde site is a potential O,O-chelator [8], but in practice the stronger O,N-chelation prevails.

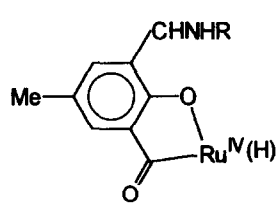

4

Geometry and bond parameters

The X-ray structure of $Ru(EtL)_2(PPh_3)Cl$ has been determined. A view of the molecule is shown in Fig. 1 and selected bond parameters are set out in Table 2. Both the EtL ligands are bonded as in motif **3**. The two phenolic oxygens lie *trans* to each other while the azomethine nitrogen atoms span *cis* positions in the distorted octahedral RuO_2N_2PCl coordination sphere. The six-membered RuC_3NO chelate rings are not quite planar due to a deviation (by 0.5–0.6 Å) of the metal atom from the excellent C_3NO plane (mean deviation, ~0.02 Å).

No other Ru^{III}-salicylaldimine species appear to have been structurally characterized and length data on authentic Ru^{III}—O bonds are rare [5,8]. The average distance in the present complex, 1.992(7) Å, compares well with that 1.981(2) Å in tris(salicylaldehydato)-ruthenium(III) [8]. In the few known [9] Ru^{II}-salicylaldimine structures, Ru^{II}—O lengths span the range 2.03–2.08 Å reflecting the increase of metal radius upon reduction. The *trans* influence [10] of PPh_3 in $Ru(EtL)_2(PPh_3)Cl$ is seen in the longer (by 0.06 Å) Ru—N(2) bond (*trans* ligand is PPh_3) compared with the Ru—N(1) bond (*trans* ligand is Cl).

A number of hydrogen atoms in the structure were directly located and these include the two aldehyde hydrogen atoms which were refined isotropically ($U = 0.08$ Å^2). The O(1), C(19), C(24), C(26) and H(26) atoms make an excellent plane (mean deviation 0.03 Å). The same applies to O(3), C(30), C(35), C(37) and H(37). The aldehyde C—H lengths are nearly equal to 1.1(1) Å. The average distance between the phenolic oxygen and aldehyde hydrogen atoms is 2.5(1) Å, suggesting the presence of weak CH···O hydrogen bonding as depicted in **3**. In contrast motif **2** is characterized by relatively stronger N—H···O hydrogen bonding between iminium hydrogen and phenolato oxygen [1,2].

Electronic structure

The complexes behave as one-electron paramagnets ($s = 1/2$) corresponding to the low-spin $d^5(t_2^5)$ configuration and are EPR-active (Table 3). The EPR spectra in frozen dichloromethane–toluene glass (77 K) are rhombic (Fig. 2) consistent with the X-ray structural geometry (C_1 symmetry). The spectra have been analysed using g-tensor theory [5,11,12] of low-spin d^5 ions (Table 3). The axial distortion (Δ) splits the t_2 shell into $e + b$ levels and the rhombic distortion (V) splits e further into two nondegenerate components (Fig. 2). Setting λ, the spin-orbit coupling constant of ruthenium(III), as 1000 cm^{-1} [13], two ligand field transitions are predicted near 4000 and 8500 cm^{-1} within the Kramers doublets (Table 3). The complexes indeed display two low intensity bands in the near-IR region at ~4500 and ~6500 cm^{-1} in

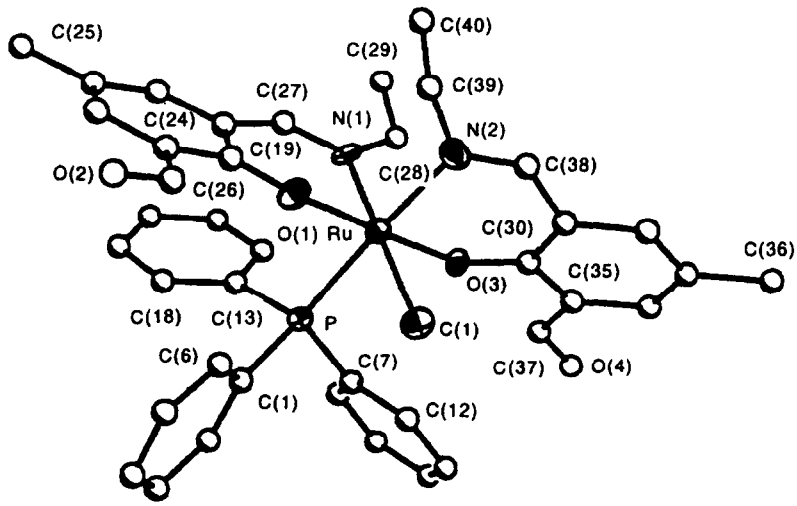

Fig. 1. Perspective view and atom labeling scheme for $Ru(EtL)_2(PPh_3)Cl$.

Table 2. Selected bond distances (Å) and angles (°) and their estimated standard deviations for $Ru(EtL)_2(PPh_3)Cl$

Ru—Cl	2.385(4)	Ru—P	2.375(3)
Ru—O(1)	1.999(7)	Ru—O(3)	1.986(7)
Ru—N(1)	2.036(9)	Ru—N(2)	2.099(10)
Cl—Ru—P	90.2(1)	Cl—Ru—O(1)	89.3(2)
P—Ru—O(1)	93.7(2)	Cl—Ru—O(3)	90.4(3)
P—Ru—O(3)	88.7(2)	O(1)—Ru—O(3)	177.6(3)
O(1)—Ru—N(1)	89.6(3)	O(3)—Ru—N(2)	89.3(3)
Cl—Ru—N(1)	178.3(3)	P—Ru—N(1)	91.2(3)
Cl—Ru—N(2)	85.9(3)	P—Ru—N(2)	175.6(3)
O(1)—Ru—N(2)	88.3(3)	O(3)—Ru—N(1)	90.7(3)
N(1)—Ru—N(2)	92.7(4)		

Table 3. Magnetic moment in the solid state (298 K), EPR g values in 1 : 1 dichloromethane/toluene glass (77 K), distortion parameters and transition energies

	μ_{eff}[a]	g_1	g_2	g_3	Δ/λ	V/λ	ν_1/λ	ν_2/λ
$Ru(EtL)_2(PPh_3)Cl$	1.90	2.364	2.106	1.878	5.966	−4.587	3.805	8.443
							(4.4)[b]	(6.7)[b]
$Ru(MeL)_2(PPh_3)Cl$	1.89	2.363	2.113	1.883	6.078	−4.577	3.917	8.546
							(4.4)[b]	(6.2)[b]

[a] B.M.
[b] Experimental values.

addition to the intense LMCT band near 16,000 cm^{-1} (Table 4, Fig. 3). In view of the many approximations involved in the theory, the agreement between calculated and experimental near-IR transition energies is quite satisfactory.

Metal redox

Bis-salicylaldiminato binding excellently stabilizes the trivalent state. This is reflected in the low ruthenium(III)/ruthenium(II) reduction potential (~ -0.4 V *vs* SCE, Table 4) of the quasireversible ($\Delta E_p = 100$ mv) cyclic voltammetric couple of eq. (1). The

$$Ru^{III}(RL)_2(PPh_3)Cl + e \rightleftharpoons Ru^{II}(RL)_2(PPh_3)Cl^- \quad (1)$$

corresponding ruthenium(IV)/ruthenium(III) couple is observed near ~ 0.9 V.

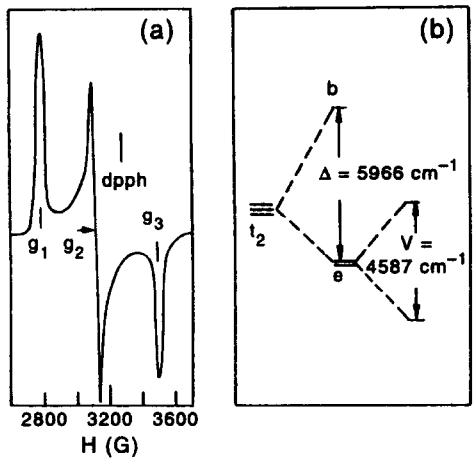

Fig. 2. (a) X-band EPR spectrum in dichloromethane-toluene (1 : 1) glass (77 K) and (b) t_2 splittings of $Ru(EtL)_2(PPh_3)Cl$.

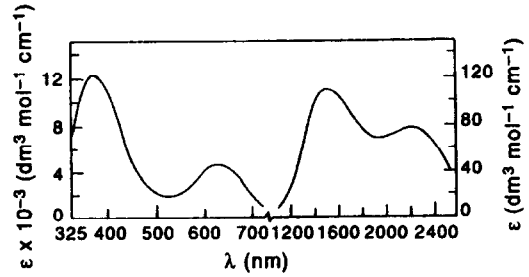

Fig. 3. Electronic spectrum of $Ru(EtL)_2(PPh_3)Cl$ in dichloromethane.

The complexes incorporating motif **2** are of type $Ru(RL')(PPh_3)_2(CO)Cl$, where Ru(RL')(CO) is motif **2**. Here the ruthenium(II) state is stabilized, the ruthenium(III)/ruthenium(II) reduction potential being ~0.5 V [2]. In this case the ruthenium(III) congeners are inherently unstable and could not be isolated.

CONCLUSION

It is shown that the Schiff mono-bases of 2,6-diformyl-4-methylphenol, HRL (R = Et, Me), **1**, react with $K_2RuCl_5(H_2O)$ affording ruthenium(III)-salicylaldimine complexes of the type $Ru^{III}(RL)_2(PPh_3)Cl$ in which the aldehyde functions remain uncoordinated. The system provides a remarkable valence specific contrast with the ruthenium(II) organometallic species (motif **2**) formed from the reaction of **1** with $Ru^{II}(PPh_3)_3Cl_2$. $Ru(EtL)_2(PPh_3)Cl$ represents the first case of structural characterization of a ruthenium(III)-salicylaldimine species. The two phenolic oxygen atoms and the two azomethine nitrogen atoms are respectively coordinated in mutually *trans* and *cis* positions. The PPh_3 molecule exerts significant trans influence on a Ru—N bond. The $Ru^{III}(RL)_2(PPh_3)Cl$ species display highly rhombic EPR spectra consistent with large axial and rhombic distortions. Predicted near-IR transitions without the Kramers doublets are observed experimentally. The complexes have relatively low metal redox potentials corresponding to stabilization of the ruthenium(III) state.

Acknowledgements—Financial support received from the Department of Science and Technology, New Delhi, Council of Scientific and Industrial Research, New Delhi, Indian National Science Academy, New Delhi, and affiliation with the Jawaharlal Nehru Centre for Advanced Scientific Research, Bangalore, India, are acknowledged.

REFERENCES

1. (a) Bag, N., Choudhury, S. B., Pramanik, A., Lahiri, G. K. and Chakravorty, A., *Inorg. Chem.*, 1990, **29**, 5013; (b) Bag, N., Choudhury, S. B., Lahiri, G. K. and Chakravorty, A., *J. Chem. Soc., Chem. Commun.*, 1990, 1626.
2. (a) Ghosh, P., Bag, N. and Chakravorty, A., *Organometallics*, 1996, **15**, 3042; (b) Ghosh, P., Pramanik, A. and Chakravorty, A., *Organometallics*, 1996, **15**, 4147; (c) Ghosh, P. and

Table 4. Electronic spectral and electrochemical data

Compound	Electronic spectra[a] λ_{max}, nm (ε^b, dm^3 mol^{-1} cm^{-1})	Electrochemical data[c] [$E_{1/2}$, V (ΔE_p, mV)] Ru^{III}/Ru^{II}	Ru^{IV}/Ru^{III}
$Ru(EtL)_2(PPh_3)Cl$	2250(80), 1500(110) 630(4840), 365(12,320)	−0.41(100)	0.95(100)
$Ru(MeL)_2(PPh_3)Cl$	2260(60), 1620(150) 620(3720), 365(11,780)	−0.51(120)	0.93(120)

[a] Solvent is dichloromethane.
[b] Extinction coefficient.
[c] Conditions: solvent, dichloromethane; supporting electrolyte, TEAP (0.1 M); working electrode, platinum; reference electrode, SCE; solute concentration, ~10^{-3} M; $E_{1/2} = 0.5(E_{pa} + E_{pc})$ at scan rate 50 mV s^{-1}, where E_{pa} and E_{pc} are anodic and cathodic peak potentials, respectively; $\Delta E_p = E_{pa} - E_{pc}$.

Chakravorty, A., *Inorg. Chem.*, 1997, **36,** 64; (d) Ghosh, P., *Polyhedron*, 1997, **16,** 1343.
3. Mercer, E. E. and Buckley, R. R., *Inorg. Chem.*, 1965, **4,** 1692.
4. (a) Ullmann, F. and Brittner, K., *Chem. Ber.*, 1909, **42,** 2539; (b) Gagne, R. R., Spiro, C. L., Smith, T. J., Hamann, C. A., Thies, T. J. and Shiemke, A. K., *J. Am. Chem. Soc.*, 1981, **103,** 4073.
5. Lahiri, G. K., Bhattacharya, S., Mukherjee, M., Mukherjee, A. K. and Chakravorty, A., *Inorg. Chem.*, 1987, **26,** 3359.
6. North, A. C. T., Phillips, D. C. and Mathews, F. A., *Acta Cryst.*, 1968, **A24,** 351.
7. Sheldrick, G. M., *SHELXTL-PLUS. Structure Determination Software Programs*. Siemens Analytical X-ray Instruments Inc., Madison, WI, 1990.
8. Bag, N., Lahiri, G. K., Bhattacharya, S., Falvello, L. R. and Chakravorty, A., *Inorg. Chem.*, 1988, **27,** 4396.
9. (a) Brunner, H., Oeschey, R. and Nuber, B., *J. Chem. Soc., Dalton Trans.*, 1996, 1499; (b) Leung, W.-H., Chan, E. Y. Y., Chow, E. K. F., Williams, I. D. and Peng, S., *J. Chem. Soc., Dalton Trans.*, 1996, 1229; (c) Mondal, S. K. and Chakravarty, A. R., *Inorg. Chem.*, 1993, **32,** 3851; (d) Odenkirk, W., Rheingold, A. L. and Bosnich, B., *J. Am. Chem. Soc.*, 1992, **114,** 6392; (e) Mondal, S. K. and Chakravarty, A. R., *J. Chem. Soc., Dalton Trans.*, 1992, 1627.
10. Huheey, J. E., Keiter, E. A. and Keiter, R. L., *Inorganic Chemistry: Principles of Structure and Reactivity*, 4th edn. HarperCollins College Publishers, NY, 1993.
11. Lahiri, G. K., Bhattacharya, S., Ghosh, B. K. and Chakravorty, A., *Inorg. Chem.*, 1987, **26,** 4344.
12. (a) Bleany, B. and O'Brien, M. C. M., *Proc. Phys. Soc. London, Sect. B*, 1956, **69,** 1216; (b) Griffith, J. S., *The Theory of Transitional Metal Ions*, Cambridge University Press, London, 1961, p. 364.
13. (a) Hill, N. J., *J. Chem. Soc., Faraday Trans.*, 1972, **2,** 427; (b) Daul, C. and Goursot, A., *Inorg. Chem.*, 1985, **24,** 3554.

Pergamon

Polyhedron Vol. 15, No. 7, pp. 1121–1127, 1996

0277-5387/96 $15.00+0.00

0277-5387(95)00348-7

SYNTHESIS, STRUCTURE AND METAL REDOX OF A FAMILY OF COPPER COMPLEXES DERIVED FROM HEXADENTATE LIGANDS INCORPORATING THIOETHER AND TRIAZENE 1-OXIDE FUNCTIONS

SUJAY PATTANAYAK, PARTHA CHAKRABORTY, SWAPAN KUMAR CHANDRA and ANIMESH CHAKRAVORTY*

Department of Inorganic Chemistry, Indian Association for the Cultivation of Science, Calcutta 700 032, India

(*Received* 26 *June* 1995; *accepted* 26 *July* 1995)

Abstract—Hexadentate ligands of type $RN(O)NN(H)C_6H_4S(CH_2)_xSC_6H_4(H)NN(O)NR$ (H_2L^1: R = Me, $x = 2$; H_2L^2: R = Ph, $x = 2$; H_2L^3: R = Me, $x = 3$; general abbreviation H_2L) have afforded copper(II) complexes of type [CuL]. The X-ray structure of $[CuL^2] \cdot 1/2CH_2Cl_2$ reveals the presence of a distorted $CuS_2N_2O_2$ coordination sphere which is strongly elongated along an OCuS axis. The axial and equatorial bond lengths are: Cu—S, 2.636(5) and 2.473(6) Å; Cu—O, 2.222(10) and 2.039(11) Å, respectively. Both the Cu—N bonds, 1.939(13) and 1.904(12) Å, lie on the equatorial plane. The structure is compared with that of $[ZnL^2] \cdot 1/2CH_2Cl_2$, which does not display the above-noted axial elongation. The findings are rationalized in terms of simple angular overlap considerations. The EPR spectrum of $[CuL^2] \cdot 1/2CH_2Cl_2$ has $g_\parallel > g_\perp$, showing that the hole lies in the $d_{x^2-y^2}$ orbital. The [CuL] complexes are electroactive in dichloromethane solutions and successive quasi-reversible responses due to the $[Cu^{II}L]/[Cu^{I}L]^-$ and $[Cu^{III}L]^+/[Cu^{II}L]$ couples are observed, the $E_{1/2}$ values being ~ -0.9 V and ~ 0.8 V vs SCE, respectively. The $E_{1/2}$ of the copper(III)–copper(II) couple lies close to that of the corresponding nickel(III)–nickel(II) couple of [NiL]. A thermodynamic rationale is provided.

The hexadentate ligand system H_2L (**1**), incorporating triazene 1-oxide and thioether functions, is known to bind a number of bivalent and trivalent 3*d* ions. The complexes are of type ML^z (**2**), having pseudo-octahedral $MS_2N_2O_2$ coordination spheres.[1–6] The ML^z species have furnished rare examples of metal–thioether binding[1,2,5,6] and of reactivity associated with such binding.[3] Herein we describe the synthesis, structure and electrochemistry of the copper(II) family [CuL]. Comparisons are made with neighbouring families: with [ZnL] in the context of copper-specific structural distortions and with [NiL] in relation to the reduction potential of the $[M^{III}L]^+/[M^{II}L]$ couple. We note in passing that thioether coordination chemistry of copper has received a good deal of attention in recent years for bioinorganic reasons.[7]

EXPERIMENTAL

Materials

Commercially available chemicals and solvents were used for the preparation of ligands and complexes. The diamines 1,2-bis(2-aminophenylthio)ethane and 1,3-bis(2-aminophenylthio) propane[8] and the hydroxylamines (*N*-methyl and *N*-phenyl)[9] were prepared as before. The ligands were synthesized by reported procedures.[4a,10,11] The purification of dichloromethane and preparation of tetraethylammonium perchlorate were done as before.[12]

*Author to whom correspondence should be addressed.

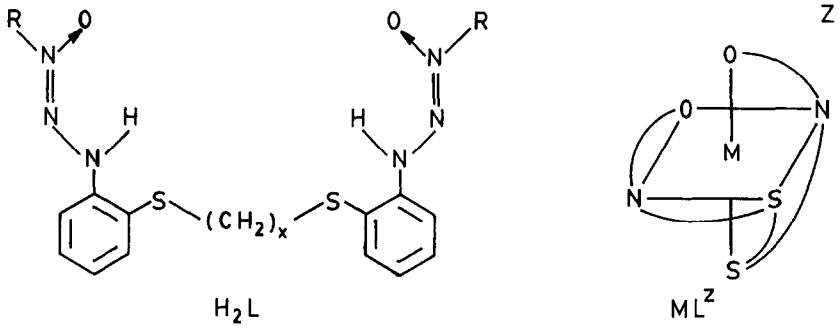

H_2L ML^Z

R = Me, x = 2 H_2L^1 Z = 0, M^{II}

R = Ph, x = 2 H_2L^2 Z = +, M^{III}

R = Me, x = 3 H_2L^3

1 2

Structures 1 and 2.

Physical measurements

Electronic and IR spectral data were collected with Hitachi 330 and Perkin–Elmer Model 783 spectrophotometers, respectively. Magnetic susceptibilities of solids were measured by using a PAR-155 vibrating sample magnetometer fitted with a Walker Scientific L75FBAL magnet. EPR spectra were recorded in the X-band using a Varian 109C spectrometer fitted with a quartz dewar, and DPPH ($g = 2.0037$) was used for calibration. Microanalytical data were collected with a Perkin–Elmer 240C elemental analyser. Redox potentials were measured using a PAR Model 370-4 electrochemistry system, as reported earlier.[13]

Synthesis of the complexes

All complexes were synthesized by similar methods. Details are given here for $[CuL^2]\cdot 1/2CH_2Cl_2$.

((1,2 - *Bis*((o - 1 - *phenyl* - 1 - *oxidotriazen* - 3 - *yl*) *phenyl*)*thio*)*ethanato*-N^3,S,O)*copper*(II) *dichloromethane adduct*. A methanolic (10 cm^3) solution of potassium hydroxide (87 mg, 1.55 mmol) was added to the straw-yellow solution of ligand H_2L^2 (400 mg, 0.78 mmol) in dichloromethane (15 cm^3). The resulting light red solution was stirred in air for 30 min. A methanolic solution (20 cm^3) of 155 mg of copper(II) acetate monohydrate (0.77 mmol) was added to the reaction mixture. Immediate precipitation of a crystalline brown compound occurred. The product was filtered, washed with water and methanol and finally dried *in vacuo* over P_4O_{10}. Yield: 382 mg (85%). Found: C, 51.1; H, 3.7; N, 13.5. Calc. for $C_{26.50}H_{23}N_6O_2S_2ClCu$: C, 51.2; H, 3.7; N, 13.6%.

The other complexes $[CuL^1]$ and $[CuL^3]$ were synthesized similarly in 82% yield. In these cases no solvent of crystallization was present. Found: C, 42.3; H, 4.0; N, 18.3. Calc. for $C_{16}H_{18}N_6O_2S_2Cu$ (CuL^1): C, 42.3; H, 4.0; N, 18.3%. Found: C, 43.5; H, 4.2; N, 18.1. Calc. for $C_{17}H_{20}N_6O_2S_2Cu$ (CuL^3): C, 43.6; H, 4.3; N, 18.0%.

X-ray structure determination

Cell parameters of a single crystal of $[CuL^2]\cdot 1/2CH_2Cl_2$ grown by slow diffusion of toluene into dichloromethane solution were determined by least-squares fits of 30 machine-centred reflections ($2\theta = 15$–$30°$). Lattice dimensions and laue groups were checked by axial photography. Data were collected at 296 K on a Nicolet R3m/V diffractometer with graphite-monochromated Mo-K_α ($\lambda = 0.71073$ Å) radiation. Two check reflections measured after every 98 reflections showed no intensity variation during ~39 h exposure to X-rays. The structure was solved by direct methods and was refined by full-matrix least-squares procedures. Due to paucity of the observed data, only the following non-hydrogen atoms were refined anisotropically: Cu, S, O, N(3), N(4), Cl(1) and C(27). Hydrogen atoms were added at calculated positions with fixed $U = 0.08$ Å^2 in the final refinement cycle. Crystallographic data and other parameters are collected in Table 1. All calculations were carried out on a MicroVax II computer with programmes of SHELXTL-PLUS.[14]

Table 1. Crystal data, intensity data collection and structural refinement for $[CuL^2] \cdot 1/2CH_2Cl_2$

Formula	$C_{26.50}H_{23}N_6O_2S_2ClCu$
Crystal size (mm)	$0.18 \times 0.22 \times 0.42$
Crystal system	Orthorhombic
Space group	*Pbcb*
a (Å)	9.622(5)
b (Å)	19.206(7)
c (Å)	28.924(11)
U (Å^3)	5345(4)
Z	8
M	620.6
D_c (g cm^{-3})	1.542
μ (Mo-K_α) (cm^{-1})	11.05
$F(000)$	2544
2θ range (°)	2–45
Total no. of reflections	4019
No. of unique reflections	3510
No. of observed reflections [$I > 2.5\sigma(I)$]	1158
Weighing scheme g in $w = 1/[\sigma^2(F) + gF^2]$	0.0001
No. of parameters refined	198
Final R	0.0770
Final R_w	0.0713
Goodness-of-fit	0.90
Largest and mean Δ/σ	0.306, 0.004
Data-to-parameter ratio	6 : 1
Largest difference peak (e Å^{-3})	0.54
Largest difference hole (e Å^{-3})	−1.15

Tables of atomic coordinates, anisotropic thermal parameters, full listings of bond lengths and angles, and observed and calculated structure factors are available as supplementary materials from the Editor.

RESULTS AND DISCUSSION

Synthesis and characterization

The H_2L ligands were synthesized by coupling appropriate tetra-azotized aromatic diamines with substituted hydroxylamines.[4a,10,11] Specific ligand abbreviations (H_2L^1, H_2L^2 and H_2L^3) are set out in **1**. The reaction of H_2L with copper(II) acetate monohydrate in mixed dichloromethane–methanol solution afforded the brown to red complexes, $[CuL^1]$, $[CuL^2] \cdot 1/2CH_2Cl_2$ and $[CuL^3]$ in excellent yields.

Selected characterization data are set out in Table 2. The complexes display N_3 and NO vibrations[15] of triazene 1-oxide chelate rings in the ranges 1390–1460 and 1210–1235 cm^{-1}, respectively. The absorption spectrum of a representative complex is shown in Fig. 1a. The band in the region 880–970 nm is associated with two shoulders, one on each side. These are assigned to split components (low symmetry) of the octahedral $t_2 \rightarrow e$ transition.

The effective magnetic moments of the complexes lie in the range 1.98–2.05 B.M. corresponding to the d^9 configuration. The EPR spectrum of a representative complex in dichloromethane–toluene glass (77 K) is shown in Fig. 1b. The spectrum is relatively broad but is grossly axial in nature, with $g_\parallel > g_\perp$ corresponding to a $(d_{x^2-y^2})^1$ ground state. This is consistent with the elongated structure revealed by the X-ray work reported below. Because of signal broadness, metal hyperfine structure could not be resolved.

X-ray structure of $[CuL^2] \cdot 1/2CH_2Cl_2$

The orthorhombic lattice consists of discrete $[CuL^2]$ and CH_2Cl_2 molecules, the latter occupying a special position (two-fold axis through the carbon atom). A perspective view of the $[CuL^2]$ molecule is shown in Fig. 2 and bond distances in the coordination sphere are given in Fig. 3. Selected bond angles are listed in Table 3. Both the thioether sulphurs are coordinated to metal and the ligand acts in hexadentate fashion, affording a $CuS_2N_2O_2$ coordination sphere.

Table 2. Electronic spectra,[a] IR spectra[b] and magnetic moments[c]

Compound	λ (nm) (ε, $dm^3mol^{-1}cm^{-1}$)	ν(NO) (cm^{-1})	$\nu(N_3)$ (cm^{-1})	μ_{eff} (B. M.)
[CuL^1]	1275[d](203), 965 (290), 630[d](270)	1235	1460	2.05
[CuL^2]·$1/2CH_2Cl_2$	1275[d](190), 960 (270), 530[d](320)	1210	1390	2.02
[CuL^3]	1275[d](204), 880 (340), 630[d](390)	1215	1410	1.98

[a] Solvent is dichloromethane.
[b] In KBr discs.
[c] In the solid state at 298 K.
[d] Shoulder.

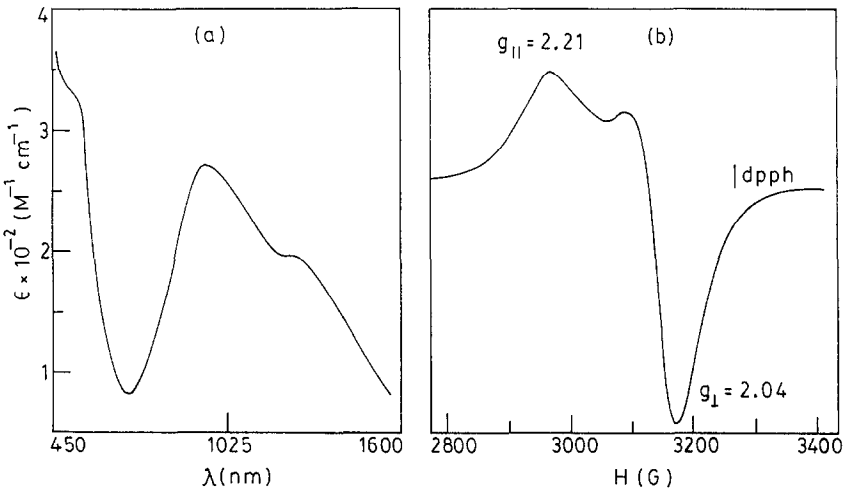

Fig. 1. (a) Electronic spectrum of [CuL^2]·$1/2CH_2Cl_2$ in dichloromethane. (b) X-band EPR spectrum of [CuL^2]·$1/2CH_2Cl_2$ in dichloromethane–toluene (1 : 1) glass at 77 K.

Angular distortions from formal octahedral symmetry are large. The angles between *trans* atoms at the metal centre are: S(1)—Cu—O(1) 160.0(4)°, S(2)—Cu—O(2) 155.0(3)° and N(3)—Cu—N(4) 174.8(6)°. The *cis* angles span a wide range, 76.0(5)–109.0(5)° (Table 3). All the five-membered chelate rings incorporating N,O- and N,S-chelation constitute good planes (mean deviation 0.02–0.04 Å). The dimethylene bridge of the five-membered CuS_2C_2 ring has *gauche* configuration.

Roughly speaking, the coordination geometry of copper(II) is a strongly elongated octahedron, with O(2)CuS(2) defining the axis of elongation (Fig. 3). The length disparity between axial and equatorial Cu—O or Cu—S bonds is ~0.2 Å. The shortest bonds on the equatorial plane are those with nitrogen.

Comparison with [ZnL^2]·$1/2CH_2Cl_2$: *copper-specific distortions*

The zinc(II) complex[5] belongs to the same space group as the copper(II) congener, and the cell dimensions of the two complexes are also very similar. However, the two complexes are far from being isometric, as can be seen in Fig. 3. This is not a radius effect, since the radii of Cu^{2+} (0.73 Å) and Zn^{2+} (0.74 Å) are nearly the same,[16] and further, the changes are not at all monotonic. For a given donor atom X, we have on average, Cu—X(ax) > Zn—X(ax) by ~0.2 Å and Cu—X(eq) < Zn—X(eq) by ~0.1 Å (ax = axial; eq = equatorial). Here, O(2)MS(2) is the axis and MS(1)O(1)N(1)N(2) is the equator.

Since the zinc(II) ion is spherical (d^{10}), the coor-

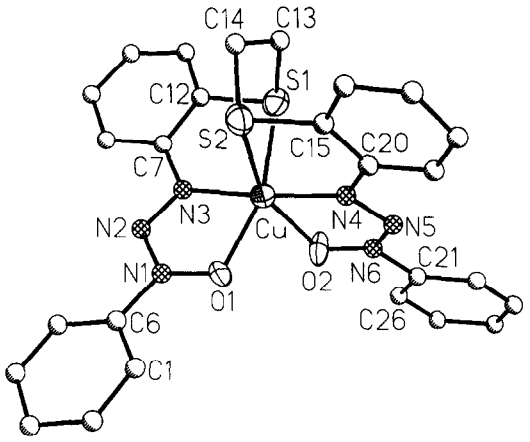

Fig. 2. Perspective view and atom labelling scheme of $[CuL^2]$ in $[CuL^2]\cdot 1/2CH_2Cl_2$ crystals with copper, oxygen and sulphur atoms represented by their 30% probability ellipsoids.

dination geometry in $[ZnL^2]$ is controlled by the natural constraints of the ligand system. The geometry is already highly distorted from the octahedron and if these were given to copper(II), the Jahn–Teller theorem will not apply. The observed "additional" distortions in $[CuL^2]$ (Fig. 3) can, however, be qualitatively rationalized in terms of anisotropy of binding, consistent with angular overlap considerations.[17]

The EPR result, $g_\parallel > g_\perp$, requires that $d_{x^2-y^2}$ lie above d_{z^2} and we have the configuration $(d_{z^2})^2(d_{x^2-y^2})^1$ for the antibonding copper d electrons. The corresponding bonding levels are, of course, doubly occupied. One therefore expects a net σ-bonding in the equatorial plane due to the $d_{x^2-y^2}$ interaction. The d_{z^2} (fully occupied) interaction, however, does not contribute to bonding and the axial ligands are held by $s+p$ orbital interactions only. In the case of zinc(II), $(d_{z^2})^2(d_{x^2-y^2})^2$, the d interactions are not effective either on the equator or the axis.[17]

Metal redox

In dichloromethane solution (0.1 M in TEAP), the [CuL] complexes display well-defined cyclic voltammograms at platinum working electrodes. Two one-electron quasi-reversible cyclic responses are observed. Representative voltammograms are shown in Fig. 4. Reduction potential (vs SCE) and coulometric data are listed in Table 4.

The responses at lower (~ -0.9 V) and higher (~ 0.8 V) potentials are assigned to the couples of eqs (1) and (2), respectively:

$$[Cu^{II}L] + e^- \rightleftharpoons [Cu^{I}L]^- \quad (1)$$

$$[Cu^{III}L]^+ + e^- \rightleftharpoons [Cu^{II}L]. \quad (2)$$

Constant potential coulometric reduction at ~ -1.2 V affords a one-electron count, but the reduced complex is too unstable for isolation. On the other hand, coulometry at $\sim$I V in cold (245 K) dichloromethane solution leads to one-electron oxidation. The oxidized solutions are stable enough for their cyclic voltammograms to be recorded. Such voltammograms are the same as those of [CuL] (Fig. 4), showing that there is no gross coordination change in going from [CuL] to $[CuL]^+$. We, however, have not succeeded in isolating salts

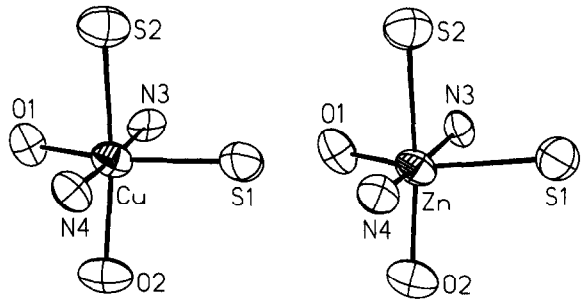

M—S(1)	2.473(6)	2.688(3)
M—S(2)	2.636(5)	2.680(4)
M—O(1)	2.039(11)	2.078(6)
M—O(2)	2.222(10)	2.056(7)
M—N(3)	1.904(12)	2.029(8)
M—N(4)	1.939(13)	2.005(8)

Fig. 3. Bond lengths (Å) within the metal coordination spheres in $[ML^2]\cdot 1/2CH_2Cl_2$ (M = Cu, Zn) with the estimated standard deviations given in parentheses.

Table 3. Selected bond angles (°)[a] for $[CuL^2] \cdot 1/2CH_2Cl_2$

S(1)—Cu—S(2)	86.8(2)	S(1)—Cu—N(3)	82.1(4)
S(2)—Cu—N(3)	95.7(5)	S(1)—Cu—N(4)	96.3(4)
S(2)—Cu—N(4)	79.2(4)	N(3)—Cu—N(4)	174.8(6)
S(1)—Cu—O(1)	160.0(4)	S(2)—Cu—O(1)	95.0(3)
N(3)—Cu—O(1)	78.0(5)	N(4)—Cu—O(1)	103.6(5)
S(1)—Cu—O(2)	93.4(4)	S(2)—Cu—O(2)	155.0(3)
N(3)—Cu—O(2)	109.0(5)	N(4)—Cu—O(2)	76.0(5)
O(1)—Cu—O(2)	93.3(4)		

[a] Estimated standard deviations are given in parentheses.

of $[CuL]^+$. We note that the d^8 complex $[Cu^{III}L]^+$ is isoelectronic with the well characterized high-spin $[Ni^{II}L]$ species.[4a]

Trend of $[M^{III}L]^+/[M^{II}L]$ *reduction potentials*: M = Cu *and* Ni

In strongly held pseudo-octahedral complexes with population in antibonding metal orbitals (d_{z^2}, $d_{x^2-y^2}$), removal of one or more electrons may become facile, leading to higher oxidation states.[4b,18] This indeed happens in the case of $[NiL]$[4a] (d^8), which displays the couple of eq. (3) with $E_{1/2}$ value of 0.75 V vs SCE. The copper couple

$$[Ni^{III}L]^+ + e^- \rightleftharpoons [Ni^{II}L] \qquad (3)$$

of eq. (2) can be similarly rationalized. The zinc complex [ZnL] is electrochemically inactive due to the stability of the d^{10} configuration.

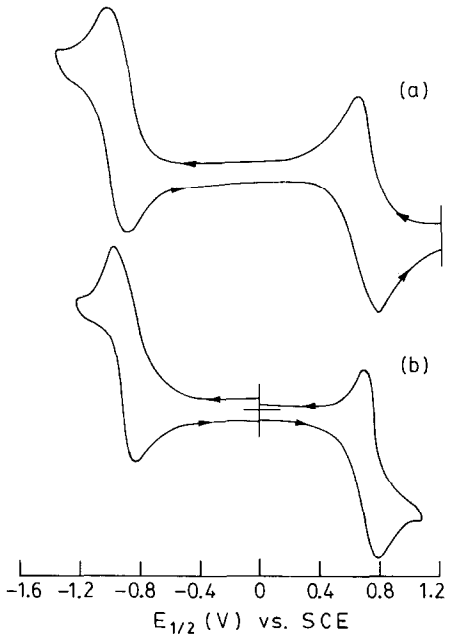

Fig. 4. Cyclic voltammograms (scan rate 50 mV s^{-1}) of $\sim 10^{-3}$ mol dm^{-3} solutions in dichloromethane (0.1 mol dm^{-3} TEAP): (a) electrogenerated $[CuL^3]^+$; (b) $[CuL^3]$.

Among similarly constituted molecules, the approximate relation of eq. (4) holds.[19-21] Here F is the Faraday, I_3 is the third ionization

$$FE_{1/2} = I_3 - \Delta H_f^\circ + k \qquad (4)$$

potential of the metal, ΔH_f° is the difference between the enthalpy of formation of the reduced, $[M^{II}L]$, and oxidized, $[M^{III}L]^+$, complexes in that order and k is a constant. The ΔH_f° parameter varies from one metal to another, an important contributing factor being the crystal field stabilization energy (CFSE).[22] In order to make a rough estimate we assume octahedral geometry and $Dq^{II} \sim 1000$ cm^{-1} and $Dq^{III} \sim 2000$ cm^{-1}.[4a,6] The crucial variable quantity is $Q = I_3 - \Delta C + P$, where ΔC equals CFSE (bivalent) minus CFSE (trivalent) and P is the pairing energy, if any.

In the case of copper, I_3 is 36.84 eV[23] and ΔC equals $-6Dq^{II} + 12Dq^{III}$ or 2.23 eV, leading to $Q = 34.61$ eV (P is zero). For nickel, I_3 is 35.16 eV,[23] ΔC is $-12Dq^{II} + 18Dq^{III}$ or 2.98 eV and P ($[NiL]^+$ is low-spin) is 2.91 eV,[24] yielding $Q = 35.09$ eV. Thus, the Q values of copper and nickel lie close to each other and so do the $E_{1/2}$ values.

CONCLUSIONS

The H_2L ligands afford stable, pseudo-octahedral copper(II) complexes of type [CuL]. The $CuS_2N_2O_2$ coordination sphere has a strong axial elongation which is absent in [ZnL]. The equatorial bond lengths, however, follow the order [CuL] < [ZnL]. These findings are qualitatively consistent with simple bonding–antibonding consideration. In [CuL] the hole lies in $d_{x^2-y^2}$ (EPR).

The [CuL] complexes display successive electrochemical Cu^{II}/Cu^{I} and Cu^{III}/Cu^{II} couples. The $E_{1/2}$ value of the Cu^{III}/Cu^{II} couple lies close to that of the corresponding Ni^{III}/Ni^{II} couple. This is in line with thermodynamic considerations.

Table 4. Electrochemical data[a]

Compound	Copper(II)–copper(I) $E_{1/2}$,[b] V (ΔE_p,[c] mV)	n[d]	Copper(III)–copper(II) $E_{1/2}$,[b] V (ΔE_p,[c] mV)	n[e]
[CuL^1]	−0.92 (90)	0.89	0.71 (90)	1.02
[CuL^2]·1/2CH_2Cl_2	−0.80 (130)	0.92	0.77 (90)	0.99
[CuL^3]	−0.91 (140)	0.88	0.75 (120)	0.92

[a] In CH_2Cl_2 (0.1 M TEAP) at a platinum electrode with an SCE reference.
[b] From cyclic voltammetry at a scan rate of 50 mV s^{-1}.
[c] Peak-to-peak separation.
[d] $n = Q/Q'$, where Q is the observed coulomb count and Q' is the calculated coulomb count for 1e transfer at 298 K.
[e] n is the ratio of observed : calculated coulomb counts at 245 K.

Acknowledgements—Financial support received from the Department of Science and Technology, New Delhi, Council of Scientific and Industrial Research, New Delhi and Jawaharlal Nehru Centre for Advanced Scientific Research, Bangalore is acknowledged.

REFERENCES

1. P. Chakraborty, S. K. Chandra and A. Chakravorty, *Inorg. Chem.* 1993, **32**, 5349.
2. P. Chakraborty, S. K. Chandra and A. Chakravorty, *Inorg. Chem.* 1994, **33**, 6429.
3. (a) P. Chakraborty, S. K. Chandra and A. Chakravorty, *Organometallics* 1993, **12**, 4726; (b) P. Chakraborty, S. Karmakar, S. K. Chandra and A. Chakravorty, *Inorg. Chem.* 1994, **33**, 816.
4. (a) S. Karmakar, S. B. Choudhury, D. Ray and A. Chakravorty, *Polyhedron* 1993, **12**, 291. (b) D. Ray, S. Pal and A. Chakravorty, *Inorg. Chem.* 1986, **25**, 2674; (c) S. Karmakar, S. B. Choudhury, D. Ray and A. Chakravorty, *Polyhedron* 1993, **12**, 2325.
5. P. Chakraborty, S. K. Chandra and A. Chakravorty, *Inorg. Chim. Acta* 1995, **229**, 477.
6. S. Pattanayak, D. K. Das, P. Chakraborty and A. Chakravorty, unpublished result.
7. (a) E. Bouwman, W. L. Driessen and J. Reedijk, *Coord. Chem. Rev.* 1990, **104**, 143; (b) E. I. Solomon, K. W. Penfield and D. E. Wilcox, *Struct. Bonding (Berlin)* 1983, **53**, 1; (c) B. P. Murphy, *Coord. Chem. Rev.* 1993, **124**, 63.
8. O. Unger, *Chem. Ber.* 1897, **30**, 607.
9. A. Chakravorty, B. Behera and P. S. Zacharias, *Inorg. Chim. Acta* 1968, **2**, 85.
10. P. S. Zacharias and A. Chakravorty, *Inorg. Chem.* 1971, **10**, 1961.
11. K. Mukkanti, Y. K. Bhoon, K. B. Pandeya and R. P. Singh, *J. Indian Chem. Soc.* 1982, **59**, 830.
12. D. Datta, P. K. Mascharak and A. Chakravorty, *Inorg. Chem.* 1981, **20**, 1673.
13. S. K. Chandra, P. Basu, D. Ray, S. Pal and A. Chakravorty, *Inorg. Chem.* 1990, **29**, 2423.
14. G. M. Sheldrick, SHELXTL-PLUS 88, Structure Determination Software Program. Nicolet Instrument Corporation, Madison (1988).
15. R. L. Dutta and R. Sharma, *J. Inorg. Nucl. Chem.* 1980, **42**, 1204.
16. R. D. Shannon, *Acta Cryst.* 1976, **A32**, 751.
17. J. K. Burdett, *Advances in Inorganic Chemistry and Radiochemistry*, Vol. 21, p. 113. Academic Press, New York (1978).
18. (a) J. G. Mohanty, R. P. Singh and A. Chakravorty, Inorg. Chem. 1975, **14**, 2178; (b) S. B. Choudhury, D. Ray and A. Chakravorty, *Inorg. Chem.* 1991, **30**, 4354.
19. S. Dutta, P. Basu and A. Chakravorty, *Inorg. Chem.* 1991, **30**, 4031.
20. R. N. Mukherjee, O. A. Rajan and A. Chakravorty, *Inorg. Chem.* 1982, **21**, 785.
21. (a) G. I. H. Hanania, D. H. Irvine, W. A. Eaton and P. George, *J. Phys. Chem.* 1967, **71**, 2022; (b) E. L. Yee, R. J. Cave, K. L. Guyer, P. D. Tyma and M. J. Weaver, *J. Am. Chem. Soc.* 1979, **101**, 1131.
22. B. N. Figgis, *Introduction to Ligand Fields*, p. 75. John Wiley, New York (1966).
23. D. F. Shriver, P. W. Atkins and C. H. Langford, *Inorganic Chemistry*, p. 638. Oxford University Press, Oxford (1991).
24. A. B. P. Lever, *Studies in Physical and Theoretical Chemistry* 33; *Inorganic Electronic Spectroscopy*, 2nd edn, p. 750. Elsevier Science, Amsterdam (1984).

Binding of Thioether Sulfur to Trivalent Chromium. A Family of $CrS_2N_2O_2$ Complexes Derived from Acyclic Ligands

Sujay Pattanayak, Diganta Kumar Das, Partha Chakraborty, and Animesh Chakravorty*

Department of Inorganic Chemistry, Indian Association for the Cultivation of Science, Calcutta 700 032, India

Received May 5, 1995

Introduction

We are interested in thioether binding of 3d-ions.[1−5] The thioether group is a poor ligand, and stable binding is best achieved with the help of macrocyclic ligands.[6,7] The problem of thioether coordination is especially acute for the hard trivalent ions, and very few authentic complexes of manganese(III)[2,8] and iron(III)[4,9] have been described. The chromium(III) situation is even worse,[10] and only very recently were two complexes, both macrocyclic, structurally characterized.[11,12]

Herein we describe a family of stable chromium complexes of coordination type $Cr^{III}S_2N_2O_2$ derived from an acyclic hexadentate ligand. A representative X-ray structure is presented along with spectra and the electrochemistry of the family.

Results and Discussion

Synthesis. The ligand system used is **1**, abbreviated H_2RxL. It was chosen because of its proven affinity for manganese(III)[2] and iron(III).[4] When stoichiometric quantities of H_2RxL and chromium(III) chloride tetrahydrate were heated in a dichloromethane−methanol mixture, the solution color changed from light green to deep brown, and upon addition of sodium perchlorate the dark-colored complex $[Cr(RxL)]ClO_4$ separated in very good yield. In acetonitrile solution the complexes behave as 1:1 electrolytes (Δ = 115−125 Ω^{-1} cm^2 M^{-1}).

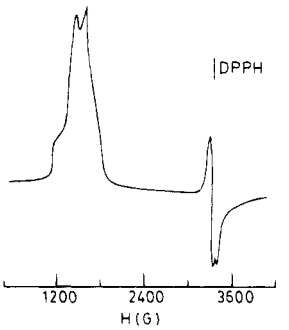

Figure 1. (a) EPR spectrum at X-band of $[Cr(Me3L)]ClO_4$ in dichloromethane−toluene (1:1) at 77 K. Instrument settings: power, 30 dB; modulation, 100 kHz; sweep center, 3000 G; sweep width, 8000 G; sweep time, 240 s, microwave frequency, 9.10 GHz.

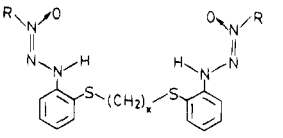

1

Magnetism, Spectra, and Electrochemistry. Selected characterization data are listed in Table 1. The magnetic moment of the complexes corresponds to the $S = {}^3/_2$ ground state. Their EPR spectra were examined in frozen (77 K) 1:1 dichloromethane−toluene solution. Two main resonance domains are g = 5.6−3.5 and $g \sim 2$, the former being more intense, corresponding to strong rhombic distortion.[13] The representative case of $[Cr(Me3L)]ClO_4$ is displayed in Figure 1.

Several electronic bands are observed in the form of shoulders in the visible region. The bands at ~850 and ~650 nm are assigned to an octahedral ν_1 transition split by the low symmetry of ligand field.[14] The average D_q value is computed to be 1360 cm^{-1}. A similar splitting has been recorded in the case of $Ni^{II}(RxL)$,[3d] for which the average D_q value is 860 cm^{-1}.

All the complexes exhibit a one-electron quasireversible cyclic voltammogram near −0.1 V versus SCE, corresponding to the metal redox potential. The $E_{1/2}$ values of the $M^{III}(RxL)^+-M^{II}(RxL)$ couple for M = Mn[2] and M = Fe[4] (both oxidation states high-spin) are known, and we can now observe the $E_{1/2}$ order Mn > Fe > Cr. Interestingly, there is a correlation between the $E_{1/2}$ values of the $M^{III}(RxL)^+-M^{II}(RxL)$ and $M^{III}(H_2O)_6^{3+}-M^{II}(H_2O)_6^{2+}$ couples.[15,16]

Structure. The structure of $[Cr(Me3L)]ClO_4 \cdot {}^1/_2CH_2Cl_2$ has been determined. A view of the cations is shown in Figure 2. The asymmetric unit contains two independent but metrically similar molecules which differ in their configurations. The two thioether sites in a given molecule have the same chiral configuration, which is enantiomeric to that in the other molecule. The configurations of the chromium sites are also mutually enantiomeric. The asymmetric unit is thus constituted

* Author to whom correspondence should be addressed. Fax: +91-33-473-2805. E-mail: icac@iacs.ernet.in.

(1) (a) Chakraborty, P.; Chandra, S. K.; Chakravorty, A. *Organometallics* **1993**, *12*, 4726. (b) Chakraborty, P.; Karmakar, S.; Chandra, S. K.; Chakravorty, A. *Inorg. Chem.* **1994**, *33*, 816. (c) Chakraborty, P.; Chandra, S. K.; Chakravorty, A. *Inorg. Chem.* **1994**, *33*, 4959.
(2) (a) Chakraborty, P.; Chandra, S. K.; Chakravorty, A. *Inorg. Chem.* **1993**, *32*, 5349. (b) Karmakar, S.; Choudhury, S. B.; Chakravorty, A. *Inorg. Chem.* **1994**, *33*, 6148.
(3) (a) Ray, D.; Pal, S.; Chakravorty, A. *Inorg. Chem.* **1986**, *25*, 2674. (b) Choudhury, S. B.; Ray, D.; Chakravorty, A. *Inorg. Chem.* **1991**, *30*, 4354. (c) Choudhury, S. B.; Ray, D.; Chakravorty, A. *J. Chem. Soc., Dalton Trans.* **1992**, 107. (d) Karmakar, S.; Choudhury, S. B.; Ray, D.; Chakravorty, A. *Polyhedron* **1993**, *12*, 291.
(4) Chakraborty, P.; Chandra, S. K.; Chakravorty, A. *Inorg. Chem.* **1994**, *33*, 6429.
(5) Chakraborty, P.; Chandra, S. K.; Chakravorty, A. *Inorg. Chim. Acta* **1995**, *229*, 477.
(6) Blake, A. J.; Schröder, M. *Adv. Inorg. Chem.* **1990**, *35*, 1.
(7) Cooper, S. R.; Rawle, S. C. *Struct. Bonding (Berlin)* **1990**, *72*, 1.
(8) (a) Doedens, R. J.; Veal, J. T.; Little, R. G. *Inorg. Chem.* **1975**, *14*, 1138. (b) Elias, H.; Schmidt, C.; Küppers, H.-J.; Wieghardt, K.; Nuber, B.; Weiss, J. *Inorg. Chem.* **1989**, *28*, 3021. (c) Tomita, M.; Matsumoto, N.; Agaki, H.; Okawa, H.; Kida, S. *J. Chem. Soc., Dalton Trans.* **1989**, 179.
(9) (a) Blake, A. J.; Holder, A. J.; Hyde, T. I.; Schröder, M. *J. Chem. Soc., Chem. Commun.* **1989**, 1433. (b) Mashiko, T.; Read, C. A.; Haller, K. J.; Kastner, M. E.; Scheidt, W. R. *J. Am. Chem. Soc.* **1981**, *103*, 5758.
(10) (a) Küppers, H.-J.; Wieghardt, K. *Polyhedron* **1989**, *8*, 1770. (b) Peerce, P. J.; Gray, H. B.; Anson, F. C. *Inorg. Chem.* **1979**, *18*, 2593. (c) Clark, R. J. H.; Natile, G. *Inorg. Chim. Acta* **1970**, *4*, 533. (d) Hughes, J.; Willey, G. R. *Inorg. Chim. Acta* **1974**, *11*, L25. (e) Vats, J. L.; Garg, N.; Sharma, S. C.; Jadav, H. S.; Saxena, R. C. *Synth. React. Inorg. Met.−Org. Chem.* **1984**, *14*, 69.
(11) Bruce, J. I.; Gahan, L. R.; Hambley, T. W.; Stranger, R. *J. Chem. Soc., Chem. Commun.* **1993**, 702.
(12) Champness, N. R.; Jacob, S. R.; Reid, G.; Frampton, C. S. *Inorg. Chem.* **1995**, *34*, 396.
(13) (a) Hempel, J. C.; Morgan, L. O.; Lewis, W. B. *Inorg. Chem.* **1970**, *9*, 2064. (b) Pedersen, E.; Toftlund, H. *Inorg. Chem.* **1974**, *13*, 1603.
(14) (a) Cavell, R. G.; Byers, W.; Day, E. D. *Inorg. Chem.* **1971**, *10*, 2710. (b) Fatta, A. M.; Lintvedt, R. L. *Inorg. Chem.* **1971**, *10*, 478.
(15) The $E_{1/2}$ values of the aquo complexes are M = Mn, 1.30 V; M = Fe, 0.50 V; M = Cr, −0.68 V.[16]
(16) Bhattacharya, S.; Mukherjee, R.; Chakravorty, A. *Inorg. Chem.* **1986**, *25*, 3448.

0020-1669/95/1334-6556$09.00/0

Table 1. Characterization Data

compound	UV−vis data[a] λ_{max}, nm (ϵ, M^{-1} cm^{-1})	$E_{1/2}$,[a-c] V (ΔE_p,[d] mV)	μ_{eff},[e] μ_B	EPR g[f] values
[Cr(Me3L)]ClO_4	840[g] (64), 650[g] (181), 430[g] (640), 375[g] (1200)	−0.12 (120)	3.93	5.54,[h] 4.61,[i] 4.26,[i] 1.99,[i] 1.97,[h] 1.95[h]
[Cr(Me2L)]ClO_4	830[g] (87), 660[g] (125), 450[g] (565), 375[g] (1636)	−0.15 (100)	3.91	4.27,[h] 3.81,[i] 3.56,[i] 2.09,[h] 2.06,[i] 1.99[i]
[Cr(Ph2L)]ClO_4	850[g] (107), 650[g] (267), 425[g] (857), 360[g] (1857)	−0.07 (140)	3.95	5.60,[h] 4.72,[i] 4.29,[h] 2.05,[i] 2.01[h]

[a] In acetonitrile at 298 K. [b] At a platinum electrode; the supporting electrolyte is tetraethylammonium perchlorate (TEAP, 0.1 M); scan rate, 50 mV s^{-1}; reference electrode, SCE; solute concentration, ~10^{-3} M. [c] $E_{1/2}$ is calculated as the average of the anodic (E_{pa}) and cathodic (E_{pc}) peak potentials. [d] $\Delta E_p = E_{pa} - E_{pc}$. [e] In the solid state at 298 K. [f] Dichloromethane−toluene (1:1) at 77 K. [g] Shoulder. [h] Weak resonance. [i] Strong resonance.

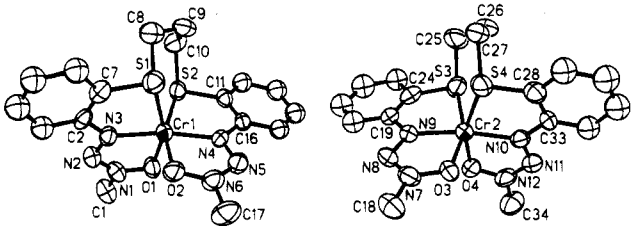

Figure 2. ORTEP plot and labeling scheme for $[Cr(Me3L)]^+$ in $[Cr(Me3L)]ClO_4 \cdot {}^1/_2CH_2Cl_2$ with all atoms represented by their 50% probability ellipsoids.

Table 2. Selected Bond Distances (Å) and Angles (deg) and Their Estimated Standard Deviations for $[Cr(Me3L)]ClO_4 \cdot {}^1/_2CH_2Cl_2$

		Distances	
Cr(1)−S(1)	2.417(3)	Cr(2)−S(3)	2.419(4)
Cr(1)−S(2)	2.445(3)	Cr(2)−S(4)	2.449(3)
Cr(1)−O(1)	1.951(6)	Cr(2)−O(3)	1.952(7)
Cr(1)−O(2)	1.958(7)	Cr(2)−O(4)	1.947(6)
Cr(1)−N(3)	1.970(6)	Cr(2)−N(9)	1.974(7)
Cr(1)−N(4)	1.984(6)	Cr(2)−N(10)	1.985(6)
O(1)−N(1)	1.338(9)	O(3)−N(7)	1.340(10)
O(2)−N(6)	1.341(8)	O(4)−N(12)	1.338(10)
N(1)−N(2)	1.271(11)	N(7)−N(8)	1.258(10)
N(2)−N(3)	1.333(10)	N(8)−N(9)	1.310(13)
N(4)−N(5)	1.322(10)	N(10)−N(11)	1.313(11)
N(5)−N(6)	1.270(13)	N(11)−N(12)	1.272(12)
		Angles	
O(1)−Cr(1)−O(2)	96.3(3)	O(3)−Cr(2)−O(4)	94.6(3)
O(1)−Cr(1)−N(3)	77.2(3)	O(3)−Cr(2)−N(9)	77.4(3)
O(1)−Cr(1)−N(4)	98.3(3)	O(3)−Cr(2)−N(10)	100.2(3)
O(1)−Cr(1)−S(1)	158.4(2)	O(3)−Cr(2)−S(3)	158.7(2)
O(1)−Cr(1)−S(2)	87.5(2)	O(3)−Cr(2)−S(4)	87.2(2)
O(2)−Cr(1)−N(3)	94.1(3)	O(4)−Cr(2)−N(9)	93.4(3)
O(2)−Cr(1)−N(4)	77.6(3)	O(4)−Cr(2)−N(10)	77.2(3)
O(2)−Cr(1)−S(1)	87.6(2)	O(4)−Cr(2)−S(3)	88.9(2)
O(2)−Cr(1)−S(2)	158.6(2)	O(4)−Cr(2)−S(4)	158.3(2)
N(3)−Cr(1)−N(4)	170.2(3)	N(9)−Cr(2)−N(10)	170.2(3)
N(3)−Cr(1)−S(1)	81.3(2)	N(9)−Cr(2)−S(3)	81.5(2)
N(3)−Cr(1)−S(2)	107.3(2)	N(9)−Cr(2)−S(4)	108.0(2)
N(4)−Cr(1)−S(1)	103.3(2)	N(10)−Cr(2)−S(3)	101.0(2)
N(4)−Cr(1)−S(2)	81.0(2)	N(10)−Cr(2)−S(4)	81.3(2)
S(1)−Cr(1)−S(2)	96.7(1)	S(3)−Cr(2)−S(4)	97.3(1)

of a racemic $[Cr(Me3L)]ClO_4$ pair and a dichloromethane molecule. Selected bond parameters are collected in Table 2.

The ligand binds the metal in hexadentate fashion, each ONS-coordinating half spanning meridionally. The $CrS_2N_2O_2$ coordination sphere is severely distorted from ideal octahedral geometry, the cis and trans angles in the sphere spanning the ranges 77.2(3)−108.0(2)° and 158.4(2)−170.2(3)°, respectively. The five-membered rings incorporating N,O and N,S chelation are satisfactorily planar (mean deviation 0.02−0.07 Å).

The Cr−S distances are of two types in each molecule, with averages of 2.418(4) and 2.447(3) Å. Interestingly in high-spin $[Fe(Me3L)]ClO_4$[4], which has only one molecule in the asymmetric unit, the Fe^{III}−S lengths are 2.557(2) and 2.533(2) Å. Thus the Cr−S length is shorter than the Fe−S length by ~0.1 Å. Part of the reason is no doubt the smaller size of the Cr^{3+} ion (ionic radii:[17] Cr^{3+}, 0.615 Å; Fe^{3+}, 0.645 Å). We also note that Fe^{3+} is significantly harder than Cr^{3+} (η values:[18] Cr^{3+}, 9.1; Fe^{3+}, 12.08), and this may selectively accentuate Cr^{III}−S binding over Fe^{III}−S binding because the thioether sulfur is soft. To our knowledge $[Cr(Me3L)]ClO_4 \cdot {}^1/_2CH_2Cl_2$ represents the first example of a structurally characterized Cr(III) complex derived from acyclic ligand supporting Cr^{III}−S (thioether) binding.

Comparisons. In the two reported structures incorporating Cr^{III}−S (thioether) binding, the coordination spheres are of types $CrSN_5$[11] and cis-CrS_4Cl_2[12] with Cr−S distances lying in the range 2.39−2.41 Å, which corresponds to the shorter distance in our complex. The D_q values of the above complexes (2120 and 1650 cm^{-1}, respectively) are higher than that in $[Cr(RxL)]ClO_4$ (1360 cm^{-1}). The chromium(III)−chromium(II) reduction potentials of the $CrSN_5$ and CrS_4Cl_2 species lie near −0.9 V versus SCE. The macrocyclic environment stabilizes (in the redox sense) the trivalent state much better than the $S_2N_2O_2$ coordination sphere does ($E_{1/2}$, −0.1 V). The EPR spectrum of $CrSN_5$ is not reported[11] while CrS_4Cl_2 is stated to give rise to a very broad signal near $g = 2$.[12] In contrast $[Cr(RxL)]ClO_4$ species display well-resolved resonances consistent with strong rhombic distortions. Thus the $[Cr(RxL)]ClO_4$ complexes have certain spectral and redox features that are distinct from those of the known macrocycles.

Concluding Remarks

The hexadentate triazene 1-oxide substituted thioether ligand family (H_2RxL readily binds chromium(III), affording stable complexes of coordination type $CrS_2N_2O_2$. The crystal structure of the complex $[Cr(Me3L)]^+$ has been determined. This is the first example of a structurally characterized nonmacrocyclic chromium(III) entity incorporating thioether coordination. Chromium(III) binds thioether sulfur better than high-spin iron(III), and a systematic search for new chromium(III)−thioether species should be rewarding.

Experimental Section

Materials. Purification of solvents and preparation of the supporting electrolyte for the electrochemical work were done as before.[19] All other chemicals and solvents were of analytical grade and were used as received.

Physical Measurements. Solution (~10^{-3} M) electrical conductivities were measured with the help of a Philips PR 9500 bridge. Magnetic susceptibilities of solids were measured by using a PAR-155 vibrating sample magnetometer fitted with a Walker Scientific L75FBAL magnet. Electronic spectra were recorded with a Hitachi 330 spectrophotometer. EPR spectra were collected in the X-band using a Varian 109C spectrometer fitted with a quartz Dewar. Calibration was done with DPPH ($g = 2.0037$). Electrochemical measurements were performed on a PAR Model 370-4 electrochemistry system, as reported earlier.[20] All potentials reported in this work are corrected for the junction

(17) Shannon, R. D. *Acta Crystallogr.* **1976**, *A32*, 751.
(18) Pearson, R. G. *Inorg. Chem.* **1988**, *27*, 734.
(19) Datta, D.; Mascharak, P. K.; Chakravorty, A. *Inorg, Chem.* **1981**, *20*, 1673.
(20) Chandra, S. K.; Chakravorty, A. *Inorg. Chem.* **1992**, *31*, 760.

contribution. A Perkin-Elmer 240C elemental analyzer was used to collect microanalytical data (C, H, N).

Preparation of Complexes. The ligands H_2RxL were prepared following the reported procedure.[3d,21-23]

Synthesis of [1,3-Bis((*o*-(1-methyl-1-oxidotriazen-3-yl)phenyl)thio)propanato-N^3,*S*,*O*]chromium(III) Perchlorate ([Cr(Me3L)]ClO_4). [*Caution! Perchlorate salts of metal complexes with organic ligands are explosive.*] A methanolic (15 mL) solution of $[Cr(H_2O)_4Cl_2]Cl\cdot 2H_2O$ (0.13 g, 0.49 mmol) was added to a dichloromethane solution (15 mL) of ligand H_2Me3L (0.20 g, 0.49 mmol), and the solution was heated at 70−80 °C for a period of 6−7 h. Addition of 0.069 g (0.49 mmol) of solid $NaClO_4\cdot H_2O$ provided a brown precipitate, which was washed with water and methanol. The product was finally dried in vacuo. The yield was 0.194 g (~71%). Anal. Calcd for $C_{17}H_{20}N_6O_6S_2ClCr$: C, 36.69; H, 3.59; N, 15.11. Found: C, 36.74; H, 3.53; N, 15.16.

The brown chelates $[Cr(Me2L)]ClO_4$ and $[Cr(Ph2L)]ClO_4$ were prepared similarly (yield ~70%). Anal. Calcd for $C_{16}H_{18}N_6O_6S_2ClCr$ ($[Cr(Me2L)]ClO_4$): C, 35.42; H, 3.32; N, 15.49. Found: C, 35.37; H, 3.38; N, 15.53. Calcd for $C_{26}H_{22}N_6O_6S_2ClCr$ ($[Cr(Ph2L)]ClO_4$): C, 46.85; H, 3.30; N, 12.61. Found: C, 46.79; H, 3.35; N, 12.57.

X-ray Structure Determination. Cell parameters of $[Cr(Me3L)]ClO_4\cdot {}^1/_2CH_2Cl_2$ (0.22 × 0.48 × 0.60 mm^3) grown by slow diffusion of *n*-hexane into dichloromethane solution were determined by least-squares fits of 30 machine-centered reflections (2θ = 15−30°). The structure was successfully solved in the space group $P\bar{1}$, and no significant correlations were present. Data were collected by the ω-scan method (2θ = 3−45°) on a Nicolet R3m/V diffractometer with graphite-monochromated Mo Kα (λ = 0.710 73 Å) radiation. Two check reflections measured after every 198 reflections showed no significant intensity reduction during an ~55 h exposure to X-rays. Data were corrected for Lorentz-polarization effects and absorption.[24] Of the 6522 reflections collected, 6495 were unique, of which 3427 satisfying $I > 3\sigma(I)$ were used for structure solution.

The structure was solved by direct methods. All non-hydrogen atoms except C(3)−C(6), C(12)−C(15), C(20)−C(23), and C(29)−C(32) were made anisotropic. Hydrogen atoms were added at calculated positions with fixed U = 0.08 $Å^2$. All refinements were performed by full-matrix least-squares procedures. The highest residual was 0.58 e/$Å^3$. All calculations were carried out on a MicroVax II computer with the programs of SHELXTL-PLUS.[25] Significant crystal data are listed in Table 3. Atomic coordinates and isotropic thermal parameters of selected atoms of the structure are given in Table 4.

Acknowledgment. We are thankful to the Department of Science and Technology, New Delhi and the Council of Scientific and Industrial Research, New Delhi for financial support. The Jawaharlal Nehru Centre for Advanced Scientific Research, Bangalore provided a Summer Research Fellowship to D.K.D.

Supporting Information Available: Tables of full listing of atomic coordinates (Table S1), complete bond distances (Table S2), angles (Table S3), anisotropic displacement parameters (Table S4), and hydrogen atom positional parameters (Table S5) (8 pages). Ordering information is given on any current masthead page.

(21) Zacharias, P. S.; Chakravorty, A. *Inorg. Chem.* **1971**, *10*, 1961.
(22) Unger, O. *Chem. Ber.* **1897**, *30*, 607.
(23) Mukkanti, K.; Bhoon, Y. K.; Pandeya, K. B.; Singh, R. P. *J. Indian Chem. Soc.* **1982**, *59*, 830.
(24) North, A. C. T.; Phillips, D. C.; Mathews, F. S. *Acta Crystallogr.* **1968**, *A24*, 351.
(25) Sheldrick, G. M. *SHELXTL-PLUS 88. Structure Determination Software Programs*; Nicolet Instrument Corp.: 5225-2 Verona Rd., Madison, WI 53711, 1988.

Table 3. Crystallographic Data for $[Cr(Me3L)]ClO_4\cdot {}^1/_2CH_2Cl_2$

chem formula	$C_{17.5}H_{21}N_6O_6S_2Cl_2Cr$
fw	598.4
color; habit	dark prismatic
space group	$P\bar{1}$
a, Å	8.484(4)
b, Å	13.538(5)
c, Å	23.476(12)
α, deg	73.56(3)
β, deg	89.34(4)
γ, deg	73.87(3)
V, $Å^3$	2477(2)
Z	4
T, °C	23
λ, Å	0.71073
ρ_{calcd}, g cm^{-3}	1.615
hkl range	h, −9 to 9; k, −13 to 14; l, 0 to 25
μ, cm^{-1}	8.94
transm coeff	0.6329−0.7210
R,[a] %	5.62
R_w,[b] %	5.98
GOF[c]	1.32

[a] $R = \sum||F_o| - |F_c||/\sum|F_o|$. [b] $R_w = [\sum w(|F_o| - |F_c|)^2/\sum w|F_o|^2]^{1/2}$; $w^{-1} = \sigma^2(|F_o|) + g|F_o|^2$; g = 0.0001. [c] Goodness of fit is defined as $[w(|F_o| - |F_c|)^2/(n_o - n_v)]^{1/2}$, where n_o and n_v denote the numbers of data and variables, respectively.

Table 4. Selected Atomic Coordinates (×10^4) and Equivalent[a] Isotropic Displacement Coefficients ($Å^2$ × 10^3) for $[Cr(Me3L)]ClO_4$

	x	y	z	U(eq)
Cr(1)	1719(2)	7971(1)	9490(1)	45(1)
O(1)	−426(7)	8233(4)	9822(3)	55(3)
O(2)	2936(7)	8106(5)	10155(3)	57(3)
N(1)	−1335(9)	9257(6)	9607(3)	53(4)
N(2)	−779(10)	9970(6)	9261(3)	51(3)
N(3)	760(9)	9534(5)	9148(3)	46(3)
N(4)	2667(8)	6451(5)	9968(3)	41(3)
N(5)	3565(9)	6269(6)	10463(3)	51(3)
N(6)	3663(9)	7143(7)	10541(3)	55(4)
S(1)	3918(3)	8348(2)	8881(1)	59(1)
S(2)	649(3)	7100(2)	8864(1)	51(1)
C(2)	1593(11)	10240(6)	8829(3)	43(4)
C(7)	3163(12)	9784(7)	8671(4)	49(4)
C(11)	1480(10)	5753(6)	9329(4)	44(4)
C(16)	2400(9)	5550(6)	9855(4)	40(3)
Cr(2)	625(2)	7862(1)	4474(1)	50(1)
O(3)	2385(7)	8295(5)	4773(3)	57(3)
O(4)	−624(7)	7866(5)	5174(3)	59(3)
N(7)	2100(10)	9364(7)	4588(3)	58(4)
N(8)	826(11)	9983(6)	4273(3)	56(4)
N(9)	−113(9)	9442(5)	4145(3)	51(3)
N(10)	1237(8)	6317(5)	4935(3)	47(3)
N(11)	622(10)	6056(6)	5453(3)	58(4)
N(12)	−315(10)	6884(7)	5563(3)	61(4)
S(3)	−1863(3)	8029(2)	3916(1)	68(1)
S(4)	2586(3)	7146(2)	3815(1)	63(1)
C(19)	−1652(12)	10048(7)	3849(4)	52(4)
C(24)	−2626(12)	9462(8)	3732(4)	59(4)
C(28)	3056(11)	5767(7)	4237(4)	54(4)
C(33)	2373(10)	5494(6)	4768(4)	45(4)

[a] Equivalent isotropic U defined as one-third of the trace of the orthogonalized U_{ij} tensor.

IC9505559